Characterisation of Skin-based THz Communication Channel for Nano-scale Body-centric Wireless Networks

Nishtha Chopra

School of Electronics Engineering and Computer Science

This dissertation is submitted for the degree of
Doctor of Philosophy

Queen Mary University of London May 2017

Declaration

I hereby declare that except where specific reference is made to the work of others, the contents of this dissertation are original and have not been submitted in whole or in part for consideration for any other degree or qualification in this, or any other university. This dissertation is my own work and contains nothing which is the outcome of work done in collaboration with others, except as specified in the text and acknowledgements.

Nishtha Chopra
May 2017

Acknowledgements

I would like to express my deepest gratitude to my supervisors, Dr.Akram Alomainy and Prof. Mike Philpott. They both have provided me with immense support to make this piece of research a worthwhile. They were prompt, encouraging and pro-active about any new idea that I had to share. Through them, I have met a lot of people in my area of research and otherwise, which has helped me to build a network of talented researchers. If I had any confusions or concerns, they were my harbour for clarity. Be it any event, conference, interview or technical writing, they have always given me the best of advice. I will always remember Dr.Akram quoting from his experience,"the graph of a PhD student", emphasizing on the focus and motivation required at step of a PhD journey. I come from a non-medical background, but with the astute guidance of Prof.Mike Philpott, I was able to grasp and apply the biology related concepts to my research. They had both given me complete freedom to explore and grow the area from an engineer's point of view and helped in resolving any challenge, I had during experimental work.

I would also like to thank my colleagues in the Antennas Group: Oleksandro shushko, Yang Zhang, Melusine Pegion, Deepak Singh Nagarkoti, Ke Yang, Darryl Smith, Max Munoz Torrico (currently the lab manager) and the list is endless for keeping the research enjoyable and informative. I will always remember our outings, lunch-time conversations, THz-TDS measurements and birthday celebrations. I was fortunate to make friends within the Cutaneous Group at Blizard Institute: Giuseppe Trigiante, Sreekanth Vootukuri Reddy, Jamie upton, Zoe Drymoussi and Rosalind Hannen and would like to thank them for helping me with the nitty-gritties of cell-culture, discussing interesting concepts and ideas to conduct my experiments.

I am grateful for having an amazing friend Abhinav Srivastava who has always been there for me through thick and thin. His presence in my life both personal and professional has been profound and significant. I would like to thank my friend Priyam Rastogi, whom I don't meet often but her encouragement has kept me on my toes while writing this thesis. Coming to a new city, specially one like buzzing London is sometimes very stressful, but I have met very helpful and genuine people as my flatmates: Mia Fogelberg, Steve Stewart, Soraia Assis, Marta Ferranti, Dhanisha Patel, in an otherwise challenging London housing.

They have brought a lot of fun and entertainment in my life. We have shared hobbies, late night talks, musicals, travel stories and a lot more.

Last but not the least, my parents, Deepa Chopra and Hemant Kumar and my sister, Jetashree Chopra, who are the backbone of my life. My parents will always be my first teachers and I couldn't have made it this far without them.

Abstract

In pursuit of enhancing the capabilities of healthcare diagnostics and monitoring, the electromagnetic spectrum has been utilized efficiently from the MHz upto THz and beyond. The era of smart phones, wearable devices and on-body networks have unfolded plethora of health applications with efficient channel communication mechanisms, faster data transfer rates and multi-user functionalities. With the advancement in material fabrication and spectroscopic techniques, a new realm of healthcare nanodevices have emerged with immense potential to garner in-depth information of the human body, real-time monitoring and tackle medical emergencies. A collection of these devices with sensing capabilities together form a nanonetwork performing computing tasks such as storage, actuation, data transfer and communication. The thesis brings forth the analysis and optimization of channel parameters; such as pathloss and molecular noise temperature, when the proposed in-body nanodevices communicate amongst each other in the terahertz (THz) range. The novel contribution of the work is mapping the optical properties of human skin by bringing together the measurement of various skin tissues and its influence on channel parameters. In the later part of the thesis, emphasis is given on the individual biological entities of the tissue contributing to channel parameters, such as collagen as an abundant protein, variation in fibrous extra-cellular matrix due to fibroblast cells and amalgamation of different layers; namely, epidermis and dermis of the skin.

Recently proposed graphene-based antennas resolve the cumbersomeness of existing medical devices by drastically reducing its size to a few hundreds of nanometres. These biocompatible nanodevices focus on exchanging the intricate details of the human body via nanoscale electromagnetic communication in the terahertz domain of the spectrum. The thesis aims to investigate the material properties of skin tissues with terahertz time domain spectroscopy and numerically evaluate the channel parameters for in-body nanoscale networks that potentially would form an essential part of a hierarchical body-centric communication network extending from inside the human body to a wider community network. The results are presented in regards to the complexity of human tissue as a channel medium. The measured refractive index and absorption coefficient data is applied to numerically calculate channel pathloss and molecular noise temperature. The results provide a real-time analysis

of tissue morphology, molecular features, hydration level and atmospheric water vapour on channel parameters. In addition to this, engineered skin substitute models: 2D collagen and 3D organotypics, are investigated to address the importance of individual biological features comprising of water dynamics and cell culture, affecting the channel parameters.

The experimental results of various tissue samples, skin substitutes and numerical evaluation of channel parameters can be used to further improve the communication capabilities of in-body nanonetworks. The original contributions on characterization of skin substitutes can be applied to study various health conditions, effects of drugs and skin ageing on a molecular level. The results presented in this thesis, foresee an increasing demand in skin substitute models due to their biological flexibility and control according to desired medical applications.

Author's Publications

Book Chapter

- Ke Yang,Chopra Nishtha; Abbasi, Qammer H.; Qaraqe, Khalid; Alomainy, Akram: 'Down scaling to the nano-scale in body-centric nano-networks' (Telecommunications, 2016), 'Advances in Body-Centric Wireless Communication: Applications and state-of-the-art', Chap. 12, pp. 375-411, **contribution from chapter 2 and 4**

Journals

- Nishtha Chopra, Ke Yang, Qammer H. Abbasi, Khalid Qaraqe, Mike Philpott and Akram Alomainy, "THz Time Domain Spectroscopy of Human Skin Tissue for In-Body Nano-networks", IEEE Transactions on THz Science and Technology,2016 **contribution from chapter 3**

- Nishtha Chopra, Ke Yang, Jamie Upton, Qammer Hussain Abbasi, Khalid Qaraqe ,Mike Philpott, Akram Alomainy, "Fibroblasts Cell Number Density based Human Skin Characterization at THz for In-body Nanonetworks", Elsevier Nano Communication Networks, 2016) **contribution from chapter 4**

- Qammer H. Abbasi, Ke Yang, Nishtha Chopra, Josep Miquel Jornet, Najah Abed AbuAli, Khalid Qaraqe, Akram Alomainy, "Nano-communication for Biomedical Applications: A Review on the State-of-the-art from Physical Layers to Novel Networking Concepts", IEEE Access,2016 **contribution from chapter 2**

- Q. H. Abbasi, H. El Sallabi, N. Chopra, K. Yang, K. Qaraqe, and A. Alomainy, "Terahertz Channel Characterization Inside the Human Skin for Nano-scale Body-Centric Networks", IEEE Transactions on THz Science and Technology (Accepted, March 2016) **contribution from chapter 2**

- K. Yang, N. Chopra, M. Munoz, Q. H. Abbasi, Y. Hao and A. Alomainy, "Effects of Non-flat Interfaces in Human Skin Tissues on the In-Vivo Tera-Hertz Communication Channel", Elsevier Nano Communication Networks, 2015 **contribution from chapter 2**

- G. Piro, K. Yang, G. Boggia, N. Chopra, L. A. Grieco, Yang Hao and A.Alomainy, "Terahertz Communications in Human Tissues at the Nano-scale for Healthcare Applications", IEEE Transactions on Nanotechnology, 2015 **contribution from chapter 2 and 3**

Conferences

- N Chopra, M Phipott, A Alomainy, QH Abbasi, K Qaraqe, RM Shubair, “THz Time Domain Characterization of Human Skin Tissue for Nano-electromagnetic Communication”, 2016 16th Mediterranean Microwave Symposium (MMS), Abu Dhabi, UAE, November 2016.

- N Chopra, J Upton, M Philpott, A Alomainy, QH Abbasi, K Qaraqe, “Characterization of Volumetric Change in Collagen using THz Time Domain Spectroscopy for In-Body Nanonetworks”, Proceedings of the 3rd ACM International Conference on Nanoscale Computing and Communication, New York, USA, September 2016.

- Nishtha Chopra, Mike Philpot, Akram Alomainy, "Investigating Electromagnetic Material Properties of Collagen at THz for Health Monitoring Applications", 5th EAI International Conference on Wireless Mobile Communication and Healthcare - "Transforming healthcare through innovations in mobile and wireless technologies", 14-16 October 2015, London, UK.

- Nishtha Chopra, Ke Yang, Qammer Abbasi , Khalid Qaraqe, Mike Philpott, Akram Alomainy, “Characterization of Human Skin Using THz Time Domain Spectroscopy for In-body Nanonetworks”,9th EAI International Conference on Bio-inspired Information and Communications Technologies, Dec 2015

- Ke Yang, Nishtha Chopra, Jamie Upton, Yang Hao, Mike Philpott and Akram Alomainy, “Characterizing Skin-Based Nano-Networks For Healthcare Monitoring Applications at THz”, 2015 IEEE AP-S Symposium on Antennas and Propagation. (Presented by Nishtha Chopra)

- K Yang, N Chopra, Q Hussain Abbasi, K Qaraqe, A Alomainy, "Towards Efficient And Comprehensive Healthcare/medical Monitoring System: Nanoscale Body-centric Networks (nano-health)", Qatar Foundation Annual Research Conference, 23-24 November 2014, Doha, Qatar.
- N Chopra, K Yang, J Upton, A Alomainy, M Philpott, Y Hao, "Understanding and characterizing nanonetworks for healthcare monitoring applications", 2014 IEEE MTT-S International Microwave Workshop Series on RF and Wireless Technologies for Biomedical and Healthcare Applications (IMWS-Bio), 8-10 December 2014, London, UK.

Table of contents

List of figures

List of tables

Chapter 1

Introduction

A worthwhile contribution to communication and networking comes from the knowledge of electromagnetic spectrum. The radio waves with frequency up to 300GHz and wavelengths less than 1mm have been immensely harnessed for communication and networking [1]. These modern communication techniques amounts to easy and effective ways of human to human interactions via smart-phones, satellite communication for entertainment and space exploration, radar system for aviation industry and slowly moving towards body area and in-body networks for medical applications. The growing interest in medical applications come with a motive to understand the source of diseases and to be able to provide a better health diagnostic system [2, 3]. On-body techniques popularly known as body area networks (BAN) are set of mobile and compact intercommunicating computing devices worn or even implanted into patients [2].

These marvels of technology and engineering, are establishing an elevating trend for the future medical monitoring devices. A gradual shift in the exploitation of electromagnetic spectrum from microwave to millimetre wave has been a stepping stone for many inventions in the field of communication, computers, electronics and medicine. Modern technology is now moving towards more collaborative applications rather than standalone and focused ones. The birth of inter-disciplinary research has penetrated the medical sciences to a level where healthcare sector is capable of diagnosing, preventing and treating even the assumed incurable diseases. They can help monitor the patient's physiology and other medical conditions. Some of the best examples include heart-rate monitors, glucose-monitors or optically based sensors fitted on earlobe fingernails or wrist. Over the years, these devices have evolved into a niche area which often referred as wearable technology [4].

Over the years, the significant growth in wireless and body-centric communication has opened doors to futuristic medical diagnostic devices and theories [5–8]. It is envisioned that medical conditions can be further improved with continuous in-body monitoring of patient's

health. Current state of the art technology dictates in microwave(50-900MHz) and millimetre wave (30-300 GHz) regions and gradually expanding in the Terahertz domain (0.1-3THz) [9, 10]. With an increasing awareness of hazardous diseases such as cancer, diabetes and demand to improve medical conditions [11], the diagnostic research is more emphasized on extracting intrinsic details of the human body, precision of measurement and efficient data transfer.

Radio enabled implantable devices with an aim to blend with the morphology and biology of the human body has paved the way for applications in drug delivery, glucose monitors, blood pressure sensing system, and eye pressure sensors [12]. While microwave is taking care of communication in the periphery of the human body and amongst devices, millimetre wave provide measuring techniques with better spatial resolution, more compact and cost-effective devices. The thrust and plethora of numerous research activities in medical electronics witnessed its first success with cardiac pacemaker. Miniaturization of devices was later possible with the advent of silicon-based semiconductor technology [13]. In the similar line of work devices such as cardioverter, defibrillators and implantable neuromodulation systems can communicate essential diagnostic information and address pathologies gastroesophageal reflux disease (GERD), sleep apnea, chronic pain obesity, hypertension and heart failure [14]. It is thus safe to assert, that wireless communication schemes and medical electronics has indeed promulgated indispensable information in the medical field. As a consequence to this widespread pool of data, it has ushered a completely new era of big data, internet-of-things and most recently internet-of-nano-things.

Advancement in communication systems applied to millimetre wave have improved health services by promoting technologies like Body Area Networks (BAN) [2]. To achieve mobility and greater flexibility, a meticulous arrangement of sensors collect healthcare data and exchange information to remote locations. For instance, an automatic real-time monitoring of patient's vitals such as blood pressure, heart-rate, body temperature etc., is possible. Despite the enormous potential of millimetre wave communication and BAN, many challenges still remain in fabricating reliable in-body sensors in hostile environment of human body.

To overcome these discrepancies, further down-scaling of devices to a length of nanometres (1-100nm) is rewarding in terms of clinical diagnosis, device performance and data collection. A conglomeration of these ingenious nanomachines or nanodevices embodied in nanonetworks [15, 16] have potential benefits of biocompatibility, in-depth analysis of human body, faster transmission rates, targeted diagnosis and sizes comparable to molecules. In terms of functionality, these are much more sophisticated than other implantable devices having features like sensing, memory, actuation, power unit, and communication. The

practical applications of this technology can only be achieved with optimization of channel medium which is the human body and hence developing novel concepts for communication systems is the key. More details on the proposed communication schemes have already been discussed extensively in chapter 1. However, here a brief overview of recent research activities in THz communication for free space and computer simulated skin models will be discussed.

In pursuit of achieving a real time understanding of in-body communication, elementary theoretical models were developed to impersonate the human body using EM simulation software. A database of different animal tissue published by Gabriel and team in 1990s [17, 18], for RF and microwave frequencies, led to development of pathloss models characterized by refractive index and absorption coefficient [19, 20]. As discussed in the further chapters, nanodevices are envisioned to communicate in the THz region of the electromagnetic spectrum, owing to their size and bandwidth of 1-10THz [21]. In addition to this, initial studies have been made to investigate the material properties of skin tissue 0.3-2THz [22–25].

1.1 Proposed Nanoscale Communication Schemes

Together with wireless technology, advances in nanotechnology and rapid synthesis of Graphene has transformed the realms of biomedical sciences [26]. Recent research in the area of drug delivery, cancer therapy, bio-sensing and bio-imaging has exploited the unique structural and physiological features of graphene and its derivatives [27, 28]. Along with Graphene, other nanomaterials like carbon nanotubes (CNTs) make excellent candidates for loading of drugs, cellular imaging, sensing other molecules and in-vivo cancer studies due to their biocompatibility and stability [29, 30]. Assimilating from the fundamentals of electromagnetic, wireless communication, medical and material science, a novel concept of nanonetworks was first introduces in 2008, which stems from the concept that a collection of nanodevices have the potential to harness the innate communication capabilities of human body, thereby allowing them to cooperate and share information [15]. Healthcare diagnosis can only be achieved if an efficient communication mechanism and data transfer is established between these nanodevices

Hence, extensive research is on-going to fabricate sensors and devices at nanometre scale in parallel to modification of existing communication and networking paradigms [16]. These revelations combining expertise from various scientific domains such as bioengineering, material science and electromagnetics are becoming a practical solution to various medical diagnostic problems. Many variants of nanoscale wireless communication have been proposed - Nano-Electromagnetic (Nano-EM), opto-ultrasonics and molecular communication

[15, 31, 32]. The thesis is conclusively focused on the operation, applications and experimental investigation of in-body Nano-EM communication. However, to provide the reader with an underlying concept of nanoscale communication, the variants can be briefly described as:

- Molecular Communication: The conceptualization of nanonetworks was first done for molecular communication based on the use of existing biological nanomachines, such as molecular motors, as components or models for the development of new nanomachines. Several biological structures found in living organisms can be considered as nanomachines such as cells [33]. A Biological nanomachine, analogous to a living cell includes: nano-biosensors, nano-actuator, bio-hybrid memory device, and control unit [15]. A nanomachine is defined as "an artificial eutactic mechanical device that relies on nanoscale components for information exchange [34].

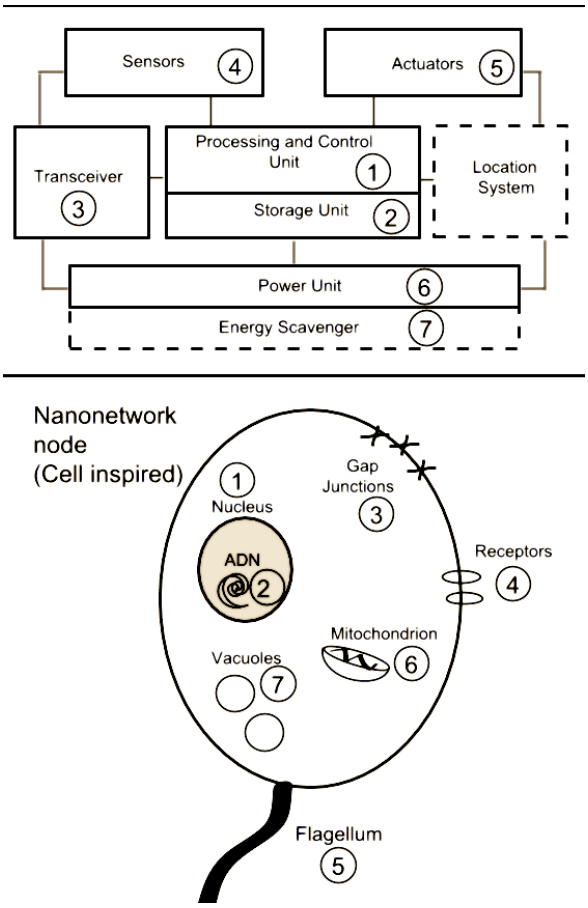

Fig. 1.1 Proposed Schematic of a Biological Nanomachine analogous to the attributes of actual human body cell [15]

Necessary features of future nanomachines are already present in a living cell, which can be defined as a self-replicating collection of nanomachines [35]. The resulting

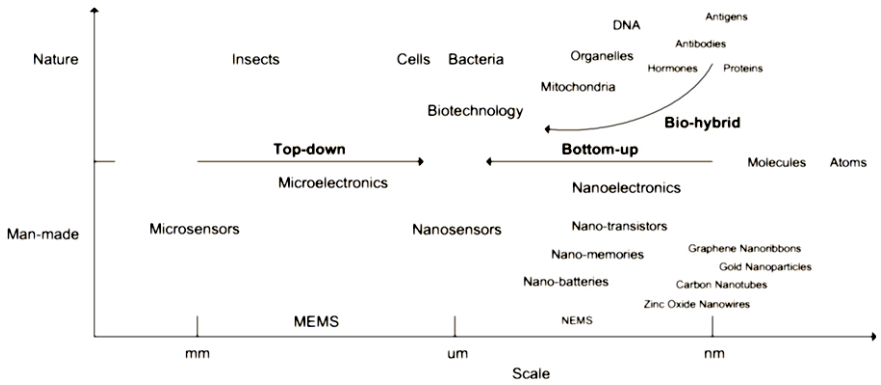

Fig. 1.2 Approaches for the development of nanoscale communication [16]

nanonetwork is based on molecular signalling, a process also used for inter-cell communication to achieve a common objective such as the growth, multiplication, control of hormonal activities or immune system responses in the human body. Molecular motor based communication is suitable for short-range communication. It is sometimes hard to predict the motion of molecules via diffusion based therefore, there is a need for more tail-like communication mechanism. Most of the intra-cell communications are based on molecular motors [33]. Molecular motors travel along molecular rails called microtubules, at a speed up to 400 mm/day [36]. The ability to move molecules makes molecular motors a feasible way to transport information packets, i.e., molecules, from the transmitter to the receiver nanomachine. As an additional advantage, molecular motors and microtubules can be used as a bio-hybrid communication interface between man-made nanomachines and biological structures [37]. A nanomachine architecture for bio-hybrid communication is shown in figure 1.1. The system has defined features similar to that of a living cell.

Another natural phenomena for communication is diffusion transport. This mechanism has been exploited in many areas, such as diffusion velocity in metals/semiconductor materials and harvesting the flow of water body in a dam for generating electricity. In all the cases, the common concept is the difference in concentration gradient and no need for an external force to trigger the process. The method is suitable for long-range communication and is also known as pheromonal communication (in case of human body cell communication). Pheromones can be defined as molecular compounds containing information that can only be decoded by specific receivers and can invoke certain reactions in them [38]. It is more of a freedom-flow based communication as there no physical link that will bind the transmitter and receiver node together. Information is encoded on the molecules, the reception of the transmitted molecules is

realized by molecular receptors located on the receiver. This phenomenon is based on the ligand-receptor interaction [39].

- Opto-Ultrasonic Communication: The motivation is to use mechanical waves stems from the natural communication mechanism between different cells of the human body. In a macroscale world, bulky robots have been engineered to perform simple tasks. In the same line of work, wireless nanorobots (also called nanomachines, nanodevices), i.e. devices of sizes ranging from one to a few hundred nanometres, have been proposed remote and distributed medical diagnosis and treatment of major diseases [40]. Molecular communication enables these nanorobots to detect and eliminate hazardous agents and pathogens inside the biological tissues, e.g., viruses and cancer cells, enabling less invasive and less aggressive treatments [41]. Moreover, a distributed networks of nano-devices could be used for organ, nervous track, or tissue replacements, i.e. bio-hybrid implants. Use of ultrasonic waves has been quite prominent in the medical field. These are mechanical waves that propagate in an elastic medium at frequencies above the upper limit for human hearing, i.e., 20 kHz. Their controlled use is a boon for many diagnostic applications such as understanding underwater life/communication [42–44] and in-body imaging [45]. In the paper, [46–48] it was illustrated that Ultrasonic waves have a strong potential to enable inter-networking among implanted devices in the human body at communication ranges spanning from a few micrometres to several centimetres.

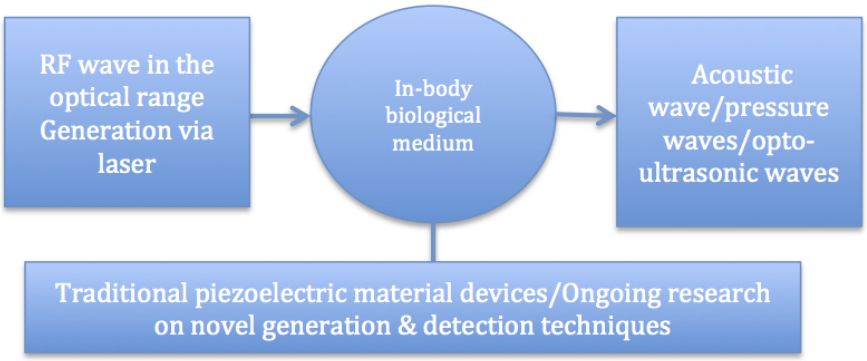

Fig. 1.3 Schematic of Opto-acoustic wave generation

This mechanism is based on the joint use of light beams and ultrasonic waves (Fig.1.3), the phenomenon known as opto-acoustics, could potentially be the foundation of a new communication paradigm to enable intra-body networking at the nano-scale [32]. Interestingly, it has been pointed out in reference [49], there is a hypothesis that techniques for studying vibrations in cellular structures, (including raman, infrared and

neutron spectroscopy) usually consider bond and small chemical group vibrations, with expected acoustic frequencies in the terahertz (THz). Higher frequency vibrations may occur more broadly in cellular processes - such as rotational and vibrational motions.

Ultrasound waves are typically generated through piezoelectric materials that convert electrical energy into mechanical energy and vice versa; or through the vibration of a thin plate, i.e. a capacitor, under a force [50]. The opto-acoustic effect refers to the generation of acoustic waves from the optical excitation of a medium and the excitation wave frequency is in the optical range. Under influence of opto-acoustic effect, the waves can be generated through various mechanisms: optical breakdown, vaporization, and thermoelastic generation. Optical breakdown provides high generation efficiency, but require extremely high laser intensities that may produce hazardous and irreversible effects in the radiated tissue. Optical energy ionizes a tissue, thus forming plasma generates a pressure wave while expanding. When the optical energy absorbed by the tissue is lower than the breakdown threshold, but exceeds the boiling threshold, e.g., 2600 J/cm^3 for water, vaporization occurs, producing an opto-ultrasonic wave [32, 51].

Thermoelastic mechanism [52, 53] has lower generation efficiency, but requires significantly lower laser intensities compared to the optical breakdown and vaporization effects. This mechanism is in general more attractive because of its low-thermal effect properties and reduces damage of the biological tissues. The energy absorbed by optical excitation generates a temperature gradient that leads to a thermal expansion, and therefore to the generation of opto-ultrasonic waves. Some adverse biological effects, which should be illustrated while proposing such a mechanism: heating effect and cavitation. The most well understood acoustic effect in biological tissues is heating. During ultrasound propagation, a portion of the energy is absorbed and converted into heat, which could lead to a temperature increase. As the wave intensity increases, the temperature rises and if it becomes higher than 38.5°, adverse biological effects may occur. Another effect caused by ultrasonic wave propagation is cavitation [32], which denotes the behaviour of gas bubbles within an acoustic field. Pressure variations of the ultrasound wave cause bubbles in the propagation medium to contract and expand. For large pressure variations, the bubble may collapse, causing serious biological effects and damaging tissues located in close proximity. To avoid potentially dangerous effects, ultrasounds at low transmission pressure levels, and consequently low transmission power levels should be employed.

- Nanoscale Electromagnetic Communication: The existence of successful biological nanomachines, which are highly optimized in terms of architecture, power consumption and communication, motivate their use as models or building blocks for new developments. In light of on-going research in the field of short range in-body communication, EM communication at nanoscale promises to offer better control, higher data rates and more reliability [54]. While, molecular communication seems like a viable solution to in-vivo diagnosis, there are many technical limitations including channel capacity, noise, interference and modulation. The speed and range of molecular communication are extremely slow and short, and vary depending on the biological materials, mechanisms used, and the environment. The communication mechanism at nanoscale defies the traditionally existing concepts. With the fabrication of such biocompatible nano-antennas, novel communication paradigm was introduced spanning from 0.1-10THz of frequencies [16].

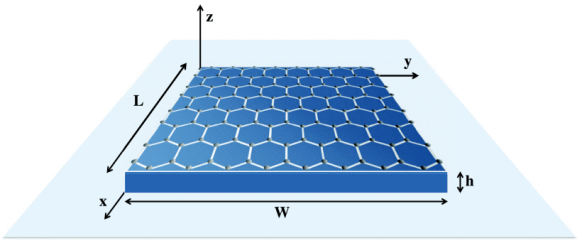

Fig. 1.4 Graphene based 2D nano-patch antenna whose width can be scaled to emit THz radiation in the desired frequency range [55]

For instance 1µm long dipole antenna is expected to emit radiation with a frequency of 1 THz whereas a metallic antenna would rate 100 THz, which is not feasible to work with [20]. Quantum effects govern the wave propagation velocity in these nanomaterials. This biological friendly radiation is generated at a dramatically lower frequency and with higher radiation efficiency with respect to their metallic antennas. Graphene has excellent properties for propagating surface plasmon polaritons (SSP) electromagnetic waves guided along the metal-dielectric interface. Graphene conductivity was calculated and propagation of SPP was studied. The coupling of incident EM radiation with corresponding SPP modes leads to resonances in such antennas leading to generation of THz radiation [56]. Thus, the principle idea of nanoscale EM communication is based on channel propagation and modelling. In the subsequent chapters more details will be provided on propagation, channel parameters and dependence on channel medium.

1.1.1 Nanonetworks Architecture and Applications

The human body is a good example of a naturally existing communication network. For instance the nervous system is composed of nerve cells, i.e., neurons, communicates the external stimulus to brain and enables communication between different systems by conveying information with molecular impulse signal known as spike [57]. The human body needs communication amongst different cells to survive, the proposed intra and inter-body nanonetworks ensures their stability without mechanically (or physically) disturbing the harmony of the in-built molecular structure of the body. Moreover, in most of the cases medicine fails to understand the root cause of the problem but once we have a monitoring network established in our body, we can extract various unknowns and treat them effectively.

The vision of nanoscale networking attempts to achieve the functionality and performance of the internet with the exception that node size is measured in nanometres and channels are physically separated by up to hundreds or thousands of nanometres [33]. In addition, nodes are assumed to be mobile and rapidly deployable. Nodes (or nanodevices) are assumed to be either self-powered or spread in and around the specific location. In a visionary sense, an ultimate application of nanoscale networking would be an automated process, where the nano-nodes are in motion communicating in a complex dynamic environment of living organisms monitoring diseased or sensitive parts of the body [58].

The intra and inter-body nanonetwork consists of [15]:

- Nano-nodes: simple and smallest nanomachines performing simple computation with limited memory. They transmit information over very short distances.
- Nano-routers: larger computational resources than nano-nodes and suitable for aggregating information coming from limited nano-devices. They control the behavior of nano-nodes by exchanging very simple control commands (on/off, sleep, read value,etc).
- Nano-micro interface devices: aggregate the information coming from nano- routers, to convey it to the microscale and vice versa. These are hybrid devices communicating in the nanoscale.
- Gateway: remote control of the entire system over the Internet. For example, in an intra-body network scenario, an advanced cellphone can forward the information it receives from a nano-micro interface in our wrist to our healthcare provider.

A brief summary on different parts of a nanodevice is provided below: [16]:

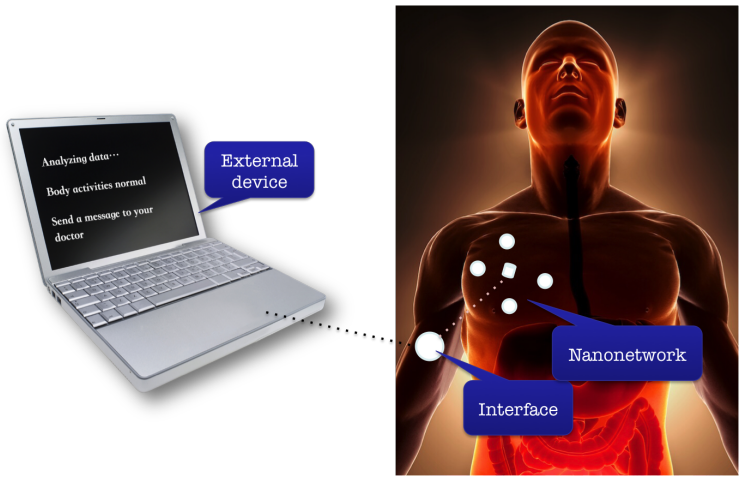

Fig. 1.5 Schematic of Nanonetwork Architecture focusing on nanoscale communication amongst collection of nano-devices inside the human skin. The information retrieved by these devices are then communicated to macroscale devices such as mobile phones, laptops etc for real-time monitoring of human health

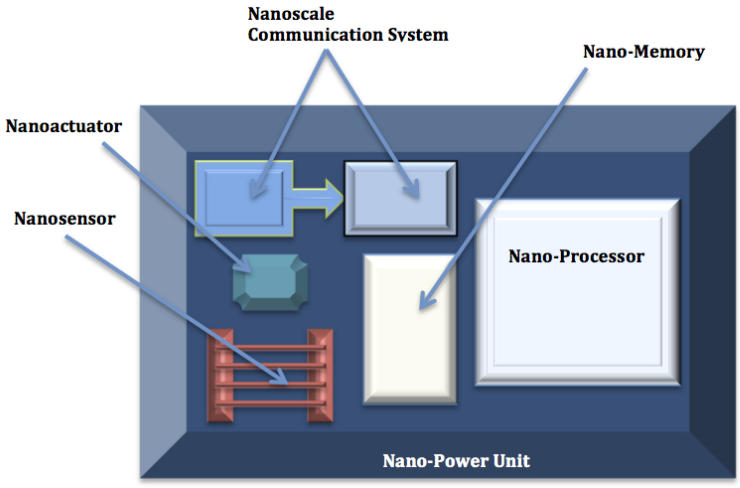

Fig. 1.6 Hypothetical in-body nano-device sensor as a part of nanonetwork (reproduced from Akyildiz et al.) [16]

- Nanoprocessor: It is responsible for all other components of the nanonetwork, can be thought of as a brain to the entire system. With the advent of nanomaterials like graphene and CNT, it is possible to fabricate tiny FET transistors and assemble for a processing unit. The nanoscale approach makes this entity less complex and high speed. It is theoretically predicted that the switching frequencies of such transistors are in the order of up to a few hundreds of terahertz, which is faster than any existing silicon FET transistor [59].

- Power unit: The unit will be able to exploit energy from external sources such as light, heat and store it for future distribution and consumption. More work is being done on Lithium nanobatteries and self-power nanobatteries [60, 61]. For a nanonetwork, it is important to consider the power unit size, energy harvested and the storage, because dealing with nanoscale physics is tedious and size and energy concepts are quite tricky.

- Actuators: It is an interface between the environment and the nanonetwork. Several sensors and/or actuators can be included in a nanomachine, e.g., temperature sensors, chemical sensors, clamps, pumps, motor or locomotion mechanisms [62].

- Communication unit: Nanonetworks are basically communication networks, this cannot blind sight the fact that they would eventually need to communicate, hence even while fabricating such devices it becomes mandatory to mind the concepts related to nanoscale communication. Nanoantenna and Nanoscale-EM transceivers are the main candidates for EM communication. Wireless communications among nano-devices cannot be achieved by simply reducing the size of a classical metallic antenna down to a few micrometers, since that would impose the use of very high resonant frequencies, in the optical range. Graphene-based plasmonic nano-antennas [63], or graphennas, just a few micrometers in size are envisaged to radiate electromagnetic waves in the terahertz band (0.1-10THz).

There are range of applications underlying the potential of nanonetworks and nanoscale communication. Some of the applications are illustrated in figure 1.7.

Necessary features of future nano-communication devices are already present in a living cell [15]. The implementation of any form in-vivo communication will need to ensure a non-disruptive operation. Since, the goal is to improve healthcare and acquire detailed information of the human body, new constraints and system requirements needs to included [64]. While, molecular communication seems like a viable solution to in-vivo diagnosis, there are many technical limitations including channel capacity, noise, interference and modulation. The speed and range of molecular communication are extremely slow and short,

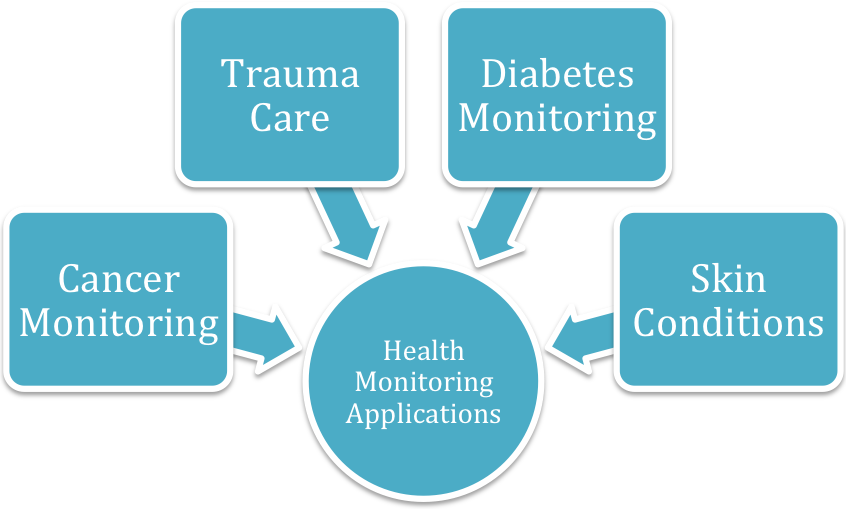

Fig. 1.7 Various applications of nanoscale electromagnetic communication devices operating in harmony as a part of nanonetwork

and vary depending on the biological materials, mechanisms used, and the environment. In addition, molecular communication experiences large signal jitters and a high loss rate because the movement of molecules is often unpredictable and the molecules arrive at a receiver bio-nanomachine after a widely varying period of time. Moreover, the molecules may degrade in the environment and not even arrive at a receiver bio-nanomachine [65]. With the current research and solutions available for molecular communication, it becomes necessary to look for alternative in-vivo communication mechanisms.

The thesis is focused on understanding and characterizing nanoscale-EM communication for healthcare diagnostic applications. Study of nanoscale-EM communication and corresponding electromagnetic properties of human body will be covered in the subsequent sections. When it comes down to cellular level specifically in-vivo communication, the mechanism is neither engineered nor is it fully accessible. However, the challenge and the obvious missing factor is detailed knowledge of the human body relevant to these electronic devices. Thus an intense research on electrical properties of the human body is vital for the operation and success of these nano-devices. Before moving towards the kernels of this thesis, some interesting questions to pay heed on would be - How nanoscale-EM communication happens within the human body ? The various organs in our body inherently communicate and transport information with each other at a cellular level (micrometres, μm in scale) thus keeping us alive. Modern day communication technologies like digital communication are a best example of harnessing the nature's way of communication [66].

Imagine a scenario where we could understand the essence of in-vivo communication in a way we understand mobile communication today; this could solve many health related

issues. However, it will be further covered that realization of in-vivo communication is not in the conventional MHz-GHz range, rather a relatively unexplored domain of the electromagnetic spectrum namely, Terahertz (THz). This part of the EM spectrum bridges the gap between electronics and photonics and extends from 0.3-30 THz [67]. Even with the limited penetration depth of THz waves in the biological medium, it is still a favourable choice for communication. The extensive and rapid growth in generation and detection techniques for THz, has led to some breakthrough in medical imaging, material characterization and space exploration [68]. However, one of the key attributes of this spectrum is its sensitivity at the cellular/molecular. The subsequent chapters of this thesis will focus on understanding in-vivo nanoscale wireless communication and thereafter channel modelling of nanoscale-EM communication for health monitoring applications.

1.2 Research Motivation

The advancement in nanomaterial research for fabrication devices has opened doors to nanoscale-EM communication. The results show that for a maximum antenna size in the order of several hundred nanometres, both a nano-dipole and a nano-patch antenna will be able to radiate electromagnetic waves in the terahertz band (0.1-10.0 THz).

The interest in THz stems from prediction of collected structural vibrational modes at the THz frequencies. These modes involving large-scale motion of entire sub-units of macromolecule are dictated by structure and have long been discussed as dynamics leading to conformational change and bimolecular function [69]. Nanoscale EM communication becomes an obvious choice due to the fact that molecular information for a human body is indeed sensitive in the THz regime. Additionally, this part of the spectrum is much safer to interact at a cellular scale that its counterparts in the microwave or gigahertz range [70]. The proposed in-vivo body nanonetworks ensures their stability without disturbing the harmony of in-built molecular structure of the body. Moreover, in most of the cases medicine fails to understand the root cause of the problem but once a monitoring network is established, one can extract various unknowns and treat them effectively.

For communication perspective, the THz Band channel is highly frequency selective and exhibits a unique distance-dependent bandwidth behaviour due to the absorption from mainly the content of biological medium, mainly water and related constituents [71]. In particular, the THz Band behaves as a single transmission window almost 10 THz wide for distances much below one meter. However, the lack of detailed database of biological medium limits the establishment of proper channel models for this communication scheme. Hence, the thesis will focus on various aspects of channel modelling such as noise and pathloss [20, 72].

Also, focus will be to characterize the biological medium and extract its electromagnetic properties.

1.3 Research Contributions

The experimental investigation of tissue optical properties, refractive index and absorption coefficient extracted using transfer function based algorithm are presented. Tissue morphology is explained in detail and validated with microscopic images. Emphasis has been given on the intricate biological features such as sweat duct cross-section and fibre distribution. The results are presented for the tissue sample which is rich in these biological features to help the reader in understanding the significance of in-depth study of tissue biology.

The samples are specifically studied for chronic dehydration and effects of water dynamics on THz frequencies using THz-time domain spectroscopy. The empirical values are then applied to numerically calculate the channel parameters for propagating THz wave in a dehydrated tissue. In chapter 4, experimental investigation of excised fresh skin tissue from different parts of the body (breast and abdomen) is done. The results highlight the differences between the absorption coefficient of different skin tissue and importance of water dynamics study inside the tissue. Also, results on variation in rotation angle of the sample holder are presented to demonstrate the variations in mechanical conformation of the tissue. The tissues are imaged using standard light microscopy, to highlight the complex layered structure with emphasis on the dermis part. The optical constants used for evaluation of channel parameters, provide an approximated in-vivo communication mechanism at short-range nanoscale level.

Further, artificial skin models are self-cultured as an alternative to excised human skin to study the intricate biological features influencing the molecular and morphological state of the skin. The results present the importance of analysing and generating a detailed data base on different layers of the skin. 2D collagen gels and 3D organotypics are artificially cultured with fibroblast and keratinocyte cell lines. Collagen gels made with fibroblast cell lines are representative of the dermis layer, hence any variation in cell number density of fibroblast, modify the optical properties and subsequently the channel parameters. Organotypics correspond to a more advanced layered structure of the skin and the results associated with its THz characterization are applied to evaluate channel parameters.

1.4 Thesis Outline

The presented thesis can be further divided into the following chapters.

- Chapter 2: In this chapter comprehensive background,definitions and models for nanocommunication is proposed. The highlight of this chapter is EM based nanocommunication working at THz band for in-body nanonetworks. This chapter discusses channel propagation models and introduction to parameters that effect the propagation of THz wave in free space. The same model is then applied to a real human skin and results for pathloss and noise temperature is presented. More details and extensive literature is provided on tissue dielectric behaviour from MHz to THz range of frequencies. Basic operation of THz Time Domain Spectroscopy (THz-TDS) in transmission geometry and its various performance features is introduced. Pulsed THz-TDS for tissue characterization and material parameter extraction algorithm is further discussed in detail.

- Chapter 3: This chapter presents the experimental work done on real skin tissue. The THz-time domain spectroscopy optical bench set-up and details of individual components are discussed. The optical parameters i.e refractive index and absorption coefficient values are compared to already published data and effect of water dynamics inside the tissue is discussed in detail. The empirical studies are made on dehydrated tissue and standard optical imaging is done to interest the reader with actual state of the tissue. Further, THz propagation channel characteristics are numerically evaluated to present the effects of dehydration of skin tissue.

- Chapter 4: This chapter provides experimental results on excised human skin from breast and abdomen part of the human body. A brief motivation is provided to highlight the importance of mapping human body in order to establish a universal nanonetwork communication channel. Tissue morphology is presented through optical microscopy images and channel parameters are evaluated. Angle-dependent THz time domain spectroscopy is also introduced to further reflect the complexity of communication inside the human body.

- Chapter 5: This chapter provide an introduction to artificial skin culture and characterization of collagen using THz time domain spectroscopy. Details about various biological parameters that could effect the communication mechanism of proposed nanonetworks is experimentally investigated and channel parameters are optimized for efficient short-range communication. Further, more complex artificial human skin tissue and comparative study of various layers of tissue is presented.

- Chapter 6: This chapter summaries the main contributions of research thereby, opening doors to further research on including intricate features of human tissue for in-body communication.

References

[1] James C Wiltse. History of millimeter and submillimeter waves. *IEEE Transactions on microwave theory and techniques*, 32(9):1118–1127, 1984.

[2] Huan-Bang Li, Kenichi Takizawa, and Ryuji Kohno. Trends and standardization of body area network (BAN) for medical healthcare. pages 1–4. IEEE, 2008.

[3] Qammer H Abbasi, Ke Yang, Nishtha Chopra, Josep Miquel Jornet, Najah Abed Abuali, Khalid A Qaraqe, and Akram Alomainy. Nano-Communication for Biomedical Applications: A Review on the State-of-the-Art From Physical Layers to Novel Networking Concepts. *IEEE Access*, 4:3920–3935, 2016.

[4] Kris Sangani. Knowledge Transfer For Medical Device Makers And Wearable Consumer Tech Companies. 2014.

[5] CS Pattichis, E Kyriacou, S Voskarides, MS Pattichis, Robert Istepanian, and Cl N Schizas. Wireless telemedicine systems: an overview. *IEEE Antennas and Propagation Magazine*, 44(2):143–153, 2002.

[6] Pantea Keikhosrokiani, Nasriah Zakaria, Norlia Mustaffa, Tat-Chee Wan, Muhammad Imran Sarwar, and Keyvan Azimi. Wireless networks in mobile healthcare. In *Mobile Health*, pages 687–726. Springer, 2015.

[7] Qammer H Abbasi, Khalid Qaraqe, Akram Alomainy, and Masood Ur Rehman. Advances in body-centric wireless communication. 2016.

[8] Maulin Patel and Jianfeng Wang. Applications, challenges, and prospective in emerging body area networking technologies. *IEEE Wireless communications*, 17(1), 2010.

[9] J Laskar, S Pinel, D Dawn, S Sarkar, B Perumana, and P Sen. The next wireless wave is a millimeter wave. *Microwave Journal*, 50(8):22, 2007.

[10] Jonathan Schepps and Arye Rosen. Microwave industry outlook-wireless communications in healthcare. *IEEE Transactions on Microwave Theory and Techniques*, 50(3):1044–1045, 2002.

[11] Harmon Eyre, Richard Kahn, Rose Marie Robertson, Nathaniel G Clark, Colleen Doyle, Yuling Hong, Ted Gansler, Thomas Glynn, Robert A Smith, and Kathryn Taubert. Preventing cancer, cardiovascular disease, and diabetes. *Circulation*, 109(25):3244–3255, 2004.

[12] John E Ferguson and A David Redish. Wireless communication with implanted medical devices using the conductive properties of the body. *Expert review of medical devices*, 8(4):427–433, 2011.

[13] Eric Y Chow, Milton M Morris, and Pedro P Irazoqui. Implantable RF medical devices: The benefits of high-speed communication and much greater communication distances in biomedical applications. *IEEE Microwave Magazine*, 14(4):64–73, 2013.

[14] Todd K Whitehurst, James P Mcgivern, and Rafael Carbunaru. Methods for treating gastrointestinal disorders. May 2013.

[15] Ian F Akyildiz, Fernando Brunetti, and Cristina Blázquez. Nanonetworks: A new communication paradigm. *Computer Networks*, 52(12):2260–2279, 2008.

[16] Ian F Akyildiz and Josep Miquel Jornet. Electromagnetic wireless nanosensor networks. *Nano Communication Networks*, 1(1):3–19, 2010.

[17] A Peyman, AA Rezazadeh, and C Gabriel. Changes in the dielectric properties of rat tissue as a function of age at microwave frequencies. *Physics in Medicine and Biology*, 46(6):1617, 2001.

[18] S Gabriel, RW Lau, and Camelia Gabriel. The dielectric properties of biological tissues: II. Measurements in the frequency range 10 Hz to 20 GHz. *Physics in medicine and biology*, 41(11):2251, 1996.

[19] Giuseppe Piro, Ke Yang, Gennaro Boggia, Nishtha Chopra, Luigi Alfredo Grieco, and Akram Alomainy. Terahertz communications in human tissues at the nano-scale for healthcare applications. *IEEE Transactions on Nanotechnology*, 14(3):404–406, 2015.

[20] Josep Miquel Jornet and Ian F Akyildiz. Channel modeling and capacity analysis for electromagnetic wireless nanonetworks in the terahertz band. *IEEE Transactions on Wireless Communications*, 10(10):3211–3221, 2011.

[21] Ian Akyildiz, Josep Jornet, and Chong Han. TeraNets: ultra-broadband communication networks in the terahertz band. *IEEE Wireless Communications*, 21(4):130–135, 2014.

[22] Vincent P Wallace, Anthony J Fitzgerald, Emma Pickwell, Richard J Pye, Philip F Taday, Niamh Flanagan, and Thomas Ha. Terahertz pulsed spectroscopy of human basal cell carcinoma. *Applied spectroscopy*, 60(10):1127–1133, 2006.

[23] AJ Fitzgerald, E Berry, NN Zinov'ev, S Homer-Vanniasinkam, RE Miles, JM Chamberlain, and MA Smith. Catalogue of human tissue optical properties at terahertz frequencies. *Journal of Biological Physics*, 29(2):123–128, 2003.

[24] SW Smye, JM Chamberlain, AJ Fitzgerald, and E Berry. The interaction between terahertz radiation and biological tissue. *Physics in medicine and biology*, 46(9):R101, 2001.

[25] Elizabeth Berry, Anthony J Fitzgerald, Nickolay N Zinov'ev, Gillian C Walker, Shervanthi Homer-Vanniasinkam, Caroline D Sudworth, Robert E Miles, J Martyn Chamberlain, and Michael A Smith. Optical properties of tissue measured using terahertz-pulsed imaging. pages 459–470. International Society for Optics and Photonics, 2003.

[26] Andre K Geim and Konstantin S Novoselov. The rise of graphene. *Nature materials*, 6(3):183–191, 2007.

[27] Q Ashton Acton. *Advances in Molecular Nanotechnology Research and Application: 2012 Edition*. ScholarlyEditions, 2012.

[28] He Shen, Liming Zhang, Min Liu, and Zhijun Zhang. Biomedical Applications of Graphene. *Theranostics*, 2(3):283–294, 2012.

[29] Sixiang Shi, Feng Chen, Emily B Ehlerding, and Weibo Cai. Surface engineering of graphene-based nanomaterials for biomedical applications. *Bioconjugate chemistry*, 25(9):1609–1619, 2014.

[30] Gianni Ciofani, Vittoria Raffa, Orazio Vittorio, Alfred Cuschieri, Tommaso Pizzorusso, Mario Costa, and Giuseppe Bardi. In vitro and in vivo biocompatibility testing of functionalized carbon nanotubes. *Carbon Nanotubes: Methods and Protocols*, pages 67–83, 2010.

[31] Stephen F. Bush. Toward in vivo nanoscale communication networks: utilizing an active network architecture. *Frontiers of Computer Science in China*, 5(3):316, 2011.

[32] G Enrico Santagati and Tommaso Melodia. Opto-ultrasonic communications for wireless intra-body nanonetworks. *Nano Communication Networks*, 5(1):3–14, 2014.

[33] Stephen F Bush. *Nanoscale Communication Networks*. Artech House, 2010.

[34] K Eric Drexler. *Nanosystems: molecular machinery, manufacturing, and computation*. John Wiley & Sons, Inc., 1992.

[35] Ralphc Merkle. Self replicating systems and molecular manufacturing. *British Interplanetary Society, Journal*, 45(10):407–413, 1992.

[36] Nobutaka Hirokawa, Shinsuke Niwa, and Yosuke Tanaka. Molecular motors in neurons: transport mechanisms and roles in brain function, development, and disease. *Neuron*, 68(4):610–638, 2010.

[37] Anita Goel and Viola Vogel. Harnessing biological motors to engineer systems for nanoscale transport and assembly. *Nat Nano*, 3(8):465–475, August 2008.

[38] Neus Roca Lacasa. Modeling the molecular communication nanonetworks. 2009.

[39] Bhalachandra L Tembre and J Andrew Mc Cammon. Ligand-receptor interactions. *Computers & Chemistry*, 8(4):281–283, 1984.

[40] James R Baker, Antonio Quintana, Lars Piehler, Mark Banazak-Holl, Donald Tomalia, and Ewa Raczka. The synthesis and testing of anti-cancer therapeutic nanodevices. *Biomedical Microdevices*, 3(1):61–69, 2001.

[41] Wei Lu, Marites P Melancon, Chiyi Xiong, Qian Huang, Andrew Elliott, Shaoli Song, Rui Zhang, Leo G Flores, Juri G Gelovani, and Lihong V Wang. Effects of photoacoustic imaging and photothermal ablation therapy mediated by targeted hollow gold nanospheres in an orthotopic mouse xenograft model of glioma. *Cancer research*, 71(19):6116–6121, 2011.

[42] Laura Galluccio, Sergio Palazzo, and G Enrico Santagati. Characterization of molecular communications among implantable biomedical neuro-inspired nanodevices. *Nano Communication Networks*, 4(2):53–64, 2013.

[43] James D Hamilton, Takashi Buma, Monica Spisar, and Matthew O'Donnell. High frequency optoacoustic arrays using etalon detection. *IEEE transactions on ultrasonics, ferroelectrics, and frequency control*, 47(1):160–169, 2000.

[44] Norman Hodgson and Horst Weber. *Optical resonators: fundamentals, advanced concepts, applications*, volume 108. Springer Science & Business Media, 2005.

[45] Armen P Sarvazyan, Matthew W Urban, and James F Greenleaf. Acoustic waves in medical imaging and diagnostics. *Ultrasound in medicine & biology*, 39(7):1133–1146, 2013.

[46] Tad Hogg and Robert A Freitas Jr. Acoustic communication for medical nanorobots. *Nano Communication Networks*, 3(2):83–102, 2012.

[47] Tommaso Melodia, Hovannes Kulhandjian, Li-Chung Kuo, and Emrecan Demirors. Advances in underwater acoustic networking. *Mobile Ad Hoc Networking: Cutting Edge Directions*, 852, 2013.

[48] John M Reid. Medical ultrasonics: Diagnostic applications of ultrasound. *Proceedings of the IRE*, 47(11):1963–1967, 1959.

[49] RP Beardsley, AV Akimov, M Henini, and AJ Kent. Coherent terahertz sound amplification and spectral line narrowing in a stark ladder superlattice. *Physical review letters*, 104(8):085501, 2010.

[50] S Boisseau, G Despesse, and B Ahmed Seddik. Electrostatic conversion for vibration energy harvesting. *arXiv preprint arXiv:1210.5191*, 2012.

[51] Frieder H Loesel, Markolf H Niemz, JF Bille, and T Juhasz. Laser-induced optical breakdown on hard and soft tissues and its dependence on the pulse duration: experiment and model. *IEEE Journal of Quantum Electronics*, 32(10):1717–1722, 1996.

[52] Markus W Sigrist and Fritz K Kneubühl. Laser-generated stress waves in liquids. *The Journal of the Acoustical Society of America*, 64(6):1652–1663, 1978.

[53] Takashi Buma, Yang Hou, Sheng-Wen Huang, Shai Ashkenazi, and Matt O ,ÄôDonnell. High frequency optoacoustic transducers for ultrasonic and photoacoustic imaging. In *Photoacoustic Imaging and Spectroscopy*, pages 223–238. CRC Press, 2009.

[54] Ekmel Ozbay. Plasmonics: merging photonics and electronics at nanoscale dimensions. *science*, 311(5758):189–193, 2006.

[55] Josep Miquel Jornet and Ian F Akyildiz. Graphene-based nano-antennas for electromagnetic nanocommunications in the terahertz band. pages 1–5. IEEE, 2010.

[56] Ignacio Llatser, Christian Kremers, Albert Cabellos-Aparicio, Eduard Alarco´ n, Dmitry N Chigrin, and Dmitry N Chigrin. Comparison of the resonant frequency in graphene and metallic nano-antennas. volume 1475, page 143, 2012.

[57] Derya Malak and Ozgur B Akan. Molecular communication nanonetworks inside human body. *Nano Communication Networks*, 3(1):19–35, 2012.

[58] Bartosz A Grzybowski and Wilhelm TS Huck. The nanotechnology of life-inspired systems. *Nature Nanotechnology*, 11(7):585–592, 2016.

[59] LA Ponomarenko, F Schedin, MI Katsnelson, R Yang, EW Hill, KS Novoselov, and AK Geim. Chaotic Dirac billiard in graphene quantum dots. *Science*, 320(5874):356–358, 2008.

[60] Fride Vullum and Dale Teeters. Investigation of lithium battery nanoelectrode arrays and their component nanobatteries. *Journal of Power Sources*, 146(1):804–808, 2005.

[61] Fride Vullum, Dale Teeters, Anton Nytén, and Josh Thomas. Characterization of lithium nanobatteries and lithium battery nanoelectrode arrays that benefit from nanostructure and molecular self-assembly. *Solid State Ionics*, 177(26):2833–2838, 2006.

[62] Chunyu Li, Erik T Thostenson, and Tsu-Wei Chou. Sensors and actuators based on carbon nanotubes and their composites: a review. *Composites Science and Technology*, 68(6):1227–1249, 2008.

[63] Josep Miquel Jornet and Ian F Akyildiz. Graphene-based nano-antennas for electromagnetic nanocommunications in the terahertz band. pages 1–5. IEEE, 2010.

[64] Sasitharan Balasubramaniam and Jussi Kangasharju. Realizing the internet of nano things: challenges, solutions, and applications. *Computer*, 46(2):62–68, 2013.

[65] Tadashi Nakano, Michael Moore, Akihiro Enomoto, and Tatsuya Suda. Molecular communication technology as a biological ICT. In *Biological functions for information and communication technologies*, pages 49–86. Springer, 2011.

[66] Nariman Farsad, Weisi Guo, and Andrew W Eckford. Tabletop molecular communication: Text messages through chemical signals. *PloS one*, 8(12):e82935, 2013.

[67] Carter M Armstrong. The truth about terahertz. *IEEE Spectrum*, 49(9), 2012.

[68] Ashish Y Pawar, Deepak D Sonawane, Kiran B Erande, and Deelip V Derle. Terahertz technology and its applications. *Drug invention today*, 5(2):157–163, 2013.

[69] Andrea G Markelz. Terahertz dielectric sensitivity to biomolecular structure and function. *IEEE Journal of Selected Topics in Quantum Electronics*, 14(1):180–190, 2008.

[70] GP Gallerano. Tera–Hertz radiation in Biological Research, Investigations on Diagnostics and study on potential Genotoxic Effects–THz-BRIDGE–Final Report. Technical report, QLK4–CT–2000–00129, 2004.

[71] Pavel Boronin, Vitaly Petrov, Dmitri Moltchanov, Yevgeni Koucheryavy, and Josep Miquel Jornet. Capacity and throughput analysis of nanoscale machine communication through transparency windows in the terahertz band. *Nano Communication Networks*, 5(3):72–82, 2014.

[72] Ke Yang, Alice Pellegrini, Max O Munoz, Alessio Brizzi, Akram Alomainy, and Yang Hao. Numerical analysis and characterization of THz propagation channel for body-centric nano-communications. *IEEE Transactions on Terahertz Science and Technology*, 5(3):419–426, 2015.

Chapter 2

Background and Literature Review

This chapter explores the properties and applications of THz radiation in various facets of research. As the background and literature proceeds, more emphasis is given on THz communication in free space, in-body communication channel parameters and knowledge of biological medium. Theory involved in channel parameters: pathloss and molecular noise temperature is discussed in detail. The basics on electromagnetic wave interaction with biological samples is provided. A brief literature review on various dielectric measurement techniques and its applications is provided covering frequencies from microwave to terahertz. The aim of this chapter is to provide the preliminaries of short-range nanocommunication, THz skin tissue characterization and in-body channel parameters.

2.1 Terahertz Radiation Properties and Applications

The terahertz (THz) region of the electromagnetic(EM) spectrum or T-rays, bridges the gap between the microwave and infrared domain, spanning from 0.1-10THz [1]. The unexplored region is now flooded with effective methods of generating and detecting THz waves [2]. Hence, there has been recent surge of application in biomedical imaging, pharmacy, security, astronomy and very recently material characterization with the help of THz-Time Domain Spectroscopy (THz-TDS) [3–7]. The Terahertz (THz) region of the electromagnetic spectrum has been of wide interest in the past few years. It is estimated that approximately 98% of the photons in the universe lie in the submillimetre and far-IR frequency range [8]. It has clearly established its niche as a potential technology aiming to unfold mysteries in the engineering and medical domain. It is crowded by innumerable spectral features associated with fundamental physical processes such as rotational transitions of molecules, large-amplitude vibrational motions of organic compounds, lattice vibrations in solids, interband transitions in semiconductors [9].

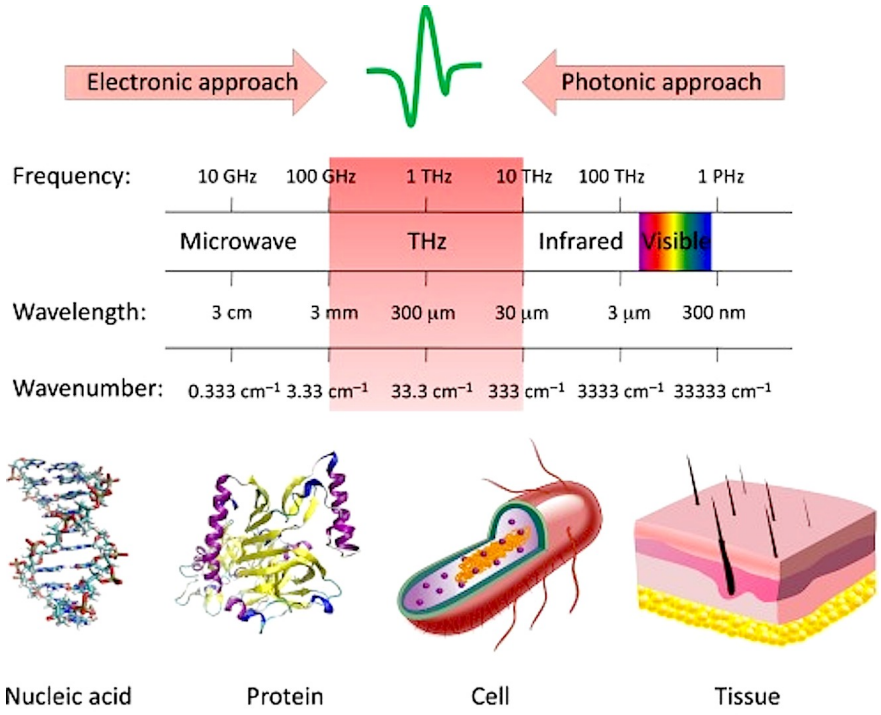

Fig. 2.1 The exploration of THz region from 100GHz to 10THz encompassing the biological spectrum from biomolecules to heterogeneous complex mammalian tissue [10]

Table 2.1 Properties of THz radiation

Attributes of THz wave	Mathematical Relation-ship	Quantitative Values
Wavelength	λ=c/f	0.3mm=300μm
Period	τ=1/f	$10^{-}12s$ = 1ps
Photon Energy	E=hf	4.14meV

T-rays are primarily used for identification of molecules and compounds, to screen explosives, drugs, weapons etc. [11]. In general, non-polar, dry, and non-metallic materials are transparent or translucent to T-ray radiation [12]. They can provide supplementary information on the sample, mainly for low density materials, chemical specifications and liquid explosives. Several liquids show very different dielectric response in the terahertz range versus their alcohol percentage for example and can thus be distinguished. THz waves can penetrate cloth, plastic, paper and other non-metallic and dry materials and, thus, provide the possibility to identify the explosives behind non-optically transparent covers. The identification can be performed either in transmission and reflection geometry. THz spectroscopy has been used to determine the carrier concentration and mobility of

doped semiconductors such as GaAs and silicon wafers [13]. Intermolecular vibrations transitions of polar molecules for both solid or liquid state made T-rays beneficial for material characterization [14], whereas polar molecules in the gas phase have their rotational transition energies spanning the microwave and T-ray frequencies [15].

In the pharmaceutical industry, T-rays have been used to study polymorphisms and chiral symmetry in drug compounds. In particular, THz TDS has been used to study polymorphisms and chiral symmetry in drug compounds [11]. Since different isomers lead to crystalline structures with varying spectra fingerprints in the THz range, polymorphic forms can be detected. Different polymorphs and chiral symmetry have an impact on the effectivity and toxicity of a drug. THz is well suited for quality control of tablet coatings that are used to control the release of active pharmaceutical ingredients. THz TDS has also been used to study phase transitions between different molecular configurations as a function of temperature and humidity [16].

THz waves have been used in imaging and spectroscopy for the diagnosis of diseased tissues, dental implants, hydration of leaves [17, 18]. The optical properties of liquids in the THz range mainly depend on the interaction and the relaxation of dipoles inside the liquid. These dipoles can be permanent dipoles in polar liquids or dipoles induced in non-polar liquids [18]. Hydrogen bonding can also have a significant effect on the THz response. Reorientation of dipoles in liquids on a picosecond (ps) time scale is essential for both chemical reactions and biological functions [19].

Recently introduced for ultra-broadband communication [20], THz waves are being investigated for short-range indoor communication [21], graphene-based antennas [22] and in-body nanonetworks [23, 24]. The microwave and gigahertz region of the EM spectrum provides a wide coverage to communication technologies. With the invention of new electronic materials and devices, number of users of wireless communication has significantly increased. Moreover, users are consuming much more digital information with mobile devices than they did with stationary personal computers connected to the wired network. The trend of achieving high data capacity wireless communications has been improved over the last a couple of decades [25]. In pursuit of never ending need for faster information exchange, THz waves has recently joined the realms of wireless communication.

2.2 Short-Range Terahertz Communication in Free-Space

With scarcity of available bandwidth limiting the achievable data rates in the GHz domain [26], the popularity of short-range broad-bandwidth THz communication with numerous medical applications is bringing the era of new wireless communication mechanism [27].

Most of the present effort towards higher data rates is aimed at enhancing the spectral efficiency of existing or currently developing microwave and millimetre-wave wireless systems. However, the spectral bandwidth of such systems is limited, and they will not be able to support data rates exceeding a few Gbps. In the long run, there is no alternative but to turn towards higher carrier frequencies [28]. THz frequencies offer large bandwidth and is unregulated, hence becomes an obvious choice for developing future communication systems [29]. It has been used mainly for space and astronomy applications, operating at cryogenic (120 K) temperatures for the detectors. Such devices can be physically large and have a cost in terms of logistics and high implementation [8]. With its ability to characterize the biological features, either by reflection or transmission geometry, THz-TDS has motivated towards cheaper, room-temperature components, and opened doors to many applications for wireless communication. THz communication is still in its infancy not only due to the lack of portable electronics and also its propagation constraints. When propagating, electromagnetic waves suffer from spreading of the energy, as well as from clear-air atmospheric and adverse weather conditions [30].

According to Friss transmission formula ($\frac{P_r}{P_e} = G_e.G_r\frac{\lambda}{4\pi.R}^2$), as the wave propagates, the final power received after free-space attenuation is proportional to square of wavelength and inversely proportional to the distance travelled [31]. In simplified terms, it relates the power received to the power transmitted between two antennas separated in space. Hence, if communicating within a distance of 10m and frequency between 300 GHz and 1 THz, the attenuation is approximately between 102 dB and 112 dB. Frequencies above 300 GHz are currently unallocated by the Federal Communications Commission [21]. The frequencies above this range, labelled as the THz domain could be utilized for novel applications communicating within a limited range. The limitation in distance is due to strong molecular absorption of these frequencies through the atmosphere (Fig. 2.2) caused by water vapour. The attenuation level in the frequency windows may not be a big problem for indoor applications, where the range is likely to be a few ten meters or less. Consequently, THz waves experience much less scattering loss caused by molecules as opposed to optical frequencies and can be used for short distances even if heavy particulates due to smoke or dust are present in the air [32].

From the current state of wireless communication research, it seems that THz frequencies are well suited for short range data exchange at a macro-scale. In the same line of work, THz communication has been proposed at nano-scale level for healthcare monitoring applications [23, 33]. Nanotechnology is enabling the development of devices on a scale ranging from one to a few hundred nanometres. At this scale, a nanomachine is defined as the most basic functional unit, integrated by nano-components and able to perform simple tasks such as sensing or actuation. Coordination and information sharing among several nanomachines

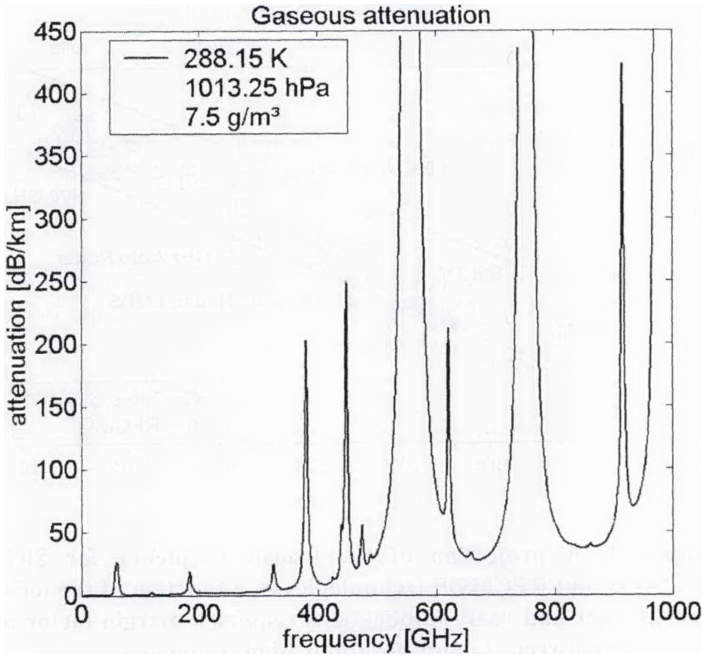

(a) Atmospheric attenuation for THz frequencies

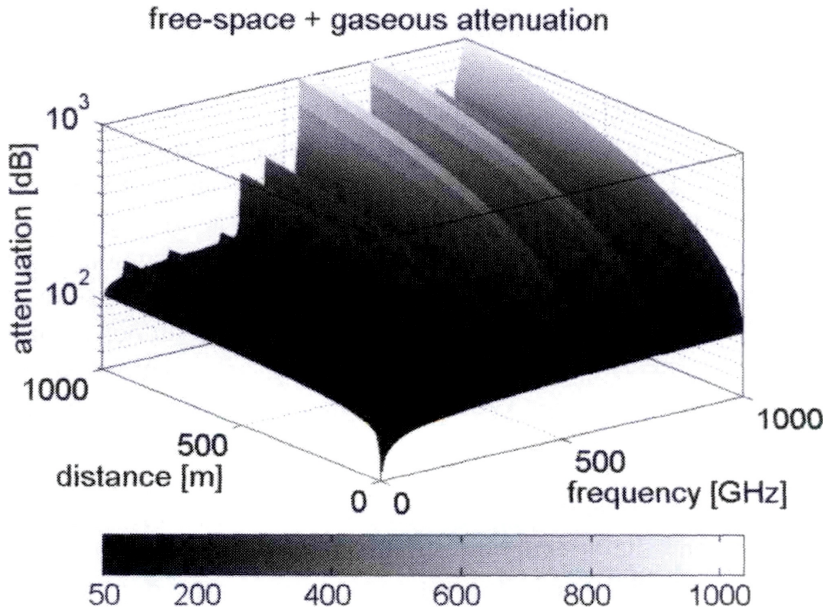

(b) Attenuation dependent on frequency and distance

Fig. 2.2 The attenuation values due to molecular absorption can reach hundreds of dB/km, but there are also a few frequency windows where the attenuation is below or near 60 dB/km [21]

will expand the potential applications of individual devices both in terms of complexity and range of operation. The resulting nanonetworks will be able to cover larger areas, to reach unprecedented locations in a non-invasive way, and to perform additional in-network processing. Moreover, the interconnection of nanoscale devices with classical net- works and ultimately the Internet defines a new networking paradigm, to which we further refer as the Internet of Nano-Things.

2.2.1 THz Communication for In-Body Nanonetworks

In-body nanonetworks are an extension to wireless body area networks (WBAN) [34], blending the two technologies with communication capabilities stretching from micro to macro scale. Recent publications in nanoscale communication, had led to development of a common framework, under the umbrella of IEEE Std 1906.1. This standard enables research and development in medical diagnostics area by focusing industry and academia on a common conceptual model, common language, and nomenclature for nanoscale communications. According to the standard, the communication mechanism for a nanodevice falls in the category of electromagnetic communication. A network of these devices is envisioned to monitor vitals of the human body such as blood pressure, glucose level etc., along with an ability to diagnose chronic health conditions. These sensors can be physically distributed around the body keeping in mind the heterogeneity of medium and work in harmony towards elevating healthcare.

The wireless technologies used to transmit information to and from the devices are crucial because they determine one of the most important aspect of communication i.e. the bandwidth available on the network. Bandwidth enables how much data can be transmitted per second. For wireless EM based nanonetworks, the range is from 0.1 – 10 THz, thereby offering a large bandwidth. This section aims to apprise the reader with THz channel parameters and performance metric essential to determine the feasibility of nanonetworks. Quantum effects cause the wave propagation at the nanoscale, which differ significantly from traditional schema. These quantum effects are due to the regular atomic structure of the nanomaterials and in the molecular composition of the transmission medium [35]. The THz band has been proposed for Ultra-broadband communication in some of recent articles [26]. The essential point to carry forward is that THz band is more likely to be suitable for short-range communication especially when the medium is lossy. To utilize the THz bandwidth keeping in mind the transmission medium, it is necessary to alter the concepts of molecular absorption, total pathloss and molecular absorption noise [36]. In this section, the aim is to review existing channel parameters for free-space with molecular variation and proposed computational skin model for in-body THz communication. Some of the key

aspects to look for are molecular absorption loss and noise due to lossy biological medium of communication. The THz (or nanoscale) communication channel is affected by two parameters: pathloss and molecular noise temperature.

The total pathloss for a travelling wave in the Terahertz band is dependent on signal frequency, transmission distance and molecular composition of the channel. It accounts for both spreading loss and molecular absorption loss. Spreading loss is the attenuation of wave when it expands while propagating through the medium whereas molecular absorption loss involves a process by which part of the wave energy is converted into internal kinetic energy of the excited molecules in the medium. Absorption from a particular molecule is not confined to a single frequency but is spread over a range of frequency [36, 37]. Hence, Molecular absorption makes the THz range highly frequency selective. In addition to this, scattering from nanoparticles and multipath propagation can affect the signal strength at the receiver [33]. The total path loss dependent on frequency and distance $A(f,d)$, for a travelling THz wave can be described as [24, 38]:

$$A(f,d)(dB) = A_{spread}(f,d) + A_{abs}(f,d) \tag{1}$$

where, f stands for frequency and d is the path length measured in metres (m). However, results presented in this thesis are calculated by fixing the path length same as the thickness of sample to be measured by THz-TDS. Hence, the thickness and path length are in millimetre (mm).

The total pathloss accounts for spreading loss, A_{spread} and molecular absorption loss, A_{abs}. As the wave propagated through the medium, it expands and results in attenuation. Hence, the spreading loss, A_{spread} can be defined as:

$$A_{spread}(f,d) = 20\log\frac{4\pi fd}{c} \tag{1a}$$

c is the speed of light

Another factor causing attenuating of THz wave is molecular absorption and depends on the concentration of channel medium. It is defined as,

$$A_{abs}(f,d) = 10\log\frac{1}{\tau(f,d)} \tag{1b}$$

where τ is the transmittance of the medium.

The factor transmittance is given by Beer-Lamberts Law [36]. It accounts for losses due to absorption coefficient as the wave propagated in a medium.

$$\tau(f,d) = \exp^{-\alpha fd} \tag{2}$$

where α is the absorption coefficient in cm^{-1}. The unit is following a standard convention of representing absorption coefficient, when measuring the samples by THz-TDS. This will help the reader to compare the data easily with other literature, without the use of conversion.

Molecular absorption does not only attenuate the transmitted signal, but it also introduces noise, termed as Molecular noise. The important parameter to measure noise is emissivity of channel. When referring radio astronomy, noise temperature is the signal-to-noise degradation of receiving system of thermal origin. To compute the equivalent noise temperature at the receiver, it is important to define the transmission bandwidth that depends on the transmission distance and the composition of the medium. Each type of molecule will have different resonant frequency; hence the power spectral density of noise has several peaks. Moreover, this type of noise only appears when transmitting, i.e. there will be no noise unless the channel is being used [36]. To compute the equivalent noise temperature at the receiver it is important to define the transmission bandwidth that depends on the transmission distance and the composition of the medium. The parameter that measures this phenomenon is the emissivity of the channel defines as:

$$\xi(f,d) = 1 - \tau(f,d) \tag{3}$$

where f is the frequency , d is the total path length and τ is the transmissivity of the medium

The main contributing factor to total noise is T_{mol}. Since the working frequency is in THz range, molecular absorption is considerably high specially if the path length has water molecules. Thus, the equivalent noise temperature (in Kelvin) due to molecular absorption is given by:

$$T_{mol}(f,d) = T_{\circ}\xi(f,d) \tag{4}$$

where, $T_{\circ}$ is the reference temperature

The total noise power is given by:

$$P_n(f,d) = K_B(T_{mol}(f,d)) + T_{electronic}(f)) \tag{5}$$

where, K_B is the Boltzmann constant

The electronic noise temperature ($T_{electronic}$) of the system is assumed to be low due to the electron transport properties of graphene [39], the main factor affecting the channel performance will be the molecular absorption noise temperature, which indicates $T_{electronic} \equiv T_{mol}$. The above equations have been used to evaluate the influence of molecular absorption noise and pathloss using HITRAN (high-temperature spectroscopic absorption parameters)

database and radiative transfer theory [40] on propagation of THz wave in freespace. The results highlight one of the attributes of THz band as being very frequency selective. The free space comprises of water and oxygen molecules, hence the channel parameters as described by equation 1 and 4 are represented as a function of distance and frequency in figure 2.3 and 2.4.

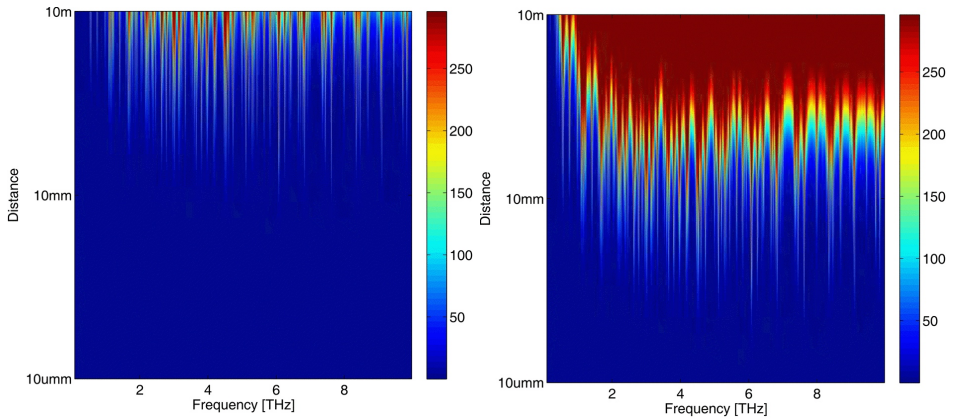

(a) 0.1% water vapour (b) 10% water vapour

Fig. 2.3 Molecular absorption noise temperature (kelvin,K) as THz wave propagate through the atmosphere with varying water vapour concentrations[36]

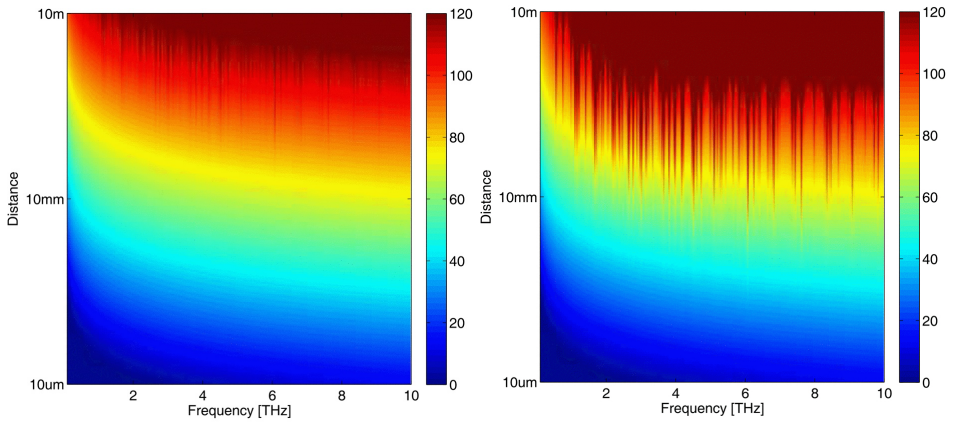

(a) 0.1% water vapour (b) 10% water vapour

Fig. 2.4 THz wave pathloss through the atmosphere. A comparison of THz propagation losses is provided if the the humidity or water vapour concentration is increased from 0.1% to 10% [36]

For a simple free space propagation with less complexity as compared to human skin, the channel parameters are significantly affected by the variation in water vapour percentage. The attenuation and noise further increases with distance and frequency, hence the working frequency range is only suitable for a few millimetre of distance. Further, to realize the

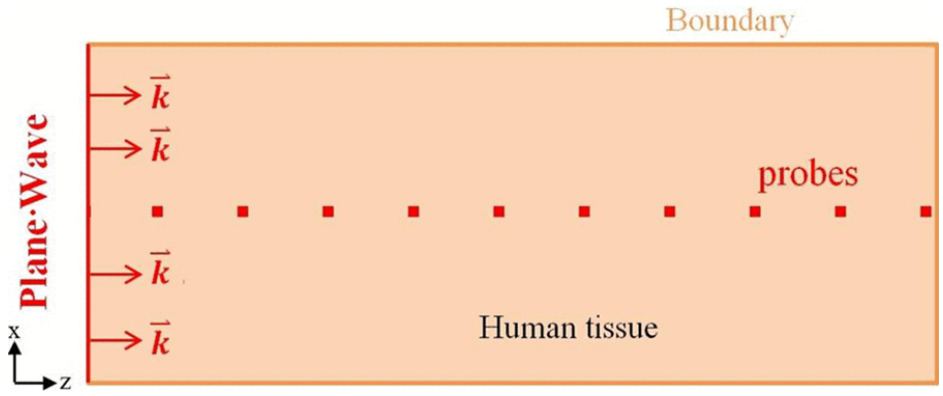

Fig. 2.5 A Homogeneous model of human skin is numerically simulated in CST Microwave Studio using a dielectric cube of mm^3 dimension. The varying electric field is monitored by equally spaced probes, where the wave is propagating in +z direction and electric field is in +x direction [24]

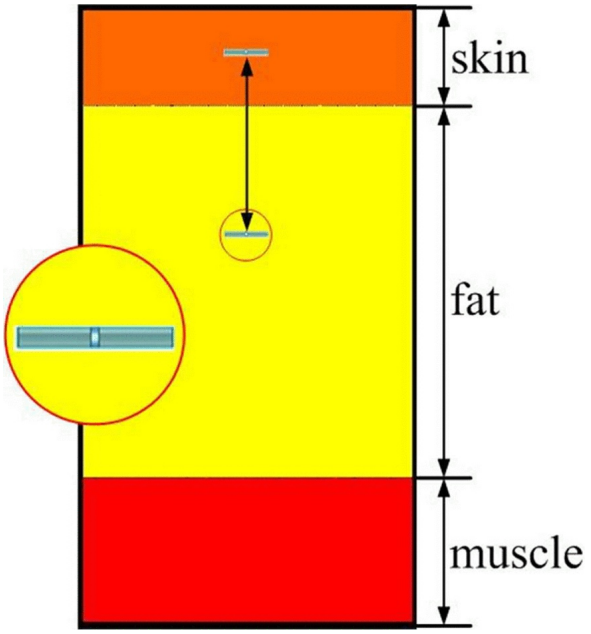

Fig. 2.6 Three layer tissue model representing skin, fat and muscle. The two dipoles are vertically located; one in skin and the other in fat [24]

feasibility of in-body nanonetworks, a homogeneous skin tissue and a three layer skin model (Fig.2.5 and 2.6) has also been proposed by incorporating the permittivity values skin in the THz domain. It was highlighted that at a millimetre distance, the path loss of the skin is around 90 dB and power loss caused by the interface (layered model) was minimum. Similarly, molecular noise temperature was evaluated to be 310 K [24]. Although these models do provide an understanding of communication mechanism inside the human body, there is still a need to map the complexity of skin properties in the THz domain with actual measurements. For instance, the effects of hydration, dehydration, molecular variation and characterization of individual skin layer. The subsequent section focuses on spectroscopy device set-up and extraction of tissue material properties in a THz domain.

2.3 Literature Review on Tissue Characterization for GHz-THz Frequencies

The motivation to nanoscale communication stems from the fact that THz radiation is sensitive to the biological medium and can sense unique spectral features. Health diagnosis has always been a field of exploration and in need of urgent development. Paragons of engineering marvels such as EEG, ECG, and Pacemaker etc.[41] have made health diagnose plausible. The present state of art for medical devices, however fails to provide a detailed analysis of human body hence the overall application and operation of such devices is limited. Till date, the dielectric properties for biological material have been restricted to MHz or GHz of range[42–45]. The initial motive to carry such studies was the stimulative increase in exposure of people to EM fields from wireless telecommunication and infrastructure. At the same time, the human body information gathered in this process was further use to model medical devices operative for diagnosing, monitoring and treating the diseases. Depending on the range of frequencies, the refractive index spectrum of biological tissues decreases with increasing frequency and can be divided into three main regions: α, β and γ dispersions occurring at low, intermediate and high frequencies from some KHz to GHz [46–48].

Nevertheless it would be interesting to note from the early literature that tissue water content significantly affects the material parameters. Human body is a complex mixture of tissue layers, blood, water, cells, proteins, DNA etc. However, to understand these properties, it is quite important to understand the basic structure, physiology and biological constitutes, skin layers and hydration. This section aims to concentrate on these parts with initial focus on skin layers. The electromagnetic (EM) material properties are defined by refractive index and absorption together. To understand the material properties of various tissues in

general, their nature can be discriminated into polar and non-polar molecules. Propagation of electromagnetic waves in materials such as dielectrics and conductors is determined by their electrical parameters [49]. The dielectric response of many polar liquids such as water, ethanol and acetone varies according to the strength of molecular dipoles and the density of dipole moments [50]. When an EM wave is propagated through a medium it will have two components: induce currents of free charges and dipole Moment resulting in re-orientation of linked charges. Earlier characterization techniques reported [46, 51, 52]were based on contact probe technique, which calculates the reflection coefficient using network analyser. For frequencies, from around 100 KHz to 100 MHz there are large changes in dielectric properties associated with the resistive nature of cell membranes. At frequencies above 100 MHz, differences between tissue types are largely lost, and at all frequencies the dielectric properties are directly associated with the tissue water content.

2.3.1 Electromagnetic Wave Behaviour in Lossy Biological Medium

A lot of differences exist for electrical properties of biological materials. These differences are determined, to a large extent, by the fluid content of the material. For example, blood and brain conduct electric current relatively well. Lungs, skin, fat, and bone are relatively poor conductors. Liver, spleen, and muscle are intermediate in their conductivities. The behaviour of biological tissues at RF and microwave frequencies is largely determined by the electro-chemical behaviour of cells and its cellular structure as well as the intra-cellular fluid in which the cells are suspended and the internal cellular materials, including the nucleus [48].

In case of a cell membrane the electrical phenomena are governed by capacitance effect and building of potential difference across it. At low frequencies (few KHz to MHz) current flows around the cells but at higher frequencies current flow may penetrate the cells. The application of an electric field within a medium causes a displacement of charge whose kinematics give rise to a frequency dependence of its bulk dielectric properties. For heterogeneous materials such as biological tissues, polarization at the interfaces is established and then decay away in time. A comprehensive review of this topic is given by Foster and Schwan [53]. There has been extensive research on various biological samples but our initial interest lies in skin tissues [54]. This section will cover most of the biological material measured so far from MHz to THz of range.

Electrical properties of a material are a measure of its ability to interact with electromagnetic energy. As this interaction results from the presence of biological entities within the material that can be affected by the electric force generated by the electromagnetic (EM) fields, a material's electrical properties are a direct consequence of its composition and

structure. Radio-frequency exposure of biological systems is usually specified in terms of physical characteristics as modulation (continuous wave or pulsed) and incident electric-field strength, incident power density, source frequency, type and zone of exposure (near or far field), and duration of exposure. The coupling of RF energy into biological systems may be quantified by the induced electric fields, power deposition, energy absorption, and the distribution and penetration into biological tissues. These quantities are all functions of its relationship to the physical configuration and dimension of the biological body [55].

An electric field results from a potential difference supported across a medium and is therefore not possible within a pure conductor. Free space has dielectric properties by virtue of the energy temporarily borrowed to create short lived virtual charges to support an electric field. Many other dielectrics exhibit phenomena which also contribute to their permittivity such as the ability to support current flow (both ionic and displacement currents) and molecular polarisation. It is normal to refer to the relative permittivity,

$$\varepsilon = \varepsilon_r * \varepsilon_0 \tag{6}$$

Where, ε_r is the relative permittivity of a material with respect to free space permittivity, ε_0. The relative permittivity of a dielectric is defined as the factor by which the capacitance of a capacitor increases when the volume between and around its plates is filled with the dielectric as compared with free space. It is known that the permittivity of a dielectric is determined by its molecular/atomic structure but no theory exists to relate the two. It is also known that permittivity is often frequency and temperature dependent, since certain phenomena which determine its permittivity are functions of frequency and temperature [56]. Furthermore, the permittivity differs for the various phases of the material which is unsurprising since the concentration of particles and their bonding differs in each phase. Various theories have been proposed to describe the permittivity of mixed dielectrics from its constituent ingredients, concentration and particle size and shape. These have been useful in describing the behaviour of solutions, suspensions and complex structures of dielectrics [57].

In non-magnetic materials such as biological tissues, an EM field primarily acts upon entities within the material that possess a net electric charge and an electric dipole moment. Polar molecules are the main source of electric dipole moments in tissues and are the additional sources. Polar molecules such as water and other biological entities such as protein structures, can translate and rotate in response to an applied sinusoidal electric field. The translation and rotation is impeded by inertia and by viscous forces. Since reorientation of polar molecules does not occur instantaneously, this gives rise to a time-dependent behaviour known as the relaxation process in biological tissues. Under the influence of RF electric

fields at frequencies up to 100 MHz molecules and cells would rearrange and form chains along the direction of the field.

In case of microwave radiation, when such lossy samples are exposed to the radiation, the release of heat is so instantaneous, that thermal phenomena of conduction, convection and radiation play only a secondary role in temperature equilibrium. The sample molecules are polarized, and dipole rotation accompanied by intermolecular friction and hysteresis takes place. For a typical soft tissue, different mechanisms dominate at different frequency ranges [52]:

At low frequencies (typically below several hundred kilohertz), the conductivity of the tissue is dominated by conduction in the electrolytes in the extracellular space. The bulk conductivity of the tissue is then a sensitive function of the volume fraction of extracellular space and the conductivity of the extracellular medium. At low frequencies (below about 0.1 MHz), electric current largely passes through the extracellular space, and the tissue conductivity is a sensitive function of the extracellular volume fraction. Any changes in the fluid distribution between intracellular and extracellular compartments can lead to a pronounced change in the low-frequency conductivity of the tissue. At low frequencies, the tissue exhibits a dispersion (the alpha dispersion), centred in the low kilohertz range, due to several physical processes. These include polarization of counter-ions near charged surfaces in the tissue and possibly the polarization of large membrane-bound structures in the tissue. At frequencies below the alpha dispersion, the relative permittivity of tissue reaches very high values, in the tens of millions. The alpha dispersion is very apparent in the permittivity but hardly noticeable in the conductivity of the tissue [58].

At RF, the tissue exhibits a dispersion (the beta dispersion), centred in the range 0.1 to 10 MHz, due to the charging of cell membranes through the intracellular and extracellular media. Above the beta dispersion, the cell membranes have negligible impedance, and the current passes through both the extracellular and intracellular media. The beta dispersion is apparent in both the permittivity and conductivity of the tissue. At microwave frequencies (above 1 GHz), the tissue exhibits a dispersion (the gamma dispersion) due to rotational relaxation of tissue water. This dispersion is centred at 20 GHz and is the same as that found in pure liquid water. In addition to these three major dispersions, other smaller dispersions occur due to rotational relaxation of bound water or tissue proteins, charging of membranes of intracellular organelles, and other effects. These dispersions overlap in frequency and lead to a broad and often featureless dielectric dispersion in tissue.

2.3.2 Tissue Measurement Techniques

The accurate measurement and deconvolution of the dielectric spectrum of polar solutions requires broadband frequency measurements across ranges as great as 1 MHz to 1 THz. Some of the techniques are briefly described in this section, aim to provide the reader with basic of measurement in microwave region of the electromagnetic spectrum [59–61].

- Vector Network Analyser

  Network Analysers (VNAs) are generally used for measuring complex reflection coefficient from RF to millimetre-wave frequencies, but techniques that were in common use before VNAs became widely available are also referred to in this section as they remain of metrological interest. Time Domain Reflectometry (TDR) can also be used to obtain complex reflection coefficients using Fourier Transform techniques. The vector network analyser (VNA) has become the standard tool and microwave source for component and circuit testing and material characterisation. Able to monitor both magnitude and phase information, VNAs are well suited to signal transmission and reflection measurements, ideal for the purpose of dielectric characterisation. Typical VNAs function with a two-port set-up with a built-in signal generator, receiver, processor and display.

  More advanced devices operate with four ports and two signal generators though such devices are beyond the need of measurements conducted within this thesis. The built-in signal generator is a continuous wave (CW) source capable of covering a large frequency range. Many modern VNAs will typically cover ranges of 1 KHz to 3-10 GHz or 50 MHz to 20-67 GHz though extensions can provide a CW source up to 1 THz. The VNA functions with stepped frequency measurements such that single frequency measurements are made before the frequency is increased and the measurement repeated. The receiver measures the magnitude and phase of the transmitted or reflect wave. In order to accurately ascertain the phase of the measurement signal a reference is split from the the source that is later combined with the measurement signal in a phase detector whose output is proportional to the phase difference. A typical measurement is made in terms of the S-parameters of a sweep. For frequencies up to 70 GHz the source signal is carried in a coaxial cable to the device or sample under measurement. Above this frequency waveguides are used due to the complexity and tolerances involved in manufacturing coaxial cables small enough to support a fundamental mode above 70 GHz.

- Coaxial Measurement and Waveguide

Methods in which the conductors have the same cross-sectional dimensions throughout the measurement volume. The important feature in this approach is that as there are no discontinuities in the conductors evanescent modes are not launched, so fundamental-mode transmission-line theory can be used. A theory that expresses complex reflection coefficient in terms of complex permittivity can be derived by satisfying electromagnetic field boundary conditions at each dielectric interface. It is easily extended to multiple layers. Open-ended coaxial sensor designs are well suited for measurements on liquids, gels, and solid materials that are malleable enough to allow perfect contact with the face of the sensor without any air gaps. They are particularly valuable where non-invasive measurements are needed.

Dielectric measurements with coaxial cables for accurate high frequency spectroscopy have only been made possible in the last few decades owing to improved manufacturing techniques. For low frequency permittivity characterisation, coaxial cables become large and for higher frequencies coaxial cables require small dimensions to suppress higher order modes and maintain accuracy. The coaxial cable comprises of a cylindrical inner and a tubular outer electrical conductor separated by a low-loss dielectric. The first advantage of using this type of transmission line is the confinement of the electric and magnetic field within the dielectric component of the cable thereby shielding the signal from external influence. The dimensions are held constant over the length of the cable thus maintaining a constant impedance for the propagating electromagnetic wave. The second notable advantage of coaxial cables is that they can be engineered to be flexible and thus bent without any or little change in the phase of the propagating wave. The properties of conducting interfaces instil boundary conditions on incident waves that, in the case of a coaxial cable waveguide confine the electromagnetic wave between the inner and outer conductor. These boundary conditions confine the type of wave that can be excited within the transmission line. Only one type of field distribution, the transverse electromagnetic (TEM) mode (no electric or magnetic field in the direction of propagation), can be excited and at any frequency within the coaxial cable. The field distribution of the mode is of a radial nature from the inner to outer conductor. At high enough frequencies other defined modes exist such as transverse electric (TE) and transverse magnetic (TM) modes. Currents exist at the surface of the conductors though the wave does not propagate into the bulk of the material. It is preferential to maintain a single mode for all frequencies when making measurements of for communication to prevent unwanted interference and loss of information.

- Resonators

The complex permittivity of polar liquids may also be measured using resonators and cavities. These may have one or two couplings, respectively for transmission or reflection measurements. Q-factors are usually measured these days by using VNAs . Measurements can be made only at resonant frequencies. In transmission measurements, resonators are normally used with weak couplings to minimize loading by the measuring instrument. For measurements on lossy materials the filling- factor — the ratio of stored electromagnetic energy in the sample on resonance to the energy in the entire volume of the resonator must be small to enable a reasonable Q-factor (e.g. 100 or more) to be obtained.

- Admittance Cell

  At lower frequencies (LF), typically below 10MHz, measurements on both solids and liquids are commonly carried out in capacitance cells – more strictly they are admittance cells because loss is also measured in them. However, liquid measurements of this type do have important implications for measurements at higher RF and Microwave frequencies, because they can be used to establish the static i.e. low frequency or liquids that contain free charge carriers. There is an important limitation to such methods namely the electrode polarization effect. If this effect is not compensated for or avoided, spurious measurement results are obtained. The measurement errors arise effectively because series impedances are set up at electrodes to which charge carriers in the liquid are attracted. The carriers tend to conglomerate, because they cannot pass into the electrode itself. Polar liquids like water and shorter chain n-alcohols do contain free charge carriers, because a portion of their molecules are ionized, and so LF measurements on such liquids generally suffer from this effect.

- Time-Domain Measurement

  Time-Domain (TD) methods for determining dielectric properties are based on the measurement of signal responses as a function of time from a specimen when it is excited with a transient signal, e.g. a pulse or a step of applied voltage. Time Domain Reflectometry (TDR), may be a treated as a distributed component in a travelling wave system, typically by being contained in part of a coaxial transmission line. TDR is the most commonly used time domain method for dielectrics. Conversion of the time-domain information in the response signal to the frequency domain provides information on specimen dielectric properties at all frequencies at which there is significant amplitude in the Fourier Transform of the stimulating pulse/step. Typically, this amplitude falls with increasing frequency, so the method usually becomes less sensitive and less accurate as one approaches the upper limits of the frequency coverage.

However the coverage of fast sampling techniques nowadays includes the whole of the microwave spectrum up to THz frequencies and above

In open literatures [3, 4, 62–65], the spectral range of 0.1 – 10 THz is exploited for wide range of applications in biomedical mainly to better understand the water dynamic, security , dental,tissue imaging, human cortical bone, protein folding and unfolding. The strong absorption of terahertz radiation by water shows that terahertz imaging is very sensitive to changes in the water content of materials, and this can therefore be exploited for biomedical applications [66, 67]. Water is a polar molecule and is highly absorbing in the THz region. Water has a simple molecular structure; it comprises two hydrogen atoms covalently bonded to one oxygen.The oxygen molecule has 4 electrons in its outer shell, two of which bond with the hydrogen atoms and two remain unshared making the oxygen atom electronegative compared with hydrogen.Individual water molecules are able to vibrate in a number of ways. In the gas state, the vibrations involve combinations of stretching and bending of the covalent bonds, including symmetrical stretching where bonds stretch in unison, asymmetrical stretching where bonds stretch in opposing directions. Symmetrical and asymmetrical stretching and bending are molecular vibrations and rocking, wagging and twisting can be thought of as restricted molecular rotations.The water vapour absorption peak in the atmosphere exists around 1.1 and 1.7 THz.

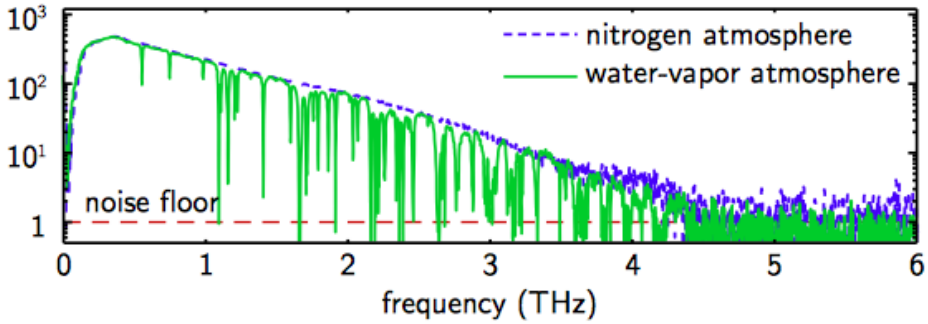

Fig. 2.7 Effects of water vapour on a T-ray pulse and its spectrum [24]

In addition, THz region is considered as safe for such applications as compared to conventional microwave frequencies. Extensive studies have been performed on skin imaging at these frequencies; Pickwell et al. [68] conducted an in vivo terahertz imaging study from 0.1 - 1.4 THz to investigate the person-to-person variations of terahertz skin properties, and demonstrated how the thickness of the stratum corneum on the palm of the hand could be measured non-invasively. THz-TDS is an ideal technology for the determination of material's parameters and detection of changes in these parameters depending on different conditions. The size of THz wave has biological relevance in regards to the following general concepts:

resolution of imaging applications, scattering properties in the biological tissues and direct molecular excitation. The THz wavelength is quite comparable to the size of the biological sample range from um to mm. The photons are known to be scattered by the structures whose size matches their wavelength, THz waves suffer minimal Rayleigh scattering and undergo Mie scattering processes as they pass through the biological tissues. A brief review on recent finding of electrical properties of various tissues and biological entities in the THz range is provided as below [69–72]:

- Artificial Skin (Collagen)

  In paper, artificial skin samples were fabricated. Integra derma regeneration templates were chosen, divided as monolayer and bilayer. The dynamic range of the THz-TDS system was approx. 0.1 to 1.5 THz. The measurement was performed in a nitrogen-based environment and polystyrene was employed as a THz transmitter material. The refractive index was reported to be 1.2 and 1.6 but no results were published on the absorption coefficient.

- Excised Human Skin

  In paper, excised human tissues were measured in the range approx. 0.5 to 2.5 THz. Skin, veins, muscles and nerves were the samples of interest. The thickness ranged from 50 to 200 um, Soft tissue samples were cut approximately to one of four thickness (50,100, 150 and 200 um). The mean refractive index was report to be 1.69.

- Excised Porcine Skin

  In the paper, the samples were divided as unfrozen and frozen/thawed tissues. The dynamic range was from 0.1 THz to 2 THz roughly. The data obtained for fresh unfrozen sample two hour post excision and similarly data obtained for frozen sample two days post excision. The results for frozen tissue was reported to be 2.5 at 0.1 THz and 2 at 2 THz and for unfrozen the refractive index was reported to be 2 at 0.1 THz and 1.7 at 2 THz.

- Hair

  The main constitute of hair is the alpha-keratin protein and water. This protein takes the 90% of the total volume while the remaining 10% is for water. This water content modifies the hair mechanical properties . Different ethnic backgrounds have their own unique features thus discriminating in colour, density and texture. In this paper, freshly excised hair samples from the two human subjects were obtained. These samples were excised using an electric shaver, and then directly placed into sterilized plastic

containers. 40 gross sections of curly and straight hair samples that varied in thickness of 0.5 and 5.0 mm; whereby each hair type and sample thickness combination.

It has been reported in [66], that THz radiation with its non-ionizing and non-invasive innateness, when exposed to cells does not express any changes in DNA repair. The human skin/tissue material properties in the THz range remain sparse and lack consistency. For the purpose of establishing EM communication in the THz range for in-body (in-vivo) nanonetworks, the focus of the subsequent section and later chapters is to construct a comprehensive database on human skin dielectric properties in the THz band. In addition to dielectric properties, aim is to provide channel model parameters for skin tissues by characterizing different layers. This is achieved by extracting the refractive index and absorption coefficient of the dermis layer from the THz time domain spectroscopy measurements on the real human skin and these parameters are further used to calculate the pathloss and noise temperature. Also the results of this paper are compared with the available literature [24], which shows the improvement in path loss and absorption coefficient measurement for dehydrated tissue.

2.4 Chapter Summary

In this chapter, fundamentals of nanoscale communication inside the human skin was provided. The concept of nanoscale communication and specifically its application to healthcare is still at its infancy. However, with increasing demands in data-rates, small-scale devices and transparent information exchange, communication THz frequencies have become the ultimate choice. Also known as millimetre waves, they have already been exploited in the field of material characterization such as weapon screening, drugs, semiconductors, atmospheric gases etc. Since their popularity in meteorology and the ability to identify spectral peaks of various molecules such as oxygen, hydrogen and water vapours, they have been recently introduced for short-range communication. The focus is given on the motivation behind using THz frequencies for nanoscale communication inside the human skin. The effectiveness of proposed nanodevices (graphene antennas) is highly dependent on medium of communication, hence THz channel parameters are studied keeping in mind the heterogeneity of human skin. Presently, the channel parameters for the free space and simplified skin tissue models (which are numerically simulated) have been proposed. However, more details on experimental characterization real human skin and effects of skin diversity on channel parameters are yet to be explored. Drawing knowledge from the existing optical properties of skin in the THz domain, water has been identified as a hindrance to extract spectral signatures of the tissue. While this is true, but at the same time variation in water

dynamics can reveal a lot of information on human health and its effect on THz channel propagation characteristics.

References

[1] Derek Abbott and Xi-Cheng Zhang. Special issue on T-ray imaging, sensing, and retection. *Proceedings of the IEEE*, 95(8):1509–1513, 2007.

[2] Daniel Mittleman. *Sensing with terahertz radiation*, volume 85. Springer, 2013.

[3] E Pickwell and VP Wallace. Biomedical applications of terahertz technology. *Journal of Physics D: Applied Physics*, 39(17):R301, 2006.

[4] Wai Lam Chan, Jason Deibel, and Daniel M Mittleman. Imaging with terahertz radiation. *Reports on progress in physics*, 70(8):1325, 2007.

[5] Calvin Yu, Shuting Fan, Yiwen Sun, and Emma Pickwell-MacPherson. The potential of terahertz imaging for cancer diagnosis: A review of investigations to date. *Quantitative imaging in medicine and surgery*, 2(1):33–45, 2012.

[6] John F Federici, Dale Gary, Robert Barat, and Zoi-heleni Michalopoulou. T-rays vs. terrorists. *IEEE Spectrum*, 44(7):47–52, 2007.

[7] Peter De Maagt, Peter Haring Bolivar, and Chris Mann. Terahertz science, engineering and systems—from space to earth applications. *Encyclopedia of RF and Microwave Engineering*, 2005.

[8] Peter H Siegel. THz instruments for space. *IEEE Transactions on Antennas and Propagation*, 55(11):2957–2965, 2007.

[9] Yun-Shik Lee. *Principles of terahertz science and technology*, volume 170. Springer Science & Business Media, 2009.

[10] Ke Yang, Qammer Hussain Abbasi, Nishtha Chopra, Max Munoz, Yang Hao, and Akram Alomainy. Effects of non-flat interfaces in human skin tissues on the in-vivo tera-hertz communication channel. *Nano Communication Networks*, 8:16–24, 2016.

[11] Josette El Haddad, Bruno Bousquet, Lionel Canioni, and Patrick Mounaix. Review in terahertz spectral analysis. *TrAC Trends in Analytical Chemistry*, 44:98–105, 2013.

[12] Withawat Withayachumnankul, Gretel M Png, Xiaoxia Yin, Shaghik Atakaramians, Inke Jones, Hungyen Lin, Benjamin Seam Yu Ung, Jegathisvaran Balakrishnan, Brian W-H Ng, and Bradley Ferguson. T-ray sensing and imaging. *Proceedings of the IEEE*, 95(8):1528–1558, 2007.

[13] D Grischkowsky, Søren Keiding, Martin Van Exter, and Ch Fattinger. Far-infrared time-domain spectroscopy with terahertz beams of dielectrics and semiconductors. *JOSA B*, 7(10):2006–2015, 1990.

[14] Masae Takahashi. Terahertz vibrations and hydrogen-bonded networks in crystals. *Crystals*, 4(2):74–103, 2014.

[15] Hungyen Lin, W Withayachumnankul, Bernd M Fischer, SP Mickan, and Derek Abbott. Gas recognition with terahertz time-domain spectroscopy and spectral catalog: a preliminary study. pages 68400X–68400X. International Society for Optics and Photonics, 2007.

[16] Shimon Y Nof, Andrew M Weiner, and Gary J Cheng. *Laser and Photonic Systems: Design and Integration*. CRC Press, 2014.

[17] Zachary D Taylor, Rahul S Singh, David B Bennett, Priyamvada Tewari, Colin P Kealey, Neha Bajwa, Martin O Culjat, Alexander Stojadinovic, Hua Lee, and Jean-Pierre Hubschman. THz medical imaging: in vivo hydration sensing. *IEEE transactions on terahertz science and technology*, 1(1):201–219, 2011.

[18] R Gente, N Born, N Voß, W Sannemann, J Léon, M Koch, and E Castro-Camus. Determination of leaf water content from terahertz time-domain spectroscopic data. *Journal of infrared, millimeter, and terahertz waves*, 34(3-4):316–323, 2013.

[19] Cecilie Rønne. Intermolecular liquid dynamics studied by THz-spectroscopy. *Department of Chemistry*, 2000.

[20] Ian Akyildiz, Josep Jornet, and Chong Han. TeraNets: ultra-broadband communication networks in the terahertz band. *IEEE Wireless Communications*, 21(4):130–135, 2014.

[21] Radoslaw Piesiewicz, Thomas Kleine-Ostmann, Norman Krumbholz, Daniel Mittleman, Martin Koch, Joerg Schoebei, and Thomas Kurner. Short-range ultra-broadband terahertz communications: Concepts and perspectives. *IEEE Antennas and Propagation Magazine*, 49(6):24–39, 2007.

[22] Ignacio Llatser, Sergi Abadal, Albert Mestres Sugranes, Albert Cabellos-Aparicio, and Eduard Alarcón. Graphene-enabled wireless networks-on-chip. pages 69–73. IEEE, 2013.

[23] Ian F Akyildiz and Josep Miquel Jornet. Electromagnetic wireless nanosensor networks. *Nano Communication Networks*, 1(1):3–19, 2010.

[24] Ke Yang, Alice Pellegrini, Max O Munoz, Alessio Brizzi, Akram Alomainy, and Yang Hao. Numerical analysis and characterization of THz propagation channel for body-centric nano-communications. *IEEE Transactions on Terahertz Science and Technology*, 5(3):419–426, 2015.

[25] Ho-Jin Song and Tadao Nagatsuma. Present and future of terahertz communications. *IEEE Transactions on Terahertz Science and Technology*, 1(1):256–263, 2011.

[26] Ian F Akyildiz, Josep Miquel Jornet, and Chong Han. Terahertz band: Next frontier for wireless communications. *Physical Communication*, 12:16–32, 2014.

[27] Qammer H Abbasi, Ke Yang, Nishtha Chopra, Josep Miquel Jornet, Najah Abed Abuali, Khalid A Qaraqe, and Akram Alomainy. Nano-Communication for Biomedical Applications: A Review on the State-of-the-Art From Physical Layers to Novel Networking Concepts. *IEEE Access*, 4:3920–3935, 2016.

[28] Alwyn J Seeds, Haymen Shams, Martyn J Fice, and Cyril C Renaud. Terahertz photonics for wireless communications. *Journal of Lightwave Technology*, 33(3):579–587, 2015.

[29] Seunghwan Kim. THz Device-to-Device Communications: Channel Measurements, Modelling, Simulation, and Antenna Design. 2016.

[30] R Wang, JQ Yao, DG Xu, JL Wang, and P Wang. The physical theory and propagation model of THz atmospheric propagation. volume 276, page 012223. IOP Publishing, 2011.

[31] Joe Allen Elder and Daniel F Cahill. *Biological effects of radiofrequency radiation*. Health Effects Research Laboratory, Office of Research and Development, US Environmental Protection Agency, 1984.

[32] Michael J Fitch and Robert Osiander. Terahertz waves for communications and sensing. *Johns Hopkins APL technical digest*, 25(4):348–355, 2004.

[33] Ian F Akyildiz and Josep Miquel Jornet. The internet of nano-things. *IEEE Wireless Communications*, 17(6):58–63, 2010.

[34] Benoît Latré, Bart Braem, Ingrid Moerman, Chris Blondia, and Piet Demeester. A survey on wireless body area networks. *Wireless Networks*, 17(1):1–18, 2011.

[35] Ignacio Llatser Martı. Exploring the Scalability Limits of Communication Networks at the Nanoscale. 2011.

[36] Josep Miquel Jornet and Ian F Akyildiz. Channel modeling and capacity analysis for electromagnetic wireless nanonetworks in the terahertz band. *IEEE Transactions on Wireless Communications*, 10(10):3211–3221, 2011.

[37] Richard M Goody and Yuk Ling Yung. *Atmospheric radiation: theoretical basis*. Oxford University Press, 1995.

[38] Josep Miquel Jornet and Ian F Akyildiz. Channel modeling and capacity analysis for electromagnetic wireless nanonetworks in the terahertz band. *IEEE Transactions on Wireless Communications*, 10(10):3211–3221, 2011.

[39] Nan Sun, Kristof Tahy, Huili Xing, Debdeep Jena, Gerald Arnold, and Steven T Ruggiero. Electrical noise and transport properties of graphene. *Journal of Low Temperature Physics*, 172(3-4):202–211, 2013.

[40] SA Clough, MW Shephard, EJ Mlawer, JS Delamere, MJ Iacono, K Cady-Pereira, S Boukabara, and PD Brown. Atmospheric radiative transfer modeling: a summary of the AER codes. *Journal of Quantitative Spectroscopy and Radiative Transfer*, 91(2):233–244, 2005.

[41] Eric Y Chow, Milton M Morris, and Pedro P Irazoqui. Implantable RF medical devices: The benefits of high-speed communication and much greater communication distances in biomedical applications. *IEEE Microwave Magazine*, 14(4):64–73, 2013.

[42] Deepak K Ghodgaonkar and Adib Bin Daud. Calculation of Debye parameters of single Debye relaxation equation for human skin in vivo. pages 71–74. Ieee, 2003.

[43] AL Bottomley, SJ Neely, SJ Wood, and JEH Tattersall. Effects of Ultrawide Band Microwave Pulses on Rat Hearts in Vitro. In *Electricity and Magnetism in Biology and Medicine*, pages 477–479. Springer, 1999.

[44] JM Alison and RJ Sheppard. Dielectric properties of human blood at microwave frequencies. *Physics in medicine and biology*, 38(7):971, 1993.

[45] Herman P Schwan. Electrical properties of tissue and cell suspensions. *Advances in biological and medical physics*, 5:147, 1957.

[46] S Gabriel, RW Lau, and Camelia Gabriel. The dielectric properties of biological tissues: II. Measurements in the frequency range 10 Hz to 20 GHz. *Physics in medicine and biology*, 41(11):2251, 1996.

[47] Camelia Gabriel. Compilation of the Dielectric Properties of Body Tissues at RF and Microwave Frequencies. Technical report, DTIC Document, 1996.

[48] R Pethig. Dielectric properties of body tissues. *Clinical Physics and Physiological Measurement*, 8(4A):5, 1987.

[49] Clive M Alabaster. The microwave properties of tissue and other lossy dielectrics. 2004.

[50] Toby H Basey-Fisher. Biosensing with microwave debye relaxation analysis. 2013.

[51] Iliana Marinova and Valentin Mateev. Determination of electromagnetic properties of human tissue. *World Acad Sci Eng Tech*, 42(4):591–595, 2010.

[52] KR FOSTER, HP SCHWAN, and MA STUCHLY. Dielectric properties of tissues and biological materials: a critical review. *Critical reviews in biomedical engineering*, 17(1):25–104, 1989.

[53] KR Foster and HP Schwan. Dielectric properties of tissues and biological materials: a critical review. *Critical reviews in biomedical engineering*, 17(1):25–104, 1988.

[54] NP Mahalik. Principle and applications of MEMS: a review. *International Journal of Manufacturing Technology and Management*, 13(2-4):324–343, 2008.

[55] Paolo Vecchia, Rüdiger Matthes, Gunde Ziegelberger, James Lin, Richard Saunders, and Anthony Swerdlow. Exposure to high frequency electromagnetic fields, biological effects and health consequences (100 kHz-300 GHz). *International Commission on Non-Ionizing Radiation Protection*, 2009.

[56] Jeffries Wyman. Studies on the dielectric constant of protein solutions I. Zein. *Journal of Biological Chemistry*, 90(2):443–476, 1931.

[57] John Barrett Hasted. *Aqueous dielectrics*. Chapman and Hall, 1973.

[58] Lawrence E Larsen and John H Jacobi. Medical applications of microwave imaging. Technical report, DTIC Document, 1985.

[59] Udo Kaatze. Techniques for measuring the microwave dielectric properties of materials. *Metrologia*, 47(2):S91, 2010.

[60] MS Venkatesh and GSV Raghavan. An overview of dielectric properties measuring techniques. *Canadian biosystems engineering*, 47(7):15–30, 2005.

[61] T Whit Athey, Maria A Stuchly, and Stanislaw S Stuchly. Measurement of radio frequency permittivity of biological tissues with an open-ended coaxial line: Part I. *IEEE Transactions on Microwave Theory and Techniques*, 30(1):82–86, 1982.

[62] SW Smye, JM Chamberlain, AJ Fitzgerald, and E Berry. The interaction between terahertz radiation and biological tissue. *Physics in medicine and biology*, 46(9):R101, 2001.

[63] James C Lin. *Electromagnetic fields in biological systems*. CRC press, 2011.

[64] AA Goryachuk, VA Begaeva, MK Khodzitsky, and AS Truloff. The optical properties and spectral features of malignant skin melanocytes in the terahertz frequency range. volume 735, page 012073. IOP Publishing, 2016.

[65] MR Stringer, DN Lund, AP Foulds, A Uddin, E Berry, RE Miles, and AG Davies. The analysis of human cortical bone by terahertz time-domain spectroscopy. *Physics in medicine and biology*, 50(14):3211, 2005.

[66] Henning Hintzsche, Christian Jastrow, Thomas Kleine-Ostmann, Uwe Kärst, Thorsten Schrader, and Helga Stopper. Terahertz electromagnetic fields (0.106 THz) do not induce manifest genomic damage in vitro. *PloS one*, 7(9):e46397, 2012.

[67] GP Gallerano. Tera–Hertz radiation in Biological Research, Investigations on Diagnostics and study on potential Genotoxic Effects–THz-BRIDGE–Final Report. Technical report, QLK4–CT–2000–00129, 2004.

[68] E Pickwell, BE Cole, AJ Fitzgerald, M Pepper, and VP Wallace. In vivo study of human skin using pulsed terahertz radiation. *Physics in Medicine and Biology*, 49(9):1595, 2004.

[69] Peter M Corridon, Ricardo Ascázubi, Courtney Krest, and Ingrid Wilke. Time-domain terahertz spectroscopy of artificial skin. pages 608007–608007. International Society for Optics and Photonics, 2006.

[70] Peter M Corridon, David Claudio, and Ingrid Wilke. Does hair impose a significant effect on the propagation of terahertz radiation in human skin? page MD4. Optical Society of America, 2007.

[71] AJ Fitzgerald, E Berry, NN Zinov'ev, S Homer-Vanniasinkam, RE Miles, JM Chamberlain, and MA Smith. Catalogue of human tissue optical properties at terahertz frequencies. *Journal of Biological Physics*, 29(2):123–128, 2003.

[72] Yiwen Sun, Ming Yiu Sy, Yi-Xiang J Wang, Anil T Ahuja, Yuan-Ting Zhang, and Emma Pickwell-MacPherson. A promising diagnostic method: Terahertz pulsed imaging and spectroscopy. *World journal of radiology*, 3(3):55, 2011.

Chapter 3

THz Characterization of Dehydrated Human Skin Tissue

This chapter presents experimental study of real human skin material parameter extraction based on Terahertz (THz) Time Domain Spectroscopy in the band 0.1 - 2.5 THz. Results in this chapter show that electromagnetic properties of the human skin distinctively affects the pathloss and noise temperature parameters of the communication link, which are vital for channel modelling of in-body nano-networks. Refractive index and absorption coefficient values are evaluated for dermis layer of the human skin. Repeatability and consistency of the data is accounted for in the experimental investigation and the morphology of the skin tissue is verified using a standard optical microscope.The measured parameters i.e. the refractive index and absorption coefficient are 2.1 and 18.45 cm^{-1}, respectively at 1 THz for a real human skin, which are vital for developing and optimizing future in-body nano-networks.

3.1 Pulsed THz-Time Domain Spectroscopy

THz-TDS is a coherent detection technique, which allows retrieving of both phase and amplitude data. Therefore, it becomes rather simple to extract the refractive index and absorption coefficient of a material in the THz band. On the other hand, FTIR and Raman use the complex models and indirect computation, such as the Kramers-Kronig to retrieve the complex dielectric constant [1]. In THz–TDS, not only the absorption but also the dispersion of the sample can be obtained by analysing the Fourier transform of the waveforms. The emergence of femtosecond lasers and photoconductive antennas during the 1980s made it possible to use THz waves for various applications [2] covering biomedical sciences, pharmacology and security.

In 1975, Bell Laboratories and the IBM T. J. Watson Research center demonstrated that ultrafast laser pulse on the order of 100 femtosecond (fs) when impinged a biased semiconductor, also known as "Auston switch" could create a picosecond (ps) current transient. This time-dependent current radiates classically in the far field and contains frequency components in the THz frequency range between 0.1 and 4 THz [3]. The THz optical bench can be aligned in two configurations: Reflection and Transmission [4]. Usually, both the configurations can be used with slight variation in alignment in regards to THz beam path length and direction. Reflection geometry is good for highly absorption materials, and transmission is convenient in terms of alignment. Hence, a more popular choice of pulsed THz-TDS in transmission mode will be discussed further in detail.

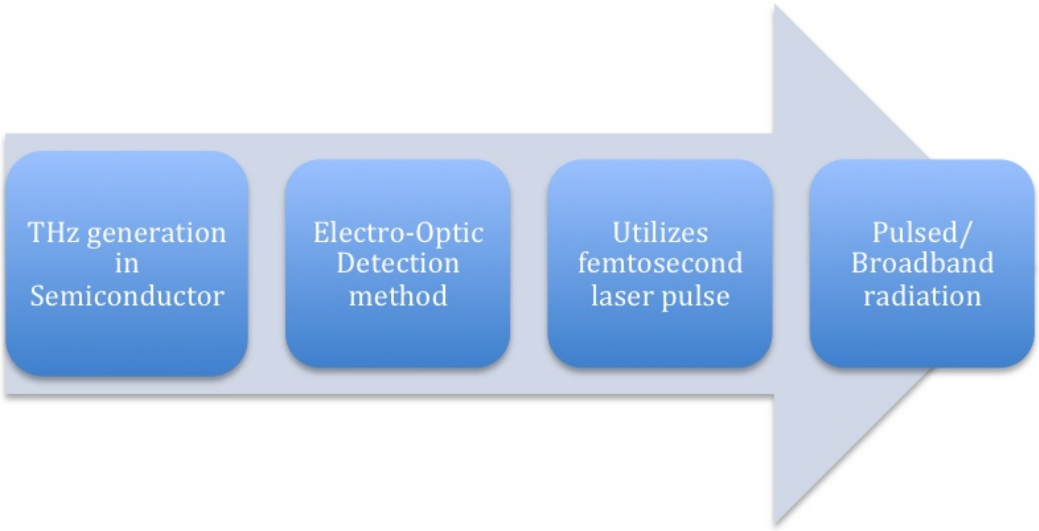

Fig. 3.1 Flowchart of THz wave generation using a semiconductor, most popular choice is low temperature gallium arsenide (LT-GaAs) and electro-optic detection based on pockel's effect

With the advancement in semiconductor technology and optics, different methods have been proposed for generation and detection of THz wave [5]. In this thesis, the focus is on generation of THz wave utilizing photocurrent in a semiconductor and detection via probing a non-linear crystal in a transmission mode [6–8]. The basic components of a pulsed THz-TDS consists of a femtosecond laser system with output power of around 1 watt, a photoconductive (PC) antenna as the THz emitter. The femtosecond pulses incident on the emitter are transformed into single-cycle electrical pulses with a period of one picosecond in the time domain [9]. The optical THz bench is complete with a mechanical delay stage, reflective optics (mirrors), a sample holder and a detector system.

A PC antenna consists of two metal strips deposited on a semiconductor substrate. Low temperature Gallium Arsenide (LT-GaAs) is extensively used for this purpose. Advantages

are its short carrier lifetime and relatively high carrier mobility [10]. The metal strips are usually made of gold for its good conductivity with a small gap at the centre. This gap is the active region where the femtosecond optical pulses are focused [11, 12]. The high intensity femtosecond optical pulses are probed with activation energy greater than the band gap of room temperature GaAs (1.43eV) [13]. This results in emission of photocarriers accelerated under the influence of an external DC bias. The photocarriers are shifted towards anode and the following recombination results in a pulsed photocurrent. The photocurrent density J(t), is related to the convolution between the laser pump intensity, P_{laser}(t), and the impulse response (qn(t)v(t)) of the photoconductive antenna [14],

$$J(t) = P_{laser}(t) * [qn(t)v(t)] \tag{7}$$

where n(t) is the photocarrier density , v(t) is the photocarrier velocity , q is the electron charge and $*$ is the convolution operator.

Thus, upon laser illumination, a rapid rise in the photocurrent can be observed, followed by a longer decay due to a finite carrier lifetime. This transient current radiates a coherent electric pulse, which, at the far field, is proportional to the first-order derivative of the photocurrent density and linearly polarised along the direction of the DC electric field [9, 14, 15]:

$$E_{THz}(t) \propto \frac{dJ(t)}{dt} \tag{8}$$

This photocurrent varies in time corresponding to the incident laser beam intensity by first rising rapidly upon generation of photocarriers, and then decaying with a time constant given by the carrier lifetime of GaAs [16]. We can treat emitter structure as a small capacitor with capacity C, bias voltage V and capacitive energy $\frac{1}{2}CV^2$ [17]. This energy is discharged when circuit is closed by the photogenerated current and radiate THz pulses. The energy of the THz pulses originates form the power supply by recharging the capacitor. The PC antenna is excited by incoming ultra-short laser pulses.

These pulses are the focused with reflective optics, transmitted through the sample in a holder and reach the detector system. A mechanical delay line or a translation stage introduces the time delay between generated and detected pulses. The electro-optic (EO) detection of THz wave is based on Pockel's effect [12], briefly it is the change of birefringence of a non-linear crystal usually ZnTe, in an external electric field. As mentioned earlier, the laser beam is bifurcated as two: pump for THz generation and probe beam for detection.The detector signal current is proportional to the THz electric field, which allows phase sensitive measurement i.e. evaluating phase difference between two samples. Both the beams should

coincide spatially and temporally, at the detector to sense any changes induced as a results of transmission through the sample. This effect is usually a change of polarization, which is turned into a change of optical power by a polariser.

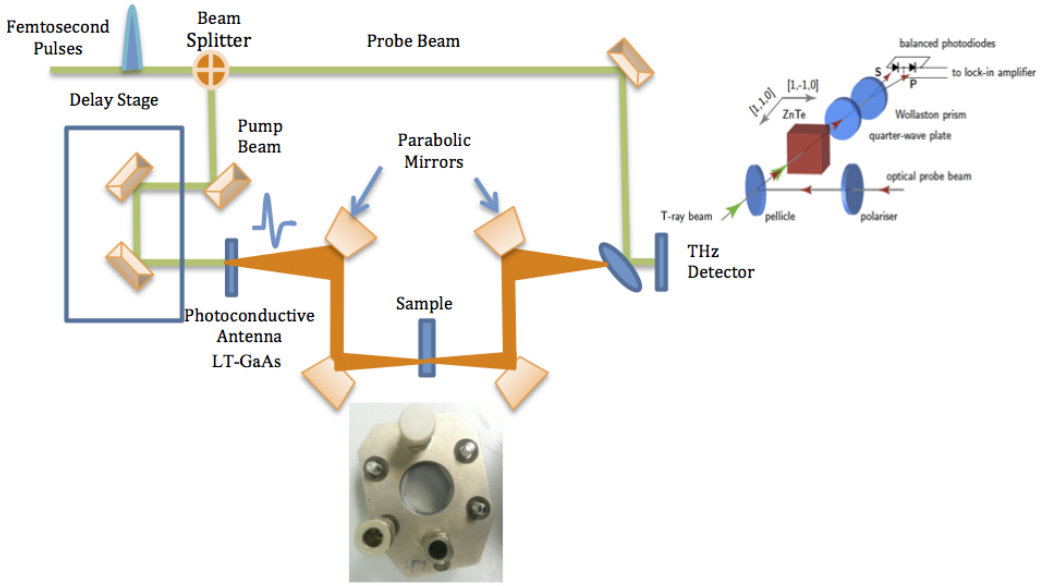

Fig. 3.2 Schematic of THz Time Domain Spectroscopy with electro-optic detection system and photoconductive generation in a transmission geometry. A metallic rotating sample holder by bruker is used to measure the skin tissues

A polarizing beam splitter, which can be viewed as a second polariser rotated 90 degrees from the first polariser, is used to split and direct the polarization rotation that the THz field induces on the probe beam and to achieve intensity modulation of the polarization [18]. This is a typical crossed polariser detection method [19, 20]. A pair of balanced photodiodes is used to analyse the split polarization rotations. The amplitude and phase of the THz-radiation pulse are measured by recording the phase change of femtosecond near infrared laser pulses travelling collinearly and simultaneously with the THz radiation pulses through the electro-optic crystal, that is, ZnTe. The electric field of the THz radiation induces a change of the refractive index of the crystal via the linear EO effect such that the crystal becomes birefringent. It is observed that EO detection is noise sensitive, and there exists a clear trade-off between the noise sensitivity and frequency response. The slow variation in the arrival time of the probe pulse, that is, sequential sampling of a repetitive signal, results in the measurement of a full waveform of a periodic signal.

3.1.1 Extraction of Material Properties

A broadband T-ray signal transmitted through or reflected from a material sample is influenced by the absorption and dispersion of the sample. A change in the transmitted signal hence relates to the optical properties of the sample, which can be extracted via the physical models of a propagating wave. The measured signal is in fact a convolution between the incident T-ray field, the optical probe pulse, and the system response. a T-ray signal that passes through a dielectric sample with parallel surfaces at a normal angle of incidence, assuming no reflections, can be expressed in the frequency domain as [21–24]:

$$E_{sample}(\omega) = \eta \frac{4\hat{n}_s(\omega)n_\circ}{(\hat{n}_s(\omega)+n_\circ)^2}.\exp[-j\hat{n}_s(\omega)\frac{\omega l}{c}].E_\circ(\omega) \tag{9}$$

where, η is the transmission factor of free air surrounding the sample; $\hat{n}_s$ is the complex refractive index of the sample; $n_\circ$ is the refractive index of free space and l is the propagation length inside the sample, which equals the sample thickness for a normal angle of incidence. Similarly, the propagation of wave through free space (reference measurement), signal measured with the same settings but in the absence of the sample is given by:

$$E_{reference}(\omega) = \eta \exp[-j\hat{n}_\circ(\omega)\frac{\omega l}{c}].E_\circ(\omega) \tag{10}$$

The material parameter extraction process requires these two spectra, $E_{sample}(\omega)$ and $E_{reference}(\omega)$, which are Fourier transformed from time-domain measurements. Normalizing the sample spectrum by the reference, or $\frac{E_{sample}(\omega)}{E_{reference}(\omega)}$, results in the complex transfer function of the sample in the frequency domain. This value is usually approximated to real value of refractive index, $n(\omega)$. Hence, the transfer function becomes:

$$H(\omega) = \frac{4n_s(\omega)n_\circ}{(n_s(\omega)+n_\circ)^2}.\exp[-k_s(\omega)\frac{\omega l}{c}]\exp[-jn_s(\omega)\frac{\omega l}{c}].E_\circ(\omega) \tag{11}$$

Taking the argument and logarithm of the simplified transfer function gives phase and amplitude of the spectra respectively. This further results in expression for refractive index and absorption coefficient:

$$n_s(\omega) = n_\circ - \frac{c}{\omega l}\angle H(\omega) \tag{12}$$

The value $\angle H(\omega)$ can be numerically solved in $Matlab^{©}$, which is the phase difference $\phi_{samp}(\omega) - \phi_{ref}(\omega)$ between the sample and the reference equivalent to the different phase velocities in the sample.

$$\alpha_s(\omega) = \frac{2}{l}[ln[\frac{4n_s(\omega)n_\circ}{(n_s(\omega)+n_\circ)^2}]] - ln|H(\omega)| \tag{13}$$

Since the data obtained is originally in time domain, the extracted parameters in frequency domain are first evaluated with Fast Fourier Transform (FFT) which provide the amplitude of the signal (Fig.3.3).

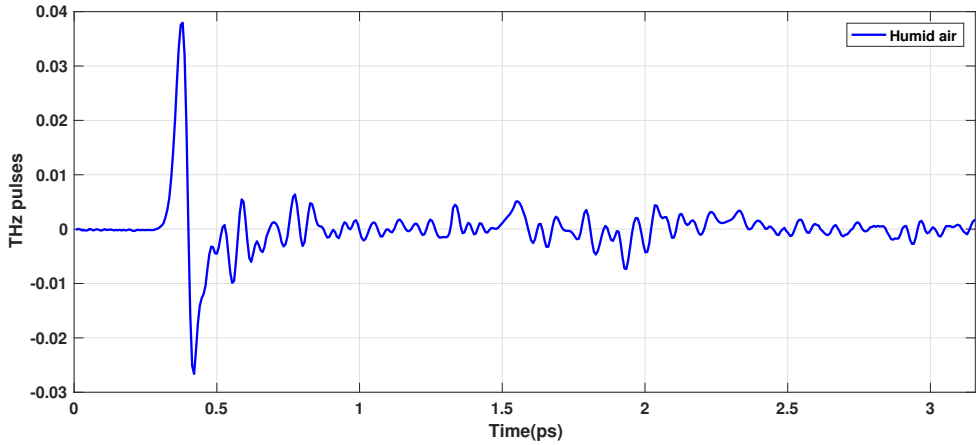

(a) THz signal transmitted through free space

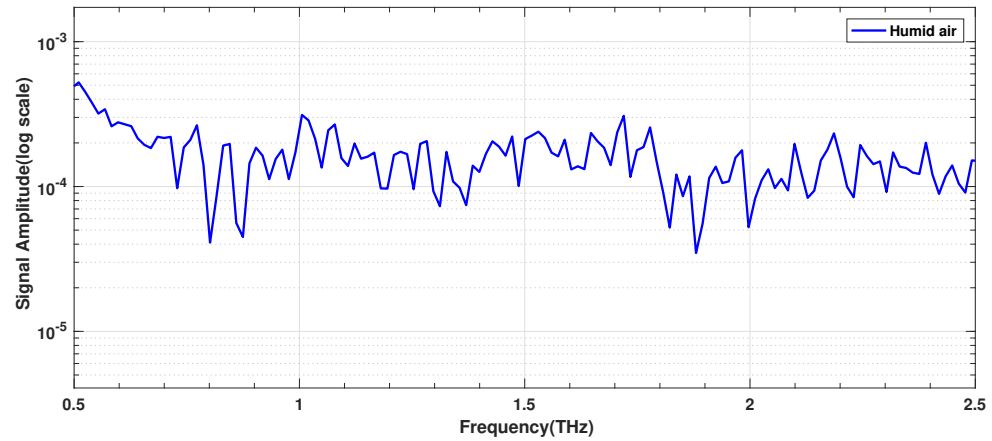

(b) Amplitude of free space signal after fast Fourier transform (FFT)

Fig. 3.3 THz signal in (a) time domain and (b) frequency domain

The signal after approximately 2.5 THz approaches the noise floor, hence it can be ignored. The amplitude as seen in Fig.3.3 (b) decrease with frequency and the bandwidth of the spectrometer is defined by the noise floor. The available amplitude extracted by Fourier transformed THz pulses gives an upper limit to the absorption coefficient of samples depending on the dynamic range. The dynamic range (DR) is defined as the signal above the noise floor in the spectrum where the noise floor level is set to 1 [17]. The air fluctuations

seem in the signal plot can be reduced by sealing the THz optical path with plastic film. The experiments both for sample and reference (free space) have been strictly conducted at a stable humidity level of RH 3-4%. The path can also be made less lossy with the help of nitrogen purging or simple by flowing dry air. However, with the current state of THz-TDS equipment available, it was only possible to carry the measurement in free space.

3.2 THz-TDS Optical Bench at Queen Mary University of London

The exposition of THz spectroscopy is the time domain measurement where pulsed THz wave is mixed with sampling optical pulses in a detector [25]. The tool utilizes similar concepts of pump-probe technique, where the optical beam is split into two parts, one of which goes through a transnational stage to provide a relative time delay.The THz-TDS at Queen Mary University of London (QMUL) [26] has a typical range of 0.1-4 THz, which provides access to broader spectral analysis.The optical bench assembly consists of a femtosecond (fs) laser source - Ti:Sapphire set to 800 nm wavelength and peak power of 1 W. It produces train of pulses at a repetition rate of 80 MHz and duration of 100 fs. The beam splitter divides the incoming radiation in two: pump and probe beam for coherent generation and detection of THz radiation. The intensity of generated THz radiation depends on the amount of incident beam and thus the splitter allows majority of pump beam to reach the emitter. The delay stage has maximum travel distance of 15cm and provides a cross-correlation measurement of THz waveform.

The delay line is mechanically controlled and for each sampled point, a different delay position is assigned. THz emitter is low Temperature (LT) GaAs photoconductive antenna with a biased voltage of 200 V and a gap size of approximately 0.5 mm, which makes the laser beam positioning easier. The femtosecond pulses are fed to this antenna with activation energy greater than the bandgap of LT-GaAs (1.43 eV). The generated photocarriers results in pulsed photocurrent, which is directly proportional to the THz field. The system is operational in transmission mode with a typical resolution of around 14.6 GHz. The radiation is focused on the sample with a help of aluminium coated off-axis parabolic mirrors of beam diameter, 2 mm. The transmitted wave without the sample is the reference data of either free space air or a transparent material. A lock-in amplifier modulates the THz signal and records the detected signal.

A ZnTe crystal is employed as an electro-optic detector with a thickness of 2 mm, which allows enough interaction length of probe beam and THz wave in the crystal [26]. A linearly

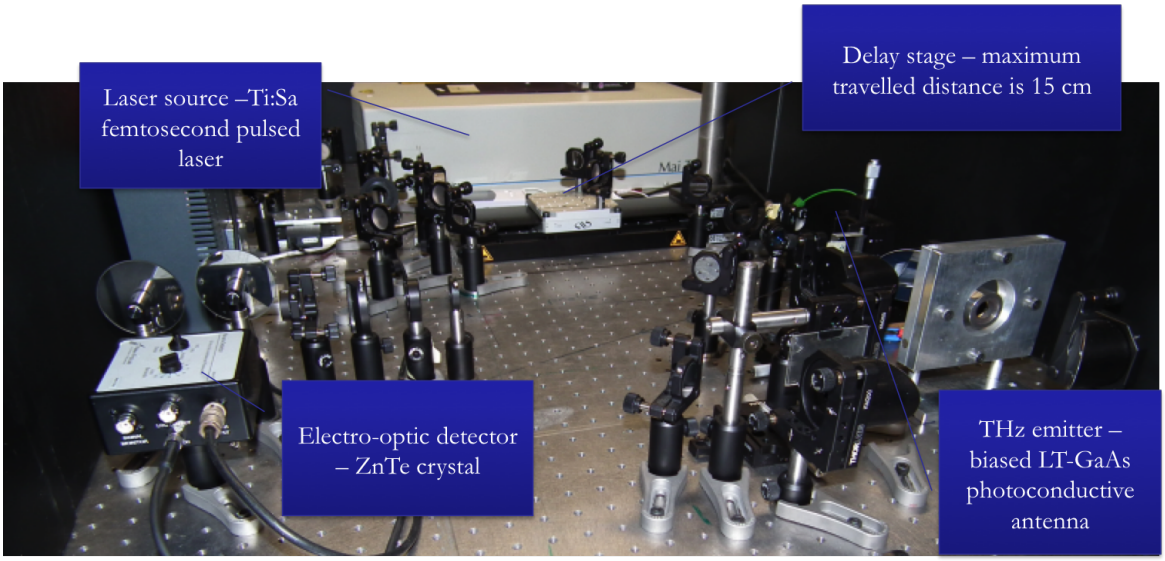

Fig. 3.4 THz-TDS optical bench aligned at Queen Mary University of London

polarized optical probe beam goes through a polariser and then travels through the EO crystal. A quarter wave plate (QWP) located after the EO crystal changes the ellipticity of the probe beam and a Wollaston prism separates the two perpendicular components of the elliptical polarization [7, 27]. Each polarization intensity is detected by a photo-diode. When no THz wave is illuminating the EO crystal, the ellipticity of the probe beam can be set so that both polarizations are equal and, therefore, the net current from the photo-diodes assembly is zero. When a THz wave illuminates the EO crystal, the electric field associated with the THz wave changes the birefringence of the material and, thus, it changes the ellipticity of the probe beam. This change in ellipticity breaks the balance between the two polarization and, therefore, a net current is generated at the photodiodes assembly that is proportional to the amplitude of the electric field of the THz wave. Autobalanced detectors based on EO sampling are commercially available.

For optical bench alignment, there are three main critical components: paths for pump beam, probe beam and detection system.The pump beam contains transnational stage providing mechanical delay, THz emitter and radiation optics.The probe beam path consists of balanced photodetector and electro-optic (EO) detection system. Both the beams have to combine at the detector, meaning the paths should be of equal length. The alignment is mostly done for THz path and detector since they probe to vibrational noises from the surroundings. It is advisable to safeguard it with compressed air cushion so that the bench is always floating.

While aligning, the pump beam should always pass through the center of the irises and could be either focused or collimated. The bench at QMUL is installed for focused

measurements. The four parabolic mirrors are placed in two pairs and the incoming THz is focused at the center, where a sample holder mount is placed. For EO detection system, ZnTe crystal, quarter wave place(QWP), wollaston prism,balanced photodiode detector and two flat mirrors are aligned consecutively. The probe beam is first made to coincide with pump beam. For final aliment, the pump beam is blocked. Overall, the alignment is very mechanical, i.e., the specific location of components cannot be calculated, it depends on direction of laser beam to getting maximum intensity. As a final step, two flat surface mirrors are used to direct the two beams accurately onto the two balanced diodes.

3.2.1 Anatomy of Human Skin

Skin layer can be divided into three major layers: epidermis, dermis and fat with definitive thickness and functionality. However, the structure is far more complex and random. In this study, the skin for in-body network is investigated for three fold reasons: firstly, most of the in-body functioning or dis-functioning affects the skin (and water concentration). Secondly, skin is rich in biological entities and structures such as blood vessels, sweat ducts, capillaries, proteins etc., and finally it is easily accessible for measurement making it a versatile subject of THz-TDS.

Skin in the human body is a protective layer, sensor of multiple parameters such as pressure and temperature. The epidermis is the thin outer layer (as shown in Fig.3.6), which can be further divided as: Stratum Corneum (SC), Keratinocytes and Basal membrane. SC consist of mature keratinocytes, which contains fibrous protein namely keratin. The layer just beneath is keratinocytes containing live cells that mature and forms SC. The deepest layer of epidermis is the basal membrane responsible for preparing new keratinocytes and replacing the old ones [28, 29]. The thickest (around 3 mm) of all is the dermis (Fig.3.5) lying just beneath epidermis, which houses vital entities such as sweat glands, hair follicles (as shown in Fig.3.5 (b and c)), and nerve endings. This layer is rich in proteins such as elastin, fibrin, fibrogen and collagen. Collagen forms an extra cellular matrix, acting as scaffolding for the dermis. The last layer of the skin is a network of collagen and fat cells, known as subcutaneous layer.

The subsequent section in this chapter aims to characterize real human skin via THz-TDS, while evaluating material properties and comparing the measured results to numerical data. The sample consists of two layers: epidermis and dermis, however, epidermis is very thin in comparison to dermis. In this work, the material properties of dermis part of the skin are investigated. The epidermis mainly consists of keratinocytes and dermis is a result of many protein structures and fibroblast cells. Although epidermis is an amalgamation of many

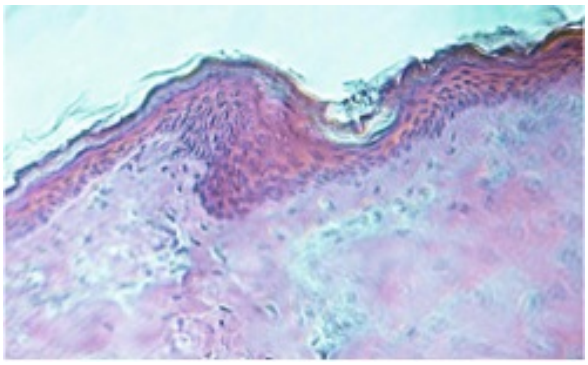

(a) Histology of breast tissue stained with H and E with traces of blood, visible as bright red lines in contract to the pink color of the remaining part

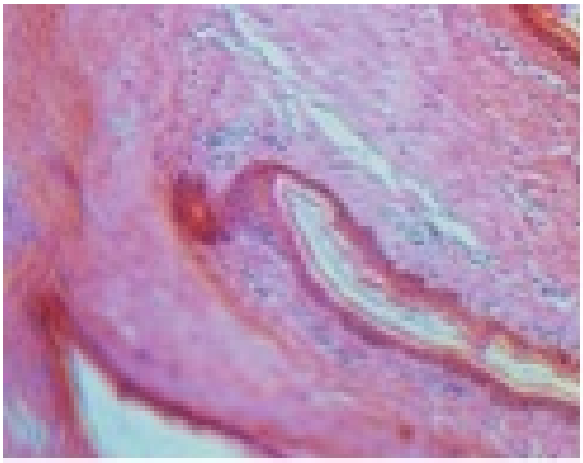

(b) Longitudinal section of the hair follicle attached to a sweat duct in the dermis layer

(c) Cross-section of oval shaped hair follicle structure. The hair follicles are mainly present in dermis layer acting as sensory receptors

Fig. 3.5 Microscopic image of real human skin presenting the two defined layers: Epidermis and Dermis. The sample sections were stained using Haematoxylin (purple/blue stain) and Eosin (red/pink stain), used for identifying nuclei and cytoplasm respectively. Stratum Corneum (SC) traces were visible in the microscopy, however the thickness is not quantifiable

different layers as explained before but this is challenging to identify at a microscopic level. However a layer of stratum corneum is slightly visible.

3.2.2 THz Time Domain Spectroscopy of The Human Skin

Human skin is mainly composed of water [30], which leads to high absorption of THz radiation during the measurement. Hence, in this section the material properties of dry skin samples are investigated, which have been stored in glycerol over the past 10 years aiding in preserving the structural integrity of the tissue. This is mainly for controlled experimental purposes and also provides the cornerstone for measuring the effects of sample dehydration at THz frequencies. Moreover, freshly excised skin samples are measured to account for parallel studies. Glycerol treated samples; specifically the dermal layer remains unperturbed, when examined in standard light microscopy. When comparing to a freshly excised skin the only change that would be expected is the hydration level. Since, these samples have been preserved for over a span of 10 years, their hydration level is expected to be low. Hence only observe shrinkage of some keratinocytes is observed, which indicated the dehydration of tissue samples [31]. To validate this morphological behaviour, the sample images were recorded through standard optical microscope (Fig.3.5).

The biological studies are performed in collaboration with the Subcutaneous group of the Blizard Institute at QMUL. The sample initially consisted of the following layers: epidermis, dermis and fat. From the measurement perspective, the main focus is investigating the different layers of the skin; for the same reason dermis layer was sliced and separated from fat, since this layer is the thickest and adobe of many biological entities. The samples were wedged between two TPX (Polymethylpentene) slabs with a spacer of known thickness. TPX is used as a sample holder, since it is transparent to THz radiation; the light is mostly transmitted through the sample with minimal absorption in TPX [33]. In this case, for reference Polymethylpenthene (TPX) polymer slabs of 2.71 mm thickness was used as it has a low-loss refractive index 1.46 and absorption coefficient was reported less than 1 cm^{-1}. The sample is measured by wedging it between TPX slabs mounted in a bruker liquid cell (sample holder) with a polytetrafluoroethylene (PTFE) spacer of thickness 200 μm. A lock-in amplifier modulates the THz signal and records the detected signal. The time domain data is recorded on the computer for air, TPX and collagen gels remotely using customized LabView® program.

These measurements are performed applying the aforementioned THz TDS system and therefore phase and amplitude information are collected and post processed using transfer equation based algorithm (section 2.3.1). The TDS pulses are generated and detected via mode locked laser. The lock-in amplifier locks and records the detected THz data for all

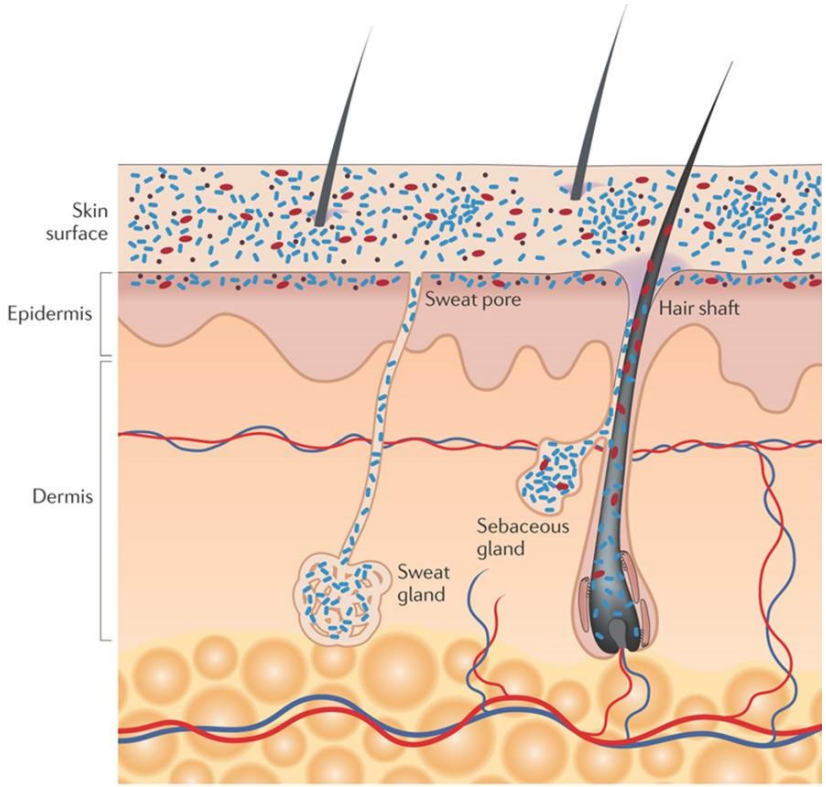

Fig. 3.6 Illustration of different layers of human skin where the skin surface is stratum corneum layer of thickness approximately less than 100 μm and just below is epidermis and dermis with an effective thickness of around 3 mm [32]

three samples – air, TPX and skin and is aided by a computer-generated program written in LabView®. In this study, the incoming THz signal consists of total 1024 consecutive samples, which are recorded at each position of the delay stage. THz-time domain data takes the form of a single pulse, with a period of 1 ps, followed by a series of attenuated pulses arising either from reflections at the interface of components within the TDS system, or from etalon (Fabry-Perot) reflections within the sample itself.

3.2.3 Skin Tissue Electric Properties Extraction

To quantify the interaction of THz wave with given samples, at least two basic material parameters needs to be determined i.e., refractive index and absorption coefficient. The measured time domain data is converted to frequency domain by using Fast Fourier Transform (FFT) to acquire amplitude and phase information.

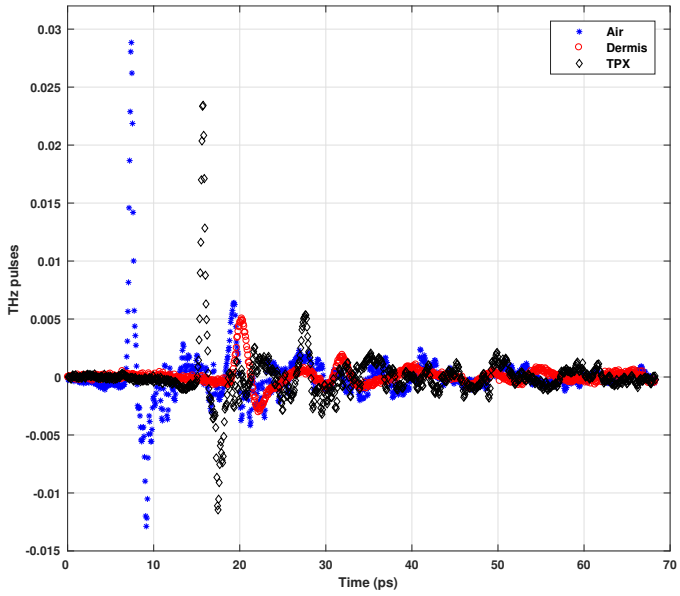

Fig. 3.7 Measured THz pulses through air, TPX and tissue. As expected the biological sample is highly attenuated and second peak is almost lost due to absorption with maximum peak value of 2.2 mV in comparison to air with second peak value of 6.7 mV

The measured time domain signal for the sample, air and TPX are shown in Fig.3.7 and it can be seen from the figure that the biological sample is highly attenuated and the second peak is almost diminished for the sample. The transmission through TPX is used as a reference data with its main peak at 15.7 ps and attenuated satellite peak at 27.6 ps. In order to extract the material properties, it is essential to have a time delay between the reference

and sample data. Figure 3.7 shows that the sample is shifted with respect to TPX with its main peak at 20 ps and satellite peak at 31.9 ps. The oscillations and attenuation in the data is due to presence of water vapour in the atmosphere.

The results for refractive index and absorption coefficient are illustrated in Fig.3.8 (a and b) respectively. Results show that refractive index values decreases and absorption coefficient increases with frequency, which depends on the sample type and dynamic range of the system. Table 3.1 shows the extracted parameters at certain chosen frequencies. The measured refractive index results are compared with [34, 35] and are in agreement with the published literature; however it's still a challenge to predict the nature and biological details of the samples.

The samples used in these papers, were either sliced porcine, in-vivo human skin or frozen samples. For in-vivo skin, the measurements were done directly on the volunteers. It is important to note that skin structure is layered and intricate; therefore it is essential to comprehend material properties of different layers of the skin. In this paper, we deliberately measured dermis layer of the skin and found out that at 1 THz the refractive index value is 2.1, which decreases to 1.8 at 1.2 THz. The absorption coefficient values are considerably low due to uniform dehydration of the sample. This amounts to the fact that water in tissue dermis layer plays a significant role when interacting with THz radiation. Repeatability of experimental techniques and hence stability of obtained parameters value is investigated by repeating each measurement four times on the same sample with the thickness intact resulting in consistent refractive index value.

Table 3.1 Measured Refractive Index and Absorption Coefficient

Frequency(THz)	Measured Refractive Index(n)	Absorption Coefficient (α,cm^{-1})
0.8	2.33	8.96
1	2.10	18.45
1.2	1.81	27.55

The presented experimental results on refractive index and absorption are utilized to evaluate the path loss and molecular absorption noise temperature of the THz channel in human tissues. These are based on radiative transfer theory and can be divided as: the spreading path loss and the absorption path loss as explained in section (2.2.1). The pathloss is as a result of absorption and spreading pathloss. These parameters significantly influence the propagation schemes. It is illustrated that the value is significantly low due to absence of water in the tissue. The noise tends to increase with the increase in frequency; however this

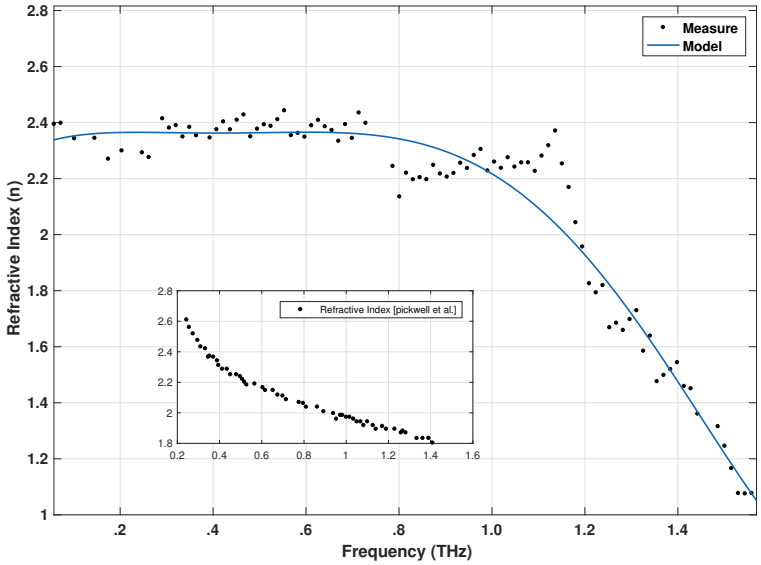

(a) Refractive index as a function of frequency

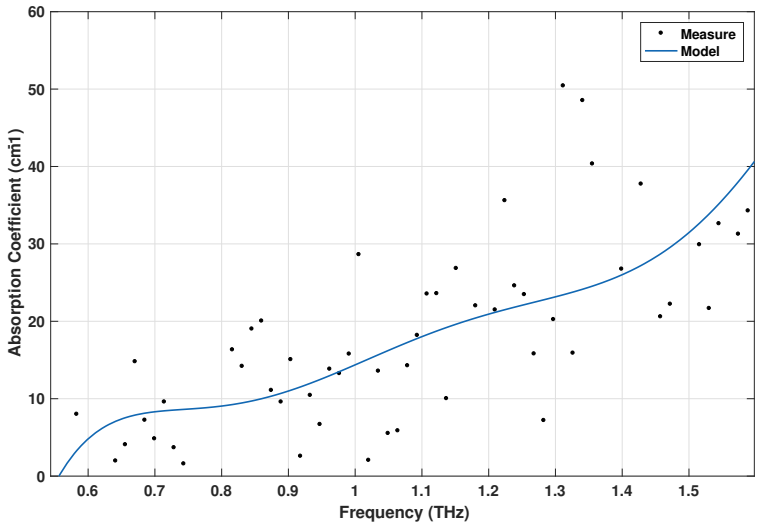

(b) Absorption coefficient as a function of frequency

Fig. 3.8 Extracted (a) refractive index, which decreases with the increasing frequency from 0.8 THz to 1.2 THz (b) absorption coefficient; the alpha value is significantly low due to the dehydration and the main absorption of THz radiation is as a result of atmospheric water vapour

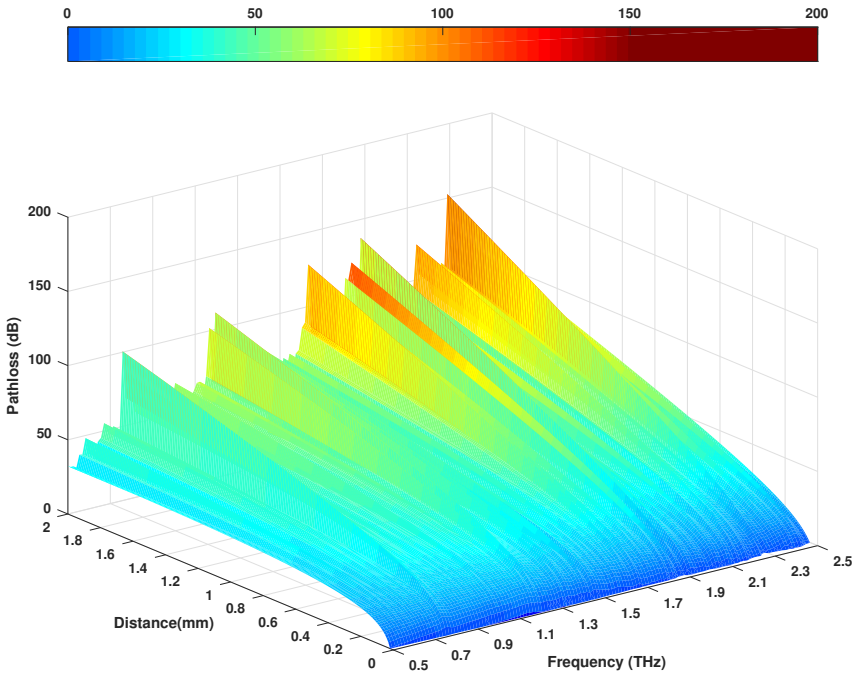

(a) Total pathloss of dehydrated dermis layer

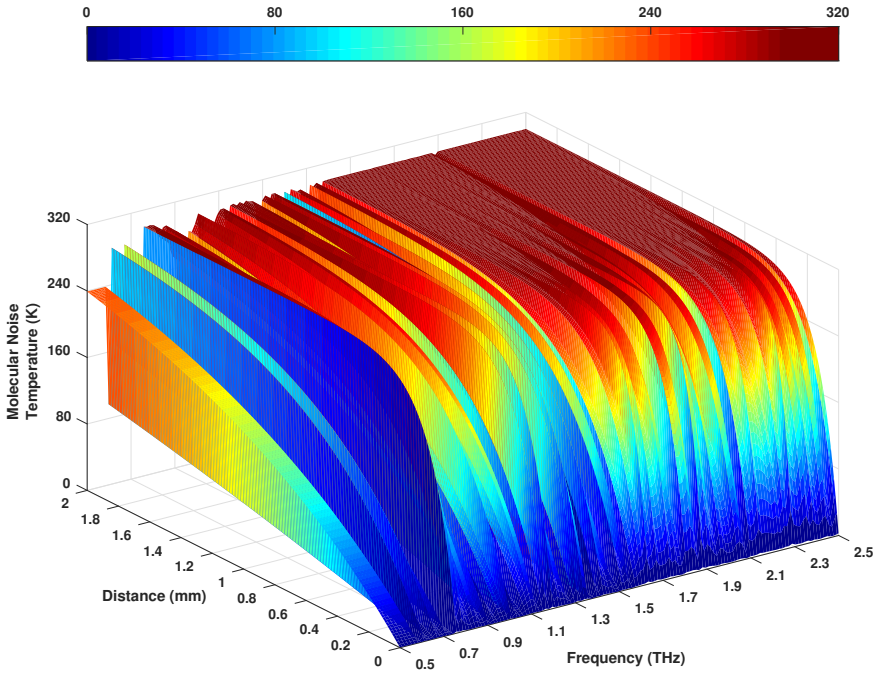

(b) Molecular noise temperature (Kelvin) of dehydrated dermis layer

Fig. 3.9 The figure illustrated (a) total pathloss and (b) molecular noise temperature as a function of distance and frequency for human skin

is rather fluctuating and not gradual owing to the fact that noise spectral density is influenced by molecular absorption.

The two-channel modelling features (i.e, path loss and noise temperature) are illustrated in Fig.3.9 (a and b) accentuating the premise of this experimental study. Total pathloss as shown in Fig.3.9 (a) is a sum of spreading and absorption pathloss and vary as a function of frequency and distance. At 1 THz and at the distance of 1 mm, the pathloss is around 52.12 dB, which gradually increases with distance and frequency. The results presented in this paper are for dehydrated sample; hence the absorption due to water is relatively low. In [36], the numerically modelled skin pathloss is around 150 dB at 1 THz, which is higher as compared to the results presented in this paper hence illustrates that water present in the dermis is the main source of attenuation and need further research. The sample has no traces of stratum corneum but thin layer of epidermis and hair follicles are still present. Thus, these results encompass attenuation due to microscopically visible biological entities present in the tissue.

The molecular noise temperature for real skin is shown in Fig.3.9 (b). It can be seen that the noise temperature increases with the increase in frequency and distance, which will lead to the rise of the noise power. Theoretical results illustrated in paper [37, 36], highlights that at a millimetre level, the noise temperature is not very high (300 K). Experimental results validates that up to 1 mm, the noise level is permissible for a communication link to exist inside the dermis layer. However, further research is needed to investigate these parameters for different layers of skin and from different parts of the body. Results in this paper highlight that the path loss is not only the function of distance and frequency but also related to the dielectric loss of human tissues.

3.3 Chapter Summary

Nano-networks aim to offer comprehensive and unambiguous healthcare solutions for medical diagnostic systems. The study of optical properties via THz TDS contributes to intricate and vital human body information. The results presented in this paper sustain consistency of the biological sample. The characterization of dehydrated sample attributes to a low absorption coefficient value as compared to fresh tissue. This study suggests that water plays a vital role even when optimizing channel models. The noise temperature results, up to 1 mm proves to be substantial for establishing communication links in the skin dermis layer. The results of this study are significant for optimizing future in-body Nano-networks inside the human body. These results aid to applications in medical sensor technologies for tumours and breast cancer owing to the sensitivity of THz-TDS to water dynamics. The next steps aim to encompass

fresh tissues while considering tissues from various parts of the body in addition to different layers of the skin to outline complete understanding of the skin properties in the THz range.

References

[1] Q Wu and X-C Zhang. Free-space electro-optic sampling of terahertz beams. *Applied Physics Letters*, 67(24):3523–3525, 1995.

[2] Xi-Cheng Zhang and Jingzhou Xu. *Introduction to THz wave photonics*, volume 29. Springer, 2010.

[3] Peter R Smith, David H Auston, and Martin C Nuss. Subpicosecond photoconducting dipole antennas. *IEEE Journal of Quantum Electronics*, 24(2):255–260, 1988.

[4] Peter Uhd Jepsen and Bernd M Fischer. Dynamic range in terahertz time-domain transmission and reflection spectroscopy. *Optics letters*, 30(1):29–31, 2005.

[5] Yun-Shik Lee. *Principles of terahertz science and technology*, volume 170. Springer Science & Business Media, 2009.

[6] C Winnewisser, P Uhd Jepsen, M Schall, V Schyja, and H Helm. Electro-optic detection of THz radiation in LiTaO 3, LiNbO 3 and ZnTe. *Applied Physics Letters*, 70(23):3069–3071, 1997.

[7] Mira Naftaly. *Terahertz metrology*. Artech House, 2015.

[8] Masahiko Tani, Shuji Matsuura, Kiyomi Sakai, and Shin-ichi Nakashima. Emission characteristics of photoconductive antennas based on low-temperature-grown GaAs and semi-insulating GaAs. *Applied optics*, 36(30):7853–7859, 1997.

[9] DH Auston, KP Cheung, and PR Smith. Picosecond photoconducting Hertzian dipoles. *Applied physics letters*, 45(3):284–286, 1984.

[10] Matthew C Beard, Gordon M Turner, and Charles A Schmuttenmaer. Subpicosecond carrier dynamics in low-temperature grown GaAs as measured by time-resolved terahertz spectroscopy. *Journal of Applied Physics*, 90(12):5915–5923, 2001.

[11] DH Auston and PR Smith. Generation and detection of millimeter waves by picosecond photoconductivity. *Applied Physics Letters*, 43(7):631–633, 1983.

[12] Ingrid Wilke and Suranjana Sengupta. Nonlinear Optical Techniques for Terahertz Pulse Generation and Detection ,Optical Rectification and Electrooptic Sampling. In *Terahertz spectroscopy: Principles and applications*, pages 41–72. CRC press, 2007.

[13] Arūnas Krotkus. Semiconductors for terahertz photonics applications. *Journal of Physics D: Applied Physics*, 43(27):273001, 2010.

[14] Lionel Duvillaret, Frédéric Garet, J-F Roux, and J-L Coutaz. Analytical modeling and optimization of terahertz time-domain spectroscopy experiments, using photoswitches as antennas. *IEEE Journal of Selected Topics in Quantum Electronics*, 7(4):615–623, 2001.

[15] Zhi-Sheng Piao, Masahiko Tani, and Kiyomi Sakai. Carrier dynamics and THz radiation in biased semiconductor structures. volume 3617, pages 49–56, 1999.

[16] Kiyomi Sakai and Masahiko Tani. Introduction to terahertz pulses. In *Terahertz optoelectronics*, pages 1–30. Springer, 2005.

[17] Matthias Clemens Hoffmann. Novel techniques in THz-time-domain-spectroscopy. 2006.

[18] Dwight L Woolard, William R Loerop, and Michael S Shur. *Terahertz Sensing Technology: Volume 1: Electronic Devices and Advanced Systems Technology*, volume 30. World Scientific, 2003.

[19] Bahaa EA Saleh, Malvin Carl Teich, and Bahaa E Saleh. *Fundamentals of photonics*, volume 22. Wiley New York, 1991.

[20] Xiaoxia Yin, Brian W-H Ng, and Derek Abbott. *Terahertz imaging for biomedical applications: pattern recognition and tomographic reconstruction*. Springer Science & Business Media, 2012.

[21] Lionel Duvillaret, Frederric Garet, and J-L Coutaz. A reliable method for extraction of material parameters in terahertz time-domain spectroscopy. *IEEE Journal of selected topics in quantum electronics*, 2(3):739–746, 1996.

[22] Lionel Duvillaret, Frederic Garet, and Jean-Louis Coutaz. Highly precise determination of optical constants and sample thickness in terahertz time-domain spectroscopy. *Applied optics*, 38(2):409–415, 1999.

[23] Timothy D Dorney, Richard G Baraniuk, and Daniel M Mittleman. Material parameter estimation with terahertz time-domain spectroscopy. *JOSA A*, 18(7):1562–1571, 2001.

[24] Withawat Withayachumnankul. Engineering aspects of terahertz time-domain spectroscopy. 2009.

[25] Martin C Nuss and Joseph Orenstein. Terahertz time-domain spectroscopy. In *Millimeter and submillimeter wave spectroscopy of solids*, pages 7–50. Springer, 1998.

[26] Nishtha Chopra, Ke Yang, Qammer H Abbasi, Khalid A Qaraqe, Mike Philpott, and Akram Alomainy. THz Time-Domain Spectroscopy of Human Skin Tissue for In-Body Nanonetworks. *IEEE Transactions on Terahertz Science and Technology*, 6(6):803–809, 2016.

[27] Trung Quan Luong. Terahertz and Infrared Spectroscopy of Confined Water. 2012.

[28] David Gawkrodger and Michael R Ardern-Jones. *Dermatology: an illustrated colour text*. Elsevier Health Sciences, 2016.

[29] Cédric Blanpain and Elaine Fuchs. Epidermal homeostasis: a balancing act of stem cells in the skin. *Nature reviews Molecular cell biology*, 10(3):207–217, 2009.

[30] HH Mitchell, TS Hamilton, FR Steggerda, and HW Bean. The chemical composition of the adult human body and its bearing on the biochemistry of growth. *Journal of Biological Chemistry*, 168:625–637, 1945.

[31] CD Richters, MJ Hoekstra, J Van Baare, JS Du Pont, and EWA Kamperdijk. Morphology of glycerol-preserved human cadaver skin. *Burns*, 22(2):113–116, 1996.

[32] Elizabeth A Grice and Julia A Segre. The skin microbiome. *Nature Reviews Microbiology*, 9(4):244–253, 2011.

[33] JR Birch and EA Nicol. The FIR optical constants of the polymer TPX. *Infrared physics*, 24(6):573–575, 1984.

[34] E Pickwell, BE Cole, AJ Fitzgerald, M Pepper, and VP Wallace. In vivo study of human skin using pulsed terahertz radiation. *Physics in Medicine and Biology*, 49(9):1595, 2004.

[35] Elizabeth Berry, Anthony J Fitzgerald, Nickolay N Zinov'ev, Gillian C Walker, Shervanthi Homer-Vanniasinkam, Caroline D Sudworth, Robert E Miles, J Martyn Chamberlain, and Michael A Smith. Optical properties of tissue measured using terahertz-pulsed imaging. pages 459–470. International Society for Optics and Photonics, 2003.

[36] Giuseppe Piro, Ke Yang, Gennaro Boggia, Nishtha Chopra, Luigi Alfredo Grieco, and Akram Alomainy. Terahertz communications in human tissues at the nano-scale for healthcare applications. *IEEE Transactions on Nanotechnology*, 14(3):404–406, 2015.

[37] Ke Yang, Alice Pellegrini, Max O Munoz, Alessio Brizzi, Akram Alomainy, and Yang Hao. Numerical analysis and characterization of THz propagation channel for body-centric nano-communications. *IEEE Transactions on Terahertz Science and Technology*, 5(3):419–426, 2015.

Chapter 4

Characterization of Freshly Excised Breast and Abdomen Skin Using THz-TDS

This chapter focuses on THz-time domain spectroscopy of freshly excised skin tissues from different parts of the body namely, breast and abdomen. Intricate biological features like the change in hydration level, fibre orientation and density of extra-cellular matrix (dermis layer) are explored. Further more experimentally evaluated material properties are extracted and applied to analytical and analysis of the THz propagation channel characteristics.

4.1 Breast and Abdomen Tissue Morphology

The characteristics of electromagnetic waves propagating inside human body at THz frequencies have been studied in , which shows that path loss has a relation with the absorption coefficient of human tissues [1]. In [2], the electrical properties (conductivity and permittivity values) of each layer have been investigated depending on the water content of each layer. The skin tissues were represented by a three-layer simplified structure i.e. stratum corneum (SC), epidermis, and dermis and dimensions are shown by standard light microscope images (Fig.4.1 and 4.3). The roughness of boundaries between the SC and epidermis was considered in the skin model as the order of magnitude for THz wavelength and roughness dimensions were comparable, since sweat glands are distributed almost all over the human body and represent a form of cooling in humans [3].

Although a virtual computational environment provides freedom to create heterogeneous layered skin structure with different thickness, boundary conditions and other electrical

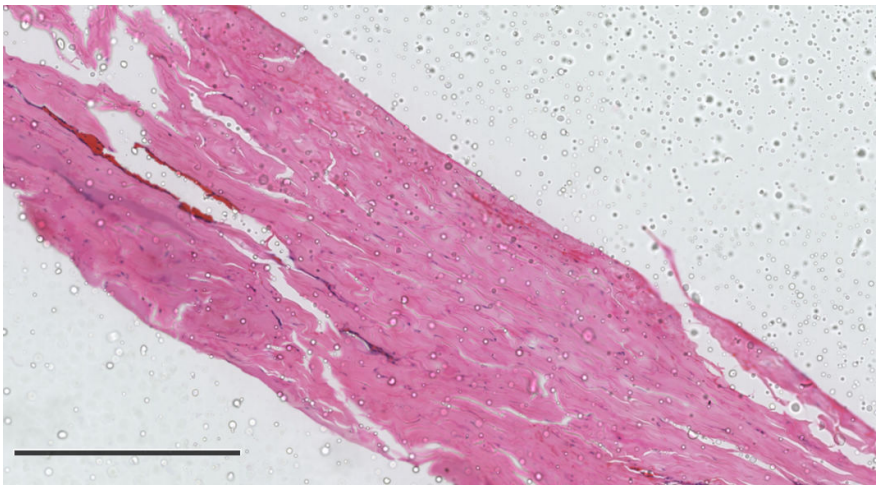

(a) Histology of breast tissue stained with H and E with traces of blood, visible as bright red lines in contract to the pink colour of the remaining part

(b) Histology of breast tissue stained with H and E with traces of Stratum Corneum layer as seem from the top by a standard light microscope

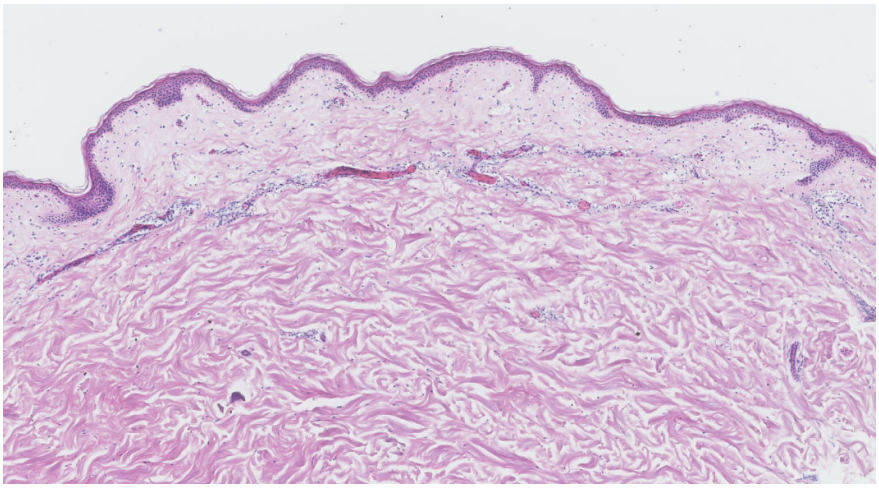

(c) Histology of breast tissue with defined layers of the skin

Fig. 4.1 Standard light microscope imaging of breast tissue focusing on the fibre orientation formation in the extra-cellular matrix.

parameters to generate propagation theories. However, it is still essential to perform experimental validation for real-time results. To address various factors involved in designing an experiment, animal tissues were initially employed, especially rats to investigate the physiological parameters. The bio-sensors and implantable antennas were inserted in the interstitial fluid under the skin to access body temperature, blood pressure and other vitals [4]. Thus with the impending nanodevices and its potential health diagnostic applications, channel parameters were evaluated in chapter 2, for dried human skin tissue with focus on the influence of hydration of the skin on pathloss and molecular noise temperature. In this chapter, channel parameters are characterized for freshly excised skin tissue from different parts of the body namely, breast and abdomen and also data is extracted for skin parameters at different angles of THz-TDS bench sample holder.

Normal human breast reduction and abdominoplasty skin specimens from female patients aged 30-35 were obtained with informed consent. The East London and City Health Authority Research Ethics Committee approved the use of redundant human skin and the protocols for obtaining patient skin biopsies (09/HO704/69). Excess adipose tissue was removed and skin samples were trimmed to 2x3 cm^{-1}. All the samples (Fig.4.5) were acquired from the Blizard Institute, Barts and London School of Medicine and Dentistry, London. The samples were obtained within a few hours of surgery and stored overnight in growth media - Dulbecco's Modified Eagle's Medium (DMEM,Sigma Aldrich) to keep the morphology intact. The human breast is an inhomogeneous mixture of fat cells and proteins, where in, water and lipid concentration is 31% and 57%, respectively [5, 6]. It is composed of the superficial epidermis which contains keratins and melanin and the underlying dense collagenous dermis which contains a very intricate network of dermal blood and vessels that lie close to the skin surface. As elsewhere on the human body, the abdominal skin is transgressed by langer lines, also called cleavage lines. This is a term used to define the direction within the skin along which the skin has the least flexibility and corresponds to the alignment of the collagen fibres within the dermis [7].

4.1.1 Tissue Measurement

THz spectroscopy of the samples was done in transmission mode by carefully wedging the samples between TPX plates. The thickness of 210 μm was defined with help of a plastic spacer. Excess water and media was removed by placing the samples for 15minutes in a 50 μm sterile cell strainer and later pat drying with a tissue paper. There were clear differences in both tissue appearances - breast tissue (Fig.4.5(a and b)) was more pink than abdominal tissue, having smooth surface with some traces of blood.

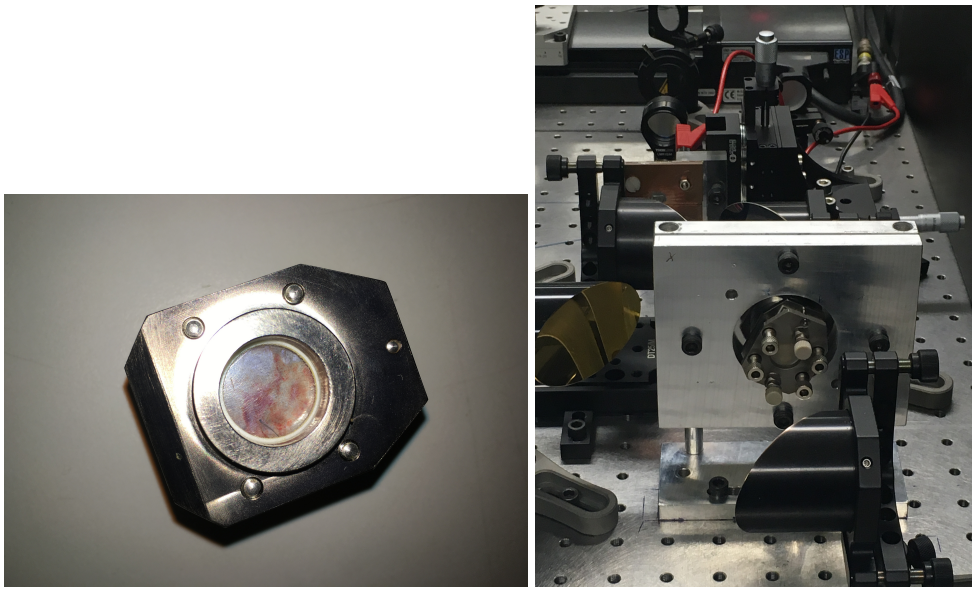

(a) (b)

Fig. 4.2 (a) The breast tissue pressed gently to a thickness of 200 μm with visible traces of blood (b) Sample holder rotated to an angle of 45° in the x-y plane with respect to the bench

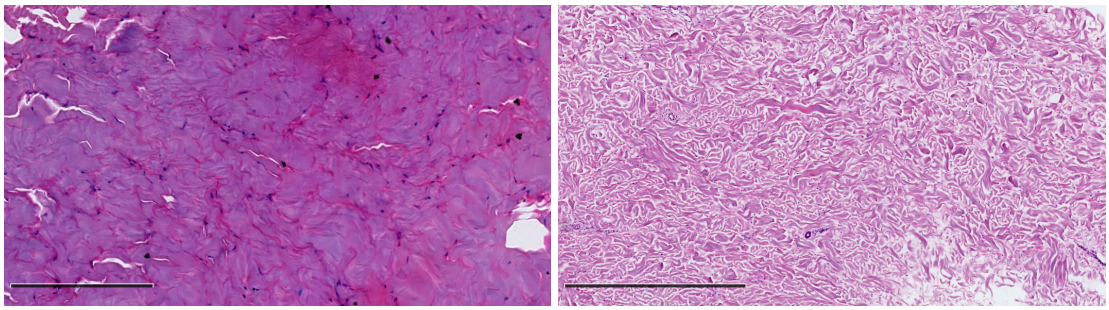

(a) Histology of abdominal tissue illustrating a dense fibrous structure

(b) Histology of abdominal tissue illustrating intricate dermis fibres

Fig. 4.3 Standard light microscopy imaging of abdominal tissue. When compared to breast tissue history, the abdominal tissue seems to have a denser extra cellular matrix

The abdominal tissue on the other hand, had surface wrinkles and traces of fat below the dermis. Once the sample are fixed to the holder on the THz optical bench, the ultra-short pulses propagate through the sample and the data acquisition happens in time-domain. Further, the same extraction procedure is followed as discussed in chapter 2.

4.2 Characterization and Extraction of Optical Parameters of Real Skin Tissues

The sample holder (Fig.4.2 and 4.4) is fixed on a magnetic mount, in a way that the incoming THz beam is transmitted through the sample at room temperature between 23-24°C. The excised tissue samples were sliced in rectangular shapes to fit the sample holder and THz scanning was performed for about 4-5 times to verify the consistency of the data. The time domain data was obtained from the measurement and Fourier transform analysis of tissue sample was done. The system is subjected to laser intensity fluctuation and electronic noise in the detection part of the bench. Moreover, varying humidity levels can result in additional water vapour peaks from the atmosphere. A typical working range frequency varies with the sample type and more importantly its hydration level. Usually, the working range is from 0.3-2.5 THz and a gradual roll-off is expected at high frequencies until the detected signal level approaches that of the noise floor.

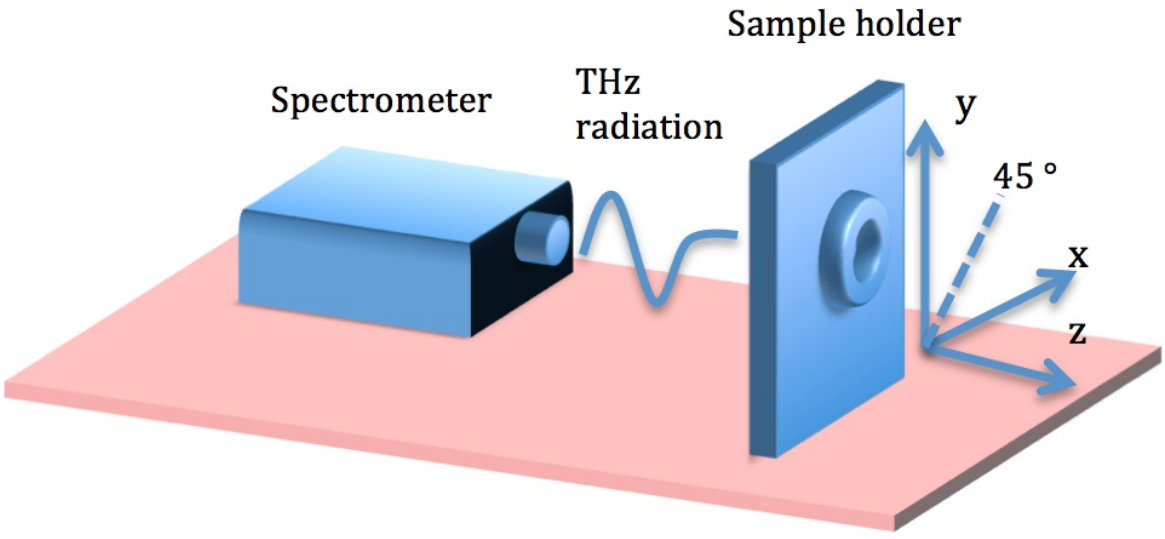

Fig. 4.4 Schematic of THz bench with sample holder rotation

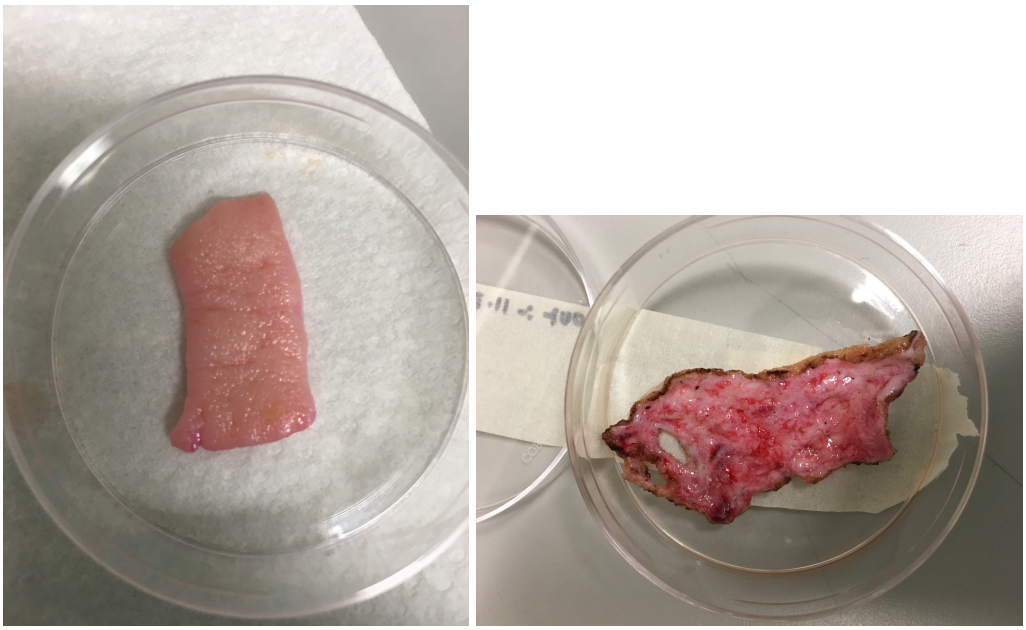

(a) Abdominal tissue (b) Breast tissue

Fig. 4.5 Freshly excised tissue sliced for THz-TDS measurement

In figure 4.6, the refractive index of breast tissue is illustrated at a rotation of 0° and 45°. The difference in phase spectra of the sample in comparison to that of reference, influences the refractive index value. In Fig.4.6a, the empirical values at 0.8THz and 1THz are 2.01 and 2.36 respectively, while the modelled values at the same frequencies are 2 and 2.43 with a root mean squared error (RMSE) of 0.068. Non-linear least square model fitting was done with the help of Matlab (version 9.1.0.441655 R2016b) software. The RMSE value provides an error difference between the measured values and predicted by a model. The goodness of the fit was ensured with R-square and adjusted R-square values as 0.998. The R-square values represent the strength of relationship between the measured and modelled values. However, it could easily overestimate the fitted model, this could be prevented by evaluating adjusted R-square values.

In figure 4.6b, the sample holder was rotated to an angle of 45 ° using a standard scale. The motivation behind this measurement was to investigate the refractive index and absorption coefficient value due to the change in tissue fibre orientation. In paper [8], angle-dependent measurement of amino acid crystals was made investigating the absorption spectra from 0° to 90°. Linearly polarized THz radiation with a rotation stage in a THz-TDS spectrometer was used to determine the direction of the oscillating dipole of the molecules in the crystals. From extensive research made in the field of imaging [9], it can be asserted that human tissue is a dense fibrous structure, which is anisotropic in nature. The fibre orientation not only

effect the image analysis, but could exaggerate certain morphological features, that could be captured by incoming linearly polarized THz wave.

The measured refractive index value of breast tissue with 45° rotation is 3.8 and 3.71 at 0.8 THz and 1THz respectively (Table 4.2), whereas modelled values at same frequencies are 3.78 and 3.7 with RMSE of 0.03. As before, the R-square and adjusted R-square value evaluated, is 0.99. Just by comparing the measured values of the figures (4.6 (a and b)), it is clear that the refractive at 45° is increased by a factor of 1.89 at 0.8 THz and 1.56 at 1 THz. The increase could be due to the fact that the THz beam has transmitted through specific regions of the tissue, which reduces the speed of propagation. The time taken by the THz wave at 1 THz, to propagate through tissue with no rotation is 3.36 ps where for rotated tissue, it is 5.04 ps. Hence, it seems that variation in orientation of the fibres could affect the propagation of THz wave inside the tissue.

In the field of biology, collagen fibre orientation affects skin ageing [10, 11], the detailed analysis of which will be formally introduced in chapter 5. Other mechanical changes such as stress (bending or twisting) of the tissue could also affect the THz communication inside the body, hence to establish an in-body network these anomalies are important to address. With the current THz setup, it is hard to exactly highlight the changes in biomolecular activity due significant water absorption. The tissue sample under test has both epidermis and dermis layer (Fig.4.1). Dermis is the dense fibrous extra-cellular matrix whereas epidermis is thin transparent-like barrier layer made of keratinocytes. Biological samples are lossy especially with high sensitivity of THz radiation to water, thus the amplitude values in frequency domain, are significantly reduced. In a natural tissue-like environment the continuum of strongly damped intermolecular modes makes featureless spectra; only at higher (4–10 THz) frequencies are some intramolecular modes in solution observed [12].

Table 4.1 Measured Refractive Index and Absorption Coefficient of breast with 0°rotation

Frequency(THz)	Measured Refractive Index(n)	Absorption Coefficient (α,cm^{-1})
0.8	2.01	181
1	2.43	158
1.2	1.82	365

Table 4.2 Measured Refractive Index and Absorption Coefficient of Breast with 45°rotation

Frequency(THz)	Measured Refractive Index(n)	Absorption Coefficient (α,cm^{-1})
0.8	3.8	9.86
1	3.71	37.09
1.2	3.5	106.3

Breast tissue characterization has been immensely popular in the field of THz imaging for cancer diagnosis. Both the absorption coefficient and refractive index were higher for tissue that contained tumour and this indicates that THz imaging could be used to detect margins of tumour [13]. The comparison between cancerous and normal tissue draws ones attention to the fact, that change in bio-molecular (mainly proteins and water molecules) activity affects the effective morphology. Having said this, the inhomogeneous behaviour of breast tissue could form complex molecular chains thereby affecting the THz optical properties.

The absorption coefficient value is a conspicuous indication of signal attenuation due to polar nature of water [14]. From figure 4.7, the absorption coefficient values increases monotonically with frequency and steeply decreases after 1.2THz due to system's dynamic range. The breast tissue at 0° has an empirical value of 161 cm^{-1} and increases upto 331 cm^{-1} at frequencies 1THz and 1.2THz respectively (Table 4.1). When the sample is rotated to 45°, the value (at same frequencies) are 37 cm^{-1} and 106 cm^{-1}. The absorption spectra was modelled with non-linear least square fitting with RMSE value of 9.05 and 13.27 for 0° and 45°. In addition to this, the R-square and adjusted R-square values for tissue with no rotation is calculates as 0.99 and 0.98, while for the later one it is 0.98 and 0.97 respectively.

On comparing both the values, the absorption spectra significantly decreases when the sample is rotated to an angle of 45°. Since tissue is a complex layered structure, there could be many variables adding to this change - 1) THz wave is sensitive to fibre orientation of the sample ; 2) the THz wave propagation is incident on a specific region of the tissue, indicating the presence of some morphological anomalies. Although more theoretical evidence is required to reason out the measured value. However, at present emphasis is given on the sensitivity of THz-TDS for heterogeneous behaviour of complex tissue.

The abdominal tissue is expected to be more lossy due to high water content and dense extra-cellular matrix. During the data acquisition, most of the time domain value before 0.9 THz were lost owing to THz-TDS electronic noise. However, the system was still able to map the data point from 0.95 THz to 1.6 THz. There scarcity of experimental data for abdomen tissue in regards to THz characterization. However, the biomolecular behaviour and morphology should be similar to skin as for other parts of the human body. The only difference one could expect is the dense extra-cellular matrix and hydration level. The

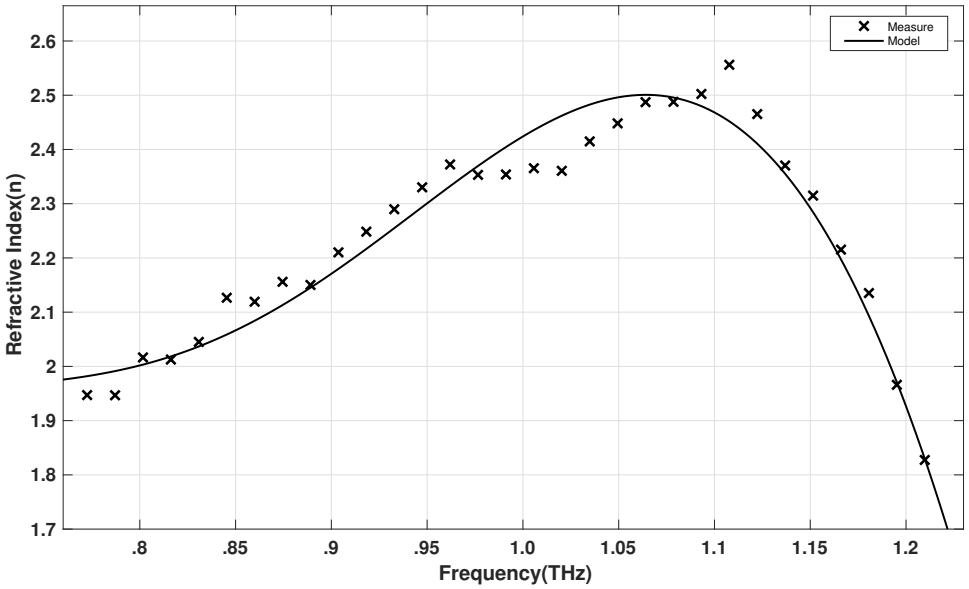

(a) Refractive index of breast tissue at 0 °angle

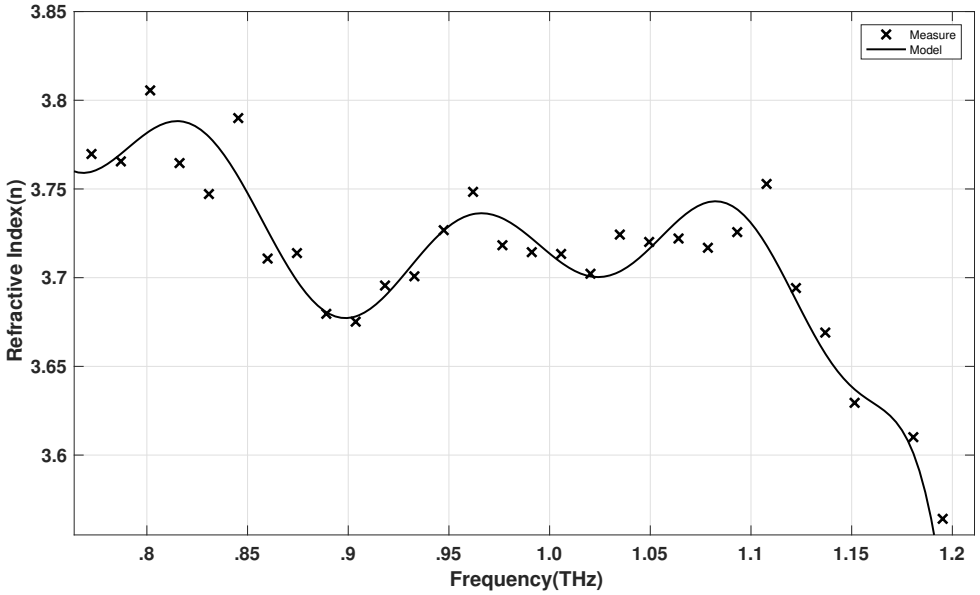

(b) The refractive index spectra of breast tissue when the sample is tilted to an angle of 45°

Fig. 4.6 Empirical value of refractive index for breast tissue ranges from 0.75THz to 1.2THz. Non-linear least square modelling is done to fit the measured value with 95% confidence interval

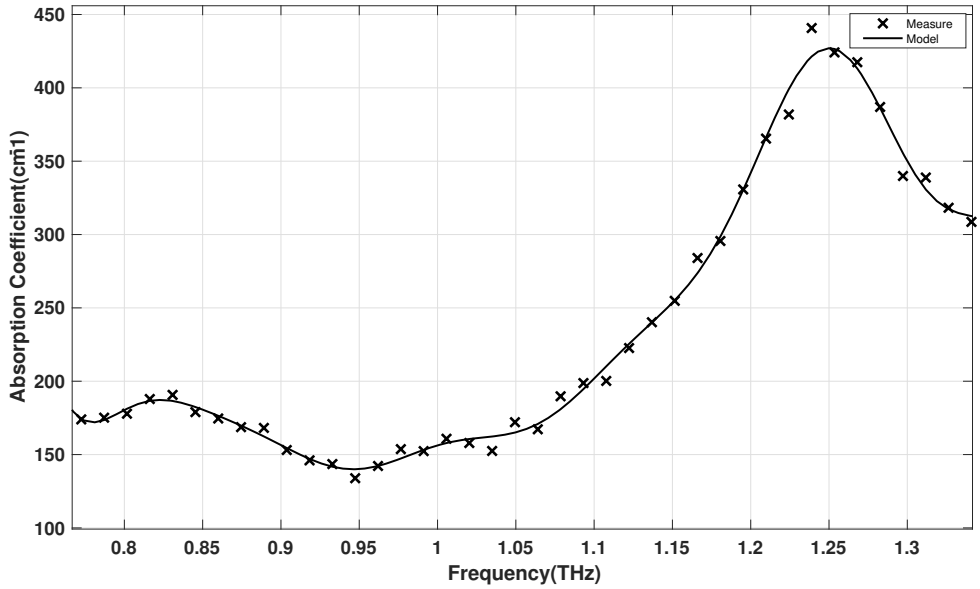

(a) Absorption coefficient of breast tissue at 0°angle with 95% confidence interval

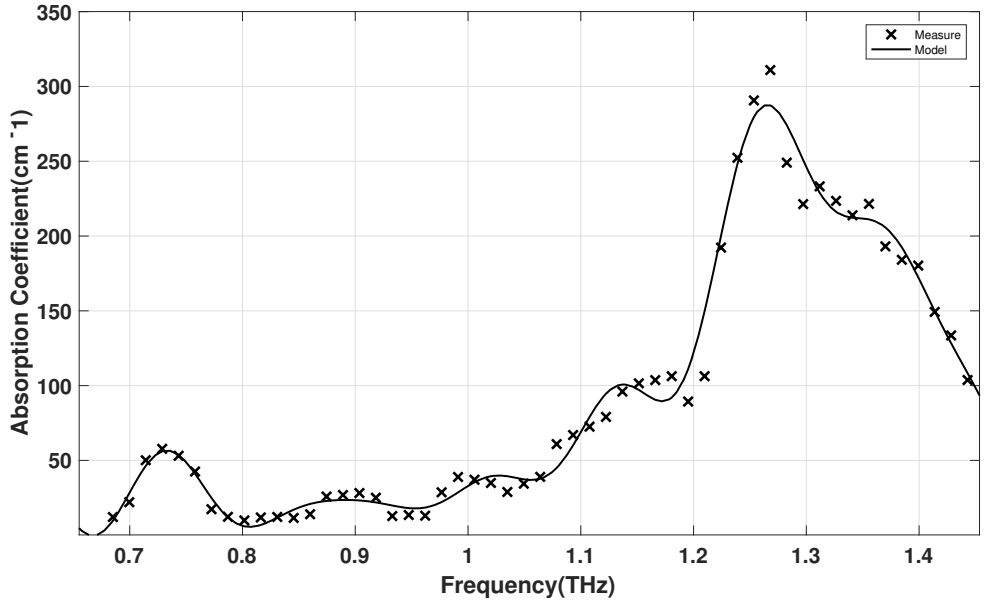

(b) Absorption Coefficient at 45° rotation with 95% confidence interval

Fig. 4.7 Absorption coefficient values of breast tissue increases as a function of frequency and roll-off data after 1.2THz neglected owing to system dynamic range and artefacts

refractive index and absorption coefficient of abdomen tissue are illustrated in figure 4.8 (a and b) respectively. The refractive index value at 1.2THz and 1.4THz is 4.2 and 3.3 respectively (Table 4.3). The refractive index value are much consistent from 1.2 THz to 1.5 THz. The RMSE value is 0.064 and R-square and adjusted R-square values are 0.99. The model values the same set of frequencies (1.2 THz and 1.4 THz) are 4.1 and 3.36 respectively. The excised abdominal tissue seems to have higher percentage of biological water as the absorption coefficient value at 1.2 THz is 198 cm^{-1} and at 1.4 THz is 186 cm^{-1}.

Table 4.3 Measured Refractive Index and Absorption Coefficient of Abdominal Tissue

Frequency(THz)	Measured Refractive Index(n)	Absorption Coefficient (α,cm^{-1})
1	4.22	151.6
1.2	4.21	212
1.4	3.3	199

Apart from the absorption due to atmospheric water vapour, the oscillatory behaviour of the plot could be because of Fabry-Perot reflection when the THz wave is transmitted through the tissue. The modelled value are similar to that of measured with RMSE of 17.85 and R-square and adjusted R-squared values of 0.90 and 0.86 respectively. The above given results represent an ex-vivo study of the optical properties. Due to the current limitations of THz-TDS set-up, in-vivo measurement is complicated and the penetration in transmission geometry will be limited to first few millimetres (stratum corneum and epidermis) of the skin. Hence ex-vivo analysis gives the freedom to study the skin layer by layer and to ensure its exactness to real live human skin, morphological freshness is important after excision.

The above parameters represent the skin properties in the THz region and consequently an effective medium for THz communication for in-vivo nanonetworks.

As already explained, the channel parameters for in-body nanodevice communication: pathloss and molecular noise temperature parameters, are a function of wave propagation distance and frequency. Figure 4.9 (a ,b and c) illustrates the pathloss for breast and abdominal tissue respectively. The empirical values of absorption coefficient and refractive index are use to numerically evaluate the channel parameters. Pathloss is defined by the properties of the medium, which in this case is the excised human skin. With the current state of art, it is challenging to investigate these parameters for live human skin. Hence, an excised skin with intact morphology is assumed to represent the structural properties of different parts of the human body. Within the available range (0.5-2 THz) for THz characterization of skin, it is very unlikely to observe any bio-molecular spectral fingerprints. Hence, the channel

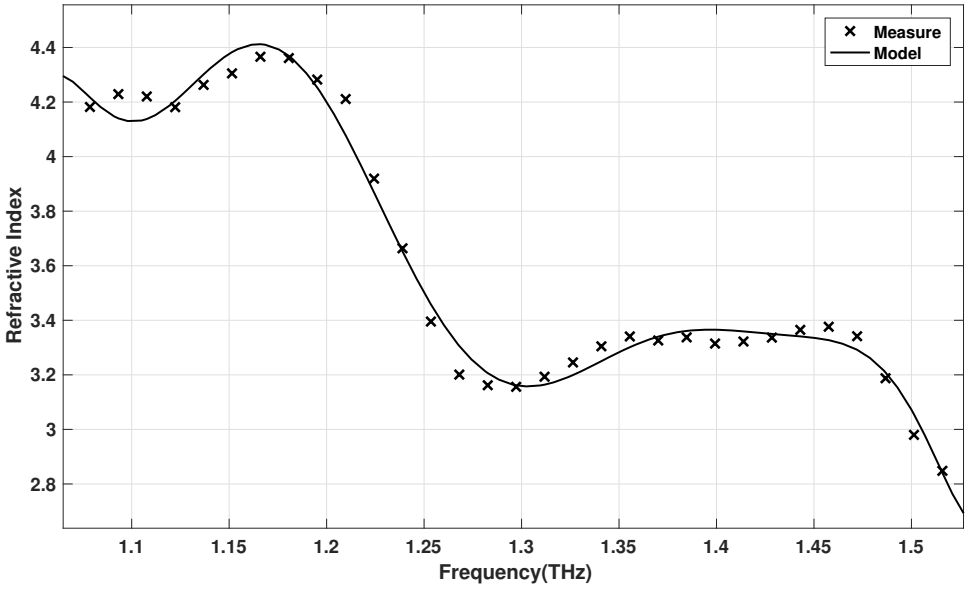

(a) The refractive index spectra for abdominal tissue with 95% confidence interval

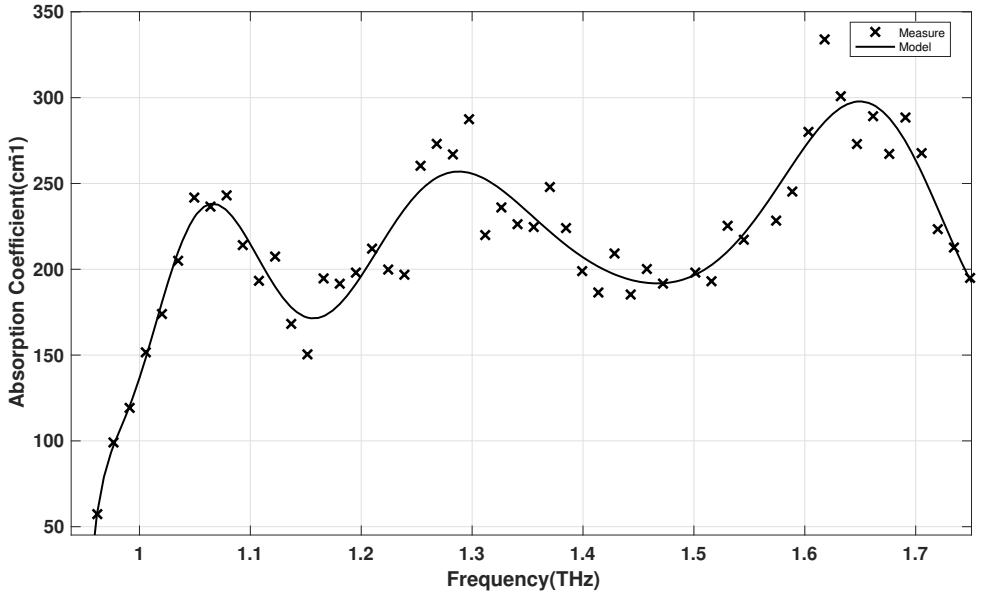

(b) The Absorption Coefficient value of abdominal tissue with 95% confidence interval

Fig. 4.8 Optical parameters of abdominal tissue (a) The refractive index calculated for abdominal tissue with a working frequency range upto 1.6 THz.The spectra below 0.95 THz is disregarded due to signal fluctuations (b) The Absorption Coefficient value at 1 THz is 250 cm^{-1} due to high water concentration of the sample and atmospheric water vapour

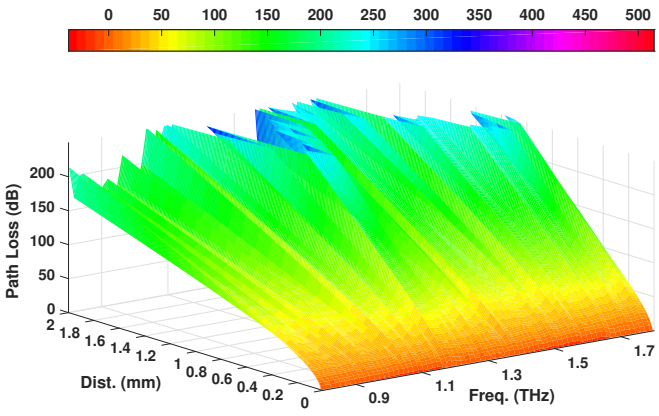

(a) The pathloss for breast tissue with 0° rotation

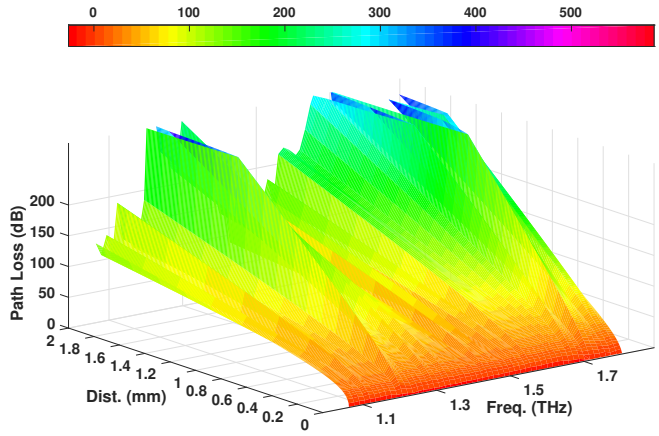

(b) The pathloss for breast tissue with 45° rotation

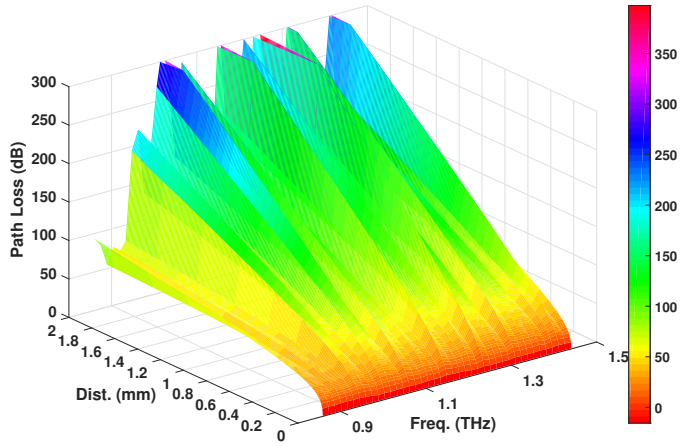

(c) The pathloss for abdominal tissue

Fig. 4.9 The pathloss values for both breast (a and b) and abdomen tissue (c) vary as a function of frequency and distance. The value vary depending on the tissue type and also the fibre orientation. The pathloss for abdomen tissue at 200 μm, 1THz is 53.34 dB where for the breast tissue at 0° rotation is 37 dB

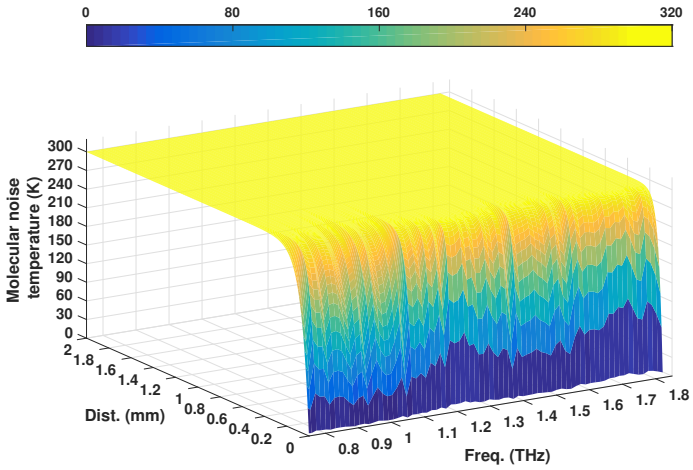

(a) Molecular noise temperature for breast tissue with 0°

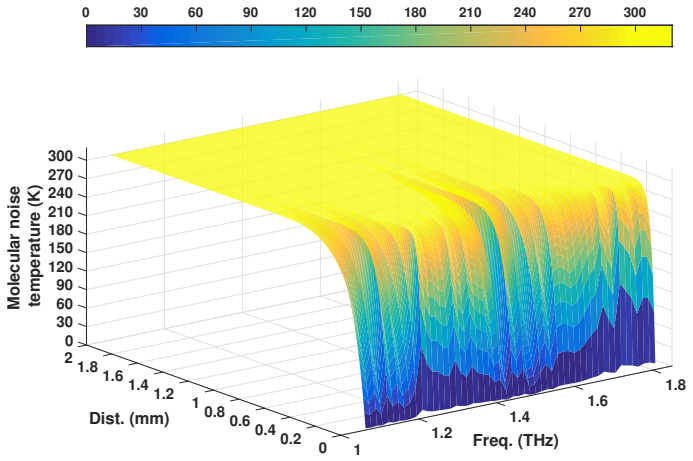

(b) Molecular noise temperature for breast tissue with 45° rotation

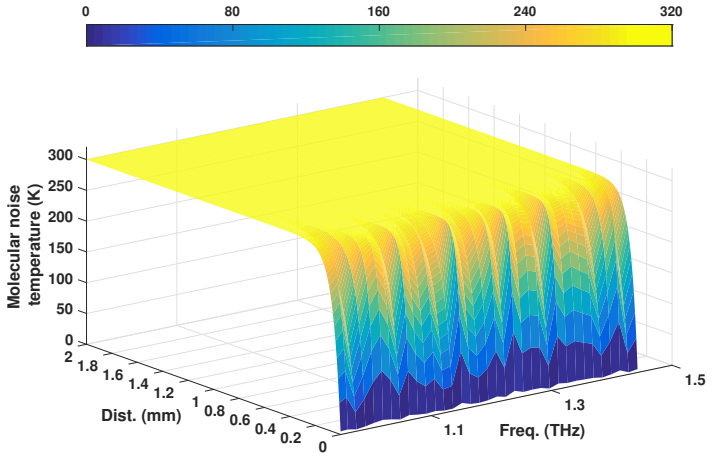

(c) The molecular noise temperature for abdominal tissue

Fig. 4.10 The molecular noise temperature for breast tissue numerically plotted for measured optical parameters. It depends on the absorption due to molecules present in the medium and increases with frequency and distance. For breast tissue with 0°, the value is almost consistent upto 1THz and then monotonically increases. Whereas for 45° rotation, the value is consistent from 1-1.1 THz. Similarly for abdominal tissue, the value to consistent upto 0.9 THz

parameters take into consideration the skin morphology of a few mm-scale. The pathloss is dependent on spreading and absorption of the propagating wave.

The breast tissue (Fig.4.9 (a and b)) at 1THz with no rotation, has a pathloss of 8 dB travelling a distance of 20 μm. To understand in terms of skin morphology (and layers), if it is assumed that the nano-devices are located just at the periphery (just below the outer most later) of stratum corneum, the signal strength is reduced to 8 dB. As the waves transmits further keeping the frequency constant, the signal strength starts to reduce by 1-2dB at a steady rate. Assuming that the path length is same as the thickness of sample measured, at 200 μm the pathloss value is 37 dB. If the frequency is increased to 1.2 THz at a distance of 200 μm ,the pathloss increases to a value of 60dB. Similarly for breast tissue at 45° rotation has a pathloss value (1 THz, 200μm) of 38 dB, suggesting that the angle dependent THz measurement could affect the pathloss as well, specially in medical emergency cases where a skin ageing, disease or an accident can change the tissue fibre orientation. Similarly for abdomen tissue, the value is relatively high (53.34 dB). This suggests that different tissue samples from the same human body vary in hydration level(and biomolecular activity), posing challenges to establish a universal communication channel mapping the entire body.

In paper [15], the total molecular absorption was computed for free space propagation. The pathloss for propagation in air was compared with 0.1 and 10% humidity. Air is a mixture of different gas molecules and water vapours. In the terahertz band, these molecules present in a standard medium significantly affects the channel performance. Due to the spreading loss, the total path loss increases with both the distance and the frequency, independently of the molecular composition of the channel. However, several peaks of attenuation can be observed due to the molecular absorption loss. The wave incurs more losses when propagation in skin as compared to free space and could vary for different tissue type. This opens door to further analysis of individual biomolecules in the skin that could potentially affect these parameters having specific absorption spectral peaks.

In an in-body communication system, the noise could have two possible sources, electronic noise of the nanodevice at the receive and molecular absorption noise of the channel. In this section, the results are presented for channel medium noise alone for both breast and abdomen tissue (Fig.4.10). At 1 THz and distance of less than 1mm, the molecular temperature noise inside human skin is expected to be much higher than free space. Hence, this further limits the transmission window for in-body communication. For instance, for breast tissue (Fig.4.10(a)), the value increases monotonically with frequency and distance, with dependence on the measured absorption coefficient values. However, in the very short range (less than 1 mm) and the presence of less water molecules could result in very low noise temperatures. On comparing the noise value between figure 4.10 (a and b), the molecular

noise temperature for instance at, 1 THz decreases for breast tissue when rotated to an angle of 45°. This again indicates the importance of taking tissue orientation as one of the factor when optimizing the channel parameters. Similarly, for abdomen tissue, the molecular noise temperature at the same frequency is higher than breast tissue (at both rotation angles), indicating the presence of higher water concentration.

4.3 Chapter Summary

The chapter provided a detailed analysis of optical properties - refractive index and absorption coefficient of different tissue type (breast and abdomen). In addition to this, angle dependent measurement was also performed on breast tissue highlighting the importance of fibre orientation and possible changes in the biomolecular activity of the tissue. The main aim of nanonetwork communication system, is to be able to map the entire body and extract information. The skin tissue data from different part of the body provide a complete medium coverage for in-vivo communication. The tissue is highly complex in terms of hydration level, fat content and various other biological entities (blood, sweat-ducts etc.). Therefore, the presented data open doors to evaluate channel capabilities for different tissue type including fibre orientation. The presence of water vapour molecules is again the main loss factor affecting the properties of the terahertz channel. Experimental investigation of individual tissue layers is challenging to study with bulk human skin samples, hence in the next chapter the reader will be introduced to skin substitutes and dwell into the intricate biological features. Within the scope of presented tissue channel parameters, the pathloss and molecular noise temperature value are relatively higher than free space and could be affected by additional tissue fibre orientation variation due to specific biomolecular activity or mechanical stress.

References

[1] Ke Yang, Alice Pellegrini, Max O Munoz, Alessio Brizzi, Akram Alomainy, and Yang Hao. Numerical analysis and characterization of THz propagation channel for body-centric nano-communications. *IEEE Transactions on Terahertz Science and Technology*, 5(3):419–426, 2015.

[2] Yuri Feldman, Alexander Puzenko, Paul Ben Ishai, Andreas Caduff, Issak Davidovich, Fadi Sakran, and Aharon J Agranat. The electromagnetic response of human skin in the millimetre and submillimetre wave range. *Physics in medicine and biology*, 54(11):3341, 2009.

[3] Ke Yang, Qammer Hussain Abbasi, Nishtha Chopra, Max Munoz, Yang Hao, and Akram Alomainy. Effects of non-flat interfaces in human skin tissues on the in-vivo tera-hertz communication channel. *Nano Communication Networks*, 8:16–24, 2016.

[4] Tuba Yilmaz, Robert Foster, and Yang Hao. Detecting vital signs with wearable wireless sensors. *Sensors*, 10(12):10837–10862, 2010.

[5] T Durduran, R Choe, JP Culver, L Zubkov, MJ Holboke, J Giammarco, B Chance, and AG Yodh. Bulk optical properties of healthy female breast tissue. *Physics in medicine and biology*, 47(16):2847, 2002.

[6] Qianqian Fang, Stefan A Carp, Juliette Selb, Greg Boverman, Quan Zhang, Daniel B Kopans, Richard H Moore, Eric L Miller, Dana H Brooks, and David A Boas. Combined optical imaging and mammography of the healthy breast: optical contrast derived from breast structure and compression. *IEEE transactions on medical imaging*, 28(1):30–42, 2009.

[7] A Prescher. Surgical anatomy. In *Incisional Hernia*, pages 45–60. Springer, 1999.

[8] Rakchanok Rungsawang, Yuko Ueno, Isao Tomita, and Katsuhiro Ajito. Angle-dependent terahertz time-domain spectroscopy of amino acid single crystals. *The Journal of Physical Chemistry B*, 110(42):21259–21263, 2006.

[9] Mark C Pierce, John Strasswimmer, B Hyle Park, Barry Cense, and Johannes F de Boer. Birefringence measurements in human skin using polarization-sensitive optical coherence tomography. *Journal of biomedical optics*, 9(2):287–291, 2004.

[10] Jane Sandby-Moller, Thomas Poulsen, and Hans Christian Wulf. Epidermal thickness at different body sites: relationship to age, gender, pigmentation, blood content, skin type and smoking habits. *Acta Dermato Venereologica*, 83(6):410–413, 2003.

[11] Sarah Lecas, Elsa Boursier, Richard Fitoussi, Katell Vié, Isabelle Momas, Nathalie Seta, and Sophie Achard. In vitro model adapted to the study of skin ageing induced by air pollution. *Toxicology Letters*, 259:60–68, 2016.

[12] Valery V Tuchin. *Handbook of photonics for biomedical science*. CRC Press, 2010.

[13] Calvin Yu, Shuting Fan, Yiwen Sun, and Emma Pickwell-MacPherson. The potential of terahertz imaging for cancer diagnosis: A review of investigations to date. *Quantitative imaging in medicine and surgery*, 2(1):33–45, 2012.

[14] Jonathan Y Suen, Michael T Fang, and Philip M Lubin. Global distribution of water vapor and cloud cover—sites for high-performance THz applications. *IEEE Transactions on Terahertz Science and Technology*, 4(1):86–100, 2014.

[15] Josep Miquel Jornet and Ian F Akyildiz. Channel modeling and capacity analysis for electromagnetic wireless nanonetworks in the terahertz band. *IEEE Transactions on Wireless Communications*, 10(10):3211–3221, 2011.

Chapter 5

THz Characterization of Skin Substitutes for In-Body Nanonetworks

This chapter presents the investigation of the electromagnetic properties of human skin tissues using Terahertz Time Domain Spectroscopy (THz-TDS). The material parameters i.e. refractive index and absorption coefficient are extracted for artificially synthesized skin model, cultured using fibroblast cells and collagen type I reagent. The increase in cell count number by 200% will cause a distinctive decrease in refractive index and absorption coefficient values. Further, a 3D model (organotypics) is introduced in section 5.2, wherein the same material parameters are investigated for a more complex structure comprising of both epidermis and dermis layer. In addition to material parameters, in-body channel parameters i.e. total pathloss and molecular noise temperature of the skin are also calculated. The results show the dependency of channel parameters on molecular features and hydration level of the skin. Such findings will pave the way for more rigorous THz channel analysis and network modelling to be applied for body-centric nano-communication specifically in the bioengineering domain.

5.1 Fibroblasts Cell Number Density based Collagen

5.1.1 Introduction

Experimental investigation and a study is performed on the material properties of artificial human skin dermis layer (2D model) in addition to in-body nano-network channel parameters within the THz range of frequencies. Skin makes an interesting choice of study, since it is the most abundant tissue present and offers dynamic analysis due to its varied hydration levels throughout the human body. The variation in tissue hydration influences the texture and

dimension, which in turn could affect the material properties. From a biology perspective, skin is a complex layered structure. However, for simplicity it can be divided into three main visibly defined layers: stratum corneum, dermis and subcutaneous fat. Out of these, dermis is the thickest and most abundant in water, hence resemble to properties of that of free water [1, 2].

Its main constituent is collagen, a fibrous protein rich in glycine and proline, that is a major component of the extracellular matrix and connective tissues. The collagen fibres are made of tiny fibrils that are arranged in individual bundles in parallel fashion of wide range of widths and thickness. They cross each other in all directions but remain parallel to the tissue surface. In the dermis, collagen fibres are believed to be a major source of light scattering [3].

Hence collagen is the most widely used for medicinal purposes such as, treating tissue burns, drug delivery system, controlling material for transdermal delivery and as surgical suture [4]. Many natural polymers and their synthetic substitutes are used as biomaterials, but the unique characteristics play an important role in the formation of tissues and organs. For instance, collagen when compared with Integra Derma, Allograft and Opsite (systhetic substitute) exhibits superior bio-compatibility and constitutes more than 30% of skin tissue. It forms extra fine fibres through its self-aggregation and cross-linking capabilities. Whereas other synthetic tissues are mainly polymer-like cultured from non-biological molecules.

The biological modelling and characterization of collagen is at its infancy and needs an in-depth investigation. The dielectric behaviour of tissues have been extensively studied from microwave to optical range of frequencies for excised animal and complex biomolecules [5, 6]. EM spectrum ranging from 0.1-10 THz bridges the gap between microwave and optical frequencies and has growing number of applications as mentioned above. Its unique spectral features and sensitivity to water, makes it a viable technique for investigating material properties of tissues, skin layers and hydration dynamics [7, 8].

Some papers [2, 9–12] have covered wide range of domains that investigate cell-protein interaction of collagen, hydration dynamics and THz TDS of artificial skin. The results published in open literature for optical properties of collagen are limited and differ in methodology. However, the material extraction techniques remain similar in most of these papers. For instance, in paper [9], Integra Derma regeneration templates divided as monolayer and bilayer were investigated for extraction of THz material parameters. Further, the data was recorded for both hydrated and dehydrated samples. The refractive index values for dehydrated monolayer and bilayer are 1.2 and 1.4 respectively. The author also experimented the hydrated samples by varying their saline concentration but no material parameters were reported. Hence, it becomes rather complex to verify any change in hydration or dehydration

level of these samples. Work done by A.G. Markelz [10], focuses on THz TDS of DNA, bovine serum albumin and collagen in the working range of 0.1-2 THz. While providing detailed analysis of other biomolecules, the work on collagen is again sparse. Experimental evaluation was done keeping in mind the humidity levels, which is important as THz wave is highly absorbed by water. Only the absorbance of collagen was reported in this paper, however it does provide some insight to hydration dependence of collagen.

Most protein molecules including collagen have been evolutionary selected to have biological activity in aqueous environments. In paper [13], protein hydration shell and its role in collagen recognition was investigated. A way to generalize the properties of these tissues is asserting water as the topological basis for all skin. There is no denying in the fact that different tissues have different water hydration level, evidently age also plays an important role. In this paper, characterization of collagen (i.e., material parameter extraction) is performed using THz TDS by varying the cell number density. The results demonstrated in this paper, enable us to develop channel parameters - pathloss and molecular noise temperature, for actual human tissue. Aim is to establish a comprehensive understanding of collagen structure and construe these novel findings to develop THz channel propagation models.

5.1.2 Biological Modelling of 2D Artificial Skin: Collagen

Collagen, in its primitive form is a complex isotropic network of tangled fibrils and restraining a randomly structured matrix of highly hydrated protein compounds [14]. The molecular arrangement into fibrils is stabilized by the formation of covalent cross-links, which finally contribute to the mechanical resilience of collagen fibrils. In this work, rat-tail type I collagen is used as a base reagent for gel preparation (Fig. 5.1). Type I is the most abundant and naturally occurs in tendons, skin, ligaments and many interstitial connective tissues. Collagen reagent together with human fibroblasts cells forms the two vital components of the gel.

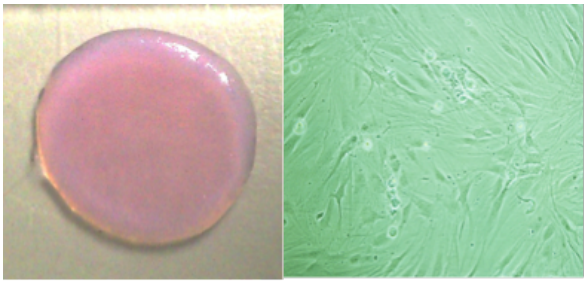

Fig. 5.1 (Left) Artificially synthesized collagen layer at the Blizard Institute, QMUL and (Right) Fibroblasts cells assisting the growth of collagen samples.

The fibroblast cells (Fig.5.1 (right)) suspended in Foetal Bovine Serum (FBS) containing essential nutrients and growth factors. In addition, the gels are supplemented with concentrated Modified Eagles Medium (MEM) which also contains a balance of nutrients for feeding the fibroblasts.In order for the gels to set, a small quantity of sodium hydroxide is added drop wise to the collagen-fibroblast mix, until the pH indicator in the MEM turns from orange to pink. The gels are then incubated (5% CO_2) for gelation at 37°C for approximately 45 minutes. Collagen gels were prepared in this study by varying the number of fibroblast cells and fixing the concentration of collagen reagent to 8 parts of 3.8 mg/ml. The cell number was estimated while observing them in a standard light microscope using a haemocytometer.

The aim is to investigate any variations in material parameters due to the differences introduced in the composition of collagen gels. Once, the initial gelation has taken place, their diameters were measured to observe any signs of contraction. They were allowed to contract to their maximum value, by keeping them in an incubator for a week. The diameter was measured again. Contraction of these gels is an important phenomenon, since the interaction of fibroblasts with collagen solution affects the thickness and overall water mass of the samples [15]. Since, it has been established that THz radiation is sensitive to changes in hydration level, it was expected to observe some unique difference in material parameters: refractive index and absorption coefficient due to the change in number of fibroblast cells.

5.1.3 Measured Material Parameter

To evaluate both phase and magnitude, Fast Fourier Transform (FFT) is applied on the data. The measured time domain signal for the different samples (collagen by varying cell concentration), air and TPX are shown in figure 5.2 and it can be seen from the figure that the biological sample is highly attenuated. The signal level attenuation of biological sample can be compared with air and TPX, where the peak intensity for collagen is reduced to 5mV for 500k cells and similarly for 300k and 100k. The oscillations and attenuation in the data is due to presence of water vapours in the atmosphere.

Sensitivity of THz radiation is dependent not only on the amount of water present but also the way in which the layers associate with water. In addition to water dynamics, the number of fibroblast cells seeded specifically for artificial skin samples, also plays an important role both in hydration level and thickness. The impact is not direct, but still is a necessary parameter to be considered while investigation optical properties of such structures. To understand the influence of number of fibroblast cells, it is necessary to review the fundamental mechanism involved in formation of collagen gels. In many types of connective tissue such as dermis layer of the skin, the matrix-secreting cells are called fibroblasts.

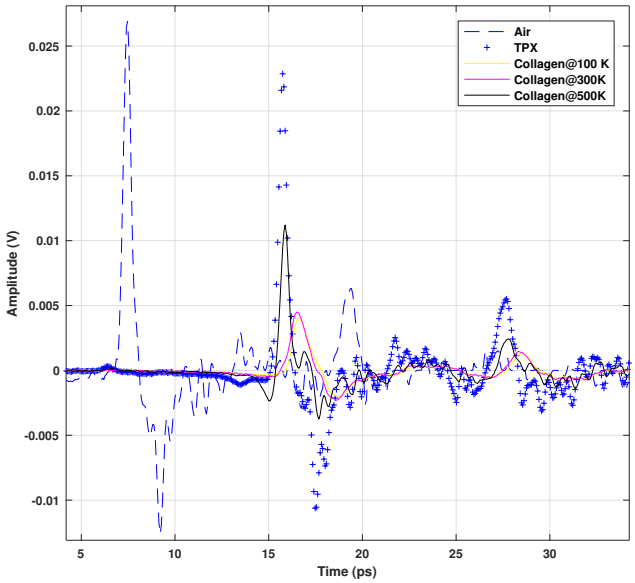

Fig. 5.2 THz transmission through reference plate TPX, air and cultured collagen samples of varying (1×10^5, 3×10^5 and 5×10^5) number of fibroblasts cells with stock solution concentration fixed.

In 1990, P. Rompre and group [11] proposed a Box-Behnken analysis to study the effects of the collagen and fibroblast concentrations on gel thickness. The results presented, verify that with increasing number of fibroblasts cells with respect to low collagen reagent concentration, the contraction increases and hence diameter of gel decreases. In the same line of work and keeping our focus on THz spectroscopy of artificial skin, the subsequent section provides details on sample preparation, cell number variation and material parameters. Referring to section 2.3.1, the same extraction algorithm was used to evaluate the refractive index and absorption coefficient of the samples (Fig.5.3 (a and b)). Table 5.1 provides cell number variation and final diameter of the samples after contraction. It can be seen from the table that with increasing number of fibroblasts cells the final diameter of the samples decreases. This highlights the fact that the capacity of cell compaction of collagen fibrils, leads to reduction in volume referred to as lattice contraction. The contraction is preceded by cell-generated force that reduces the water mass between collagen fibres [15].

In this work, the thickness of the samples were deliberately kept constant so as to avoid any variation in refractive index values due to change in thickness. At 1 THz, the refractive index of the samples from 100k to 500k decreases consistently (as shown in Fig.5.3(a)). This suggests that concentration of water molecules do play a definitive role in changing the intrinsic nature of collagen. Sensitivity of THz radiation is dependent not only on the amount of water present but also the way in which the layers associate with water. The collagen

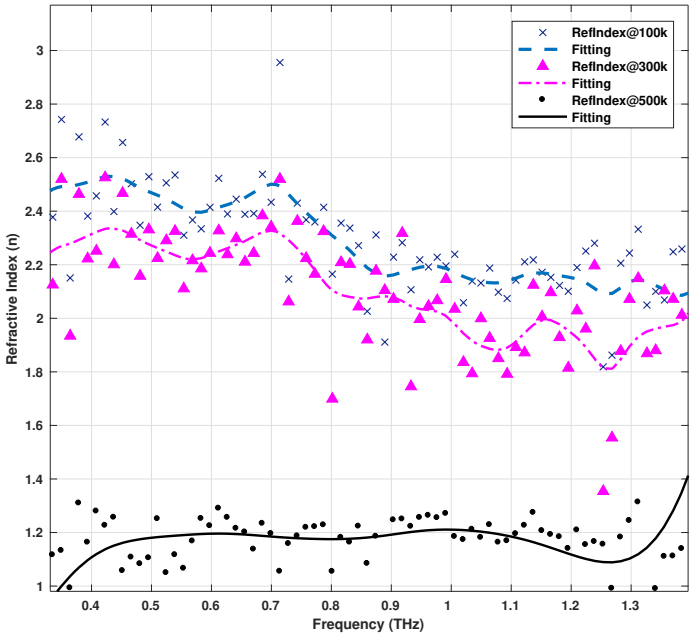

(a) Refractive index of collagen samples of varying (1×10^5, 3×10^5 and 5×10^5) number of fibroblasts cells with stock solution concentration fixed

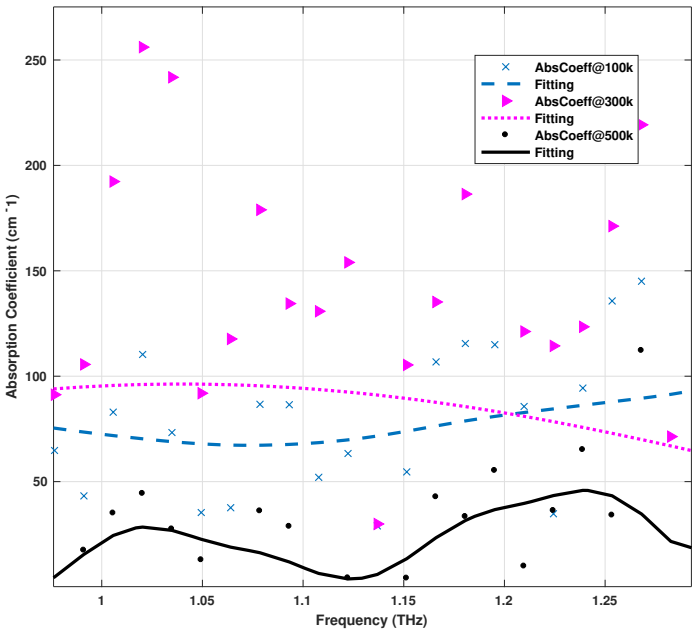

(b) Absorption coefficient of collagen samples of varying (1×10^5, 3×10^5 and 5×10^5) number of fibroblasts cells with stock solution concentration fixed

Fig. 5.3 (a) Refractive Index ranging from 0.5-1.3 THz illustrates that with increasing frequency the value decreases. For samples with 100k and 300k, the value of refractive index is 2.2 and 2 respectively at 1 THz. However, for sample with 500k cells the value decreases to 1.2 highlighting the dynamics of collagen protein and water molecules. (b) The absorption coefficient calculated for 100k, 300k and 500k cells; the extra water outside the sample was carefully removed without excessively dehydrating the samples. The measured absorption coefficient is dependent on the hydration level and structure of collagen

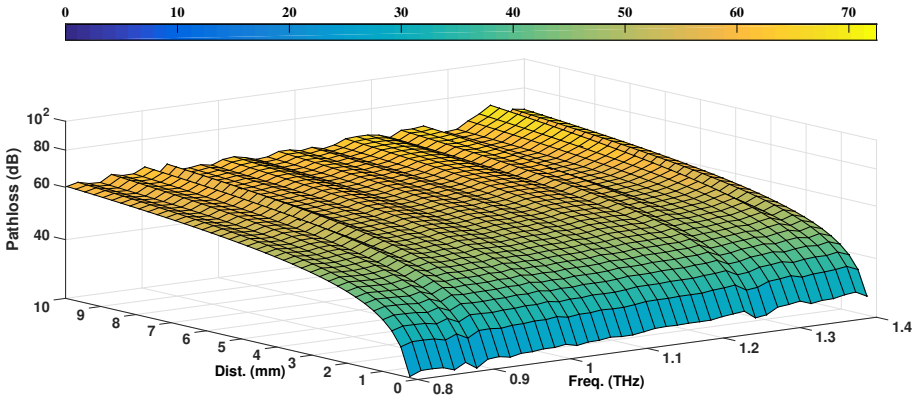

(a) Coll1 – 100k cells

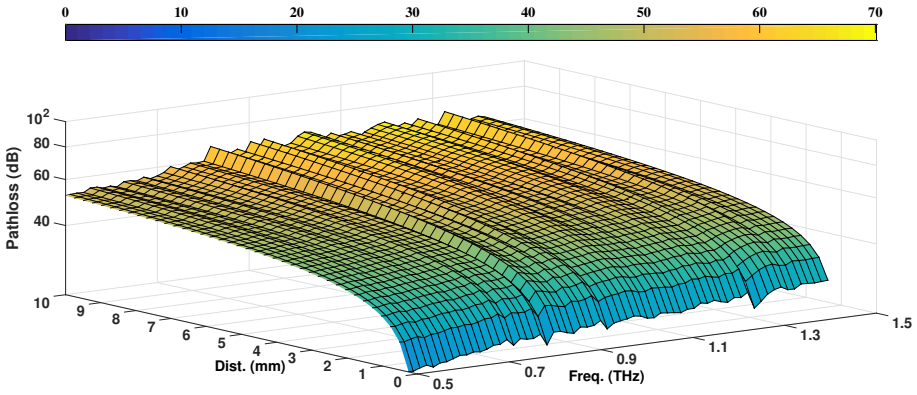

(b) Coll1 – 300k cells

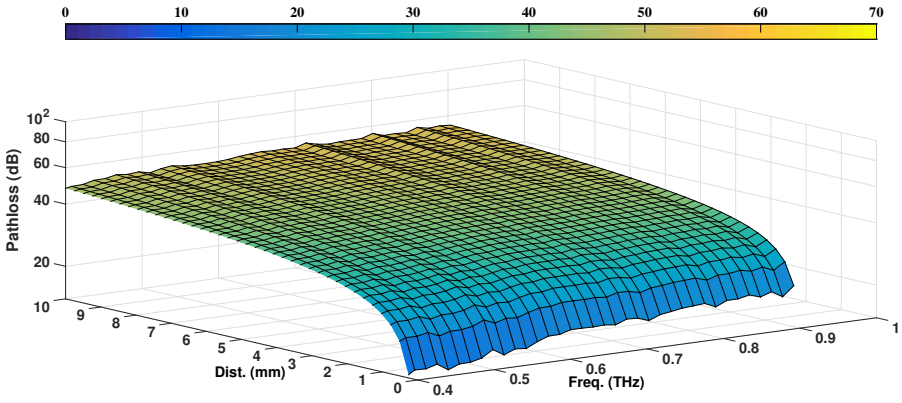

(c) Coll1 – 500k cells

Fig. 5.4 Total pathloss as a function of frequency and distance for three different cell number densities

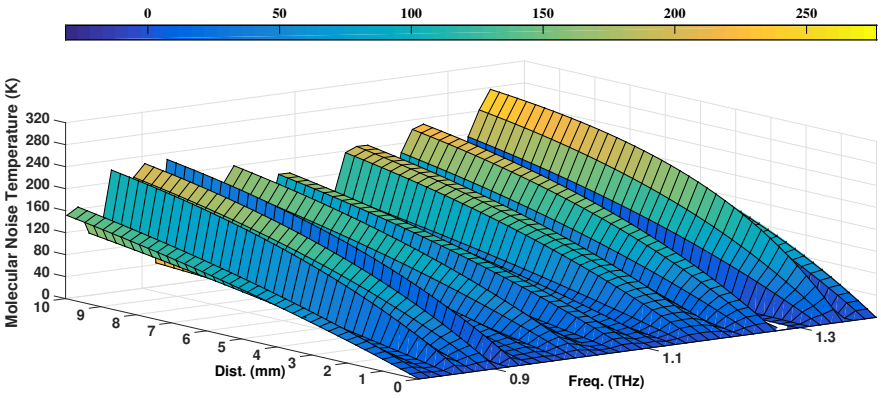

(a) Coll1 – 100k cells

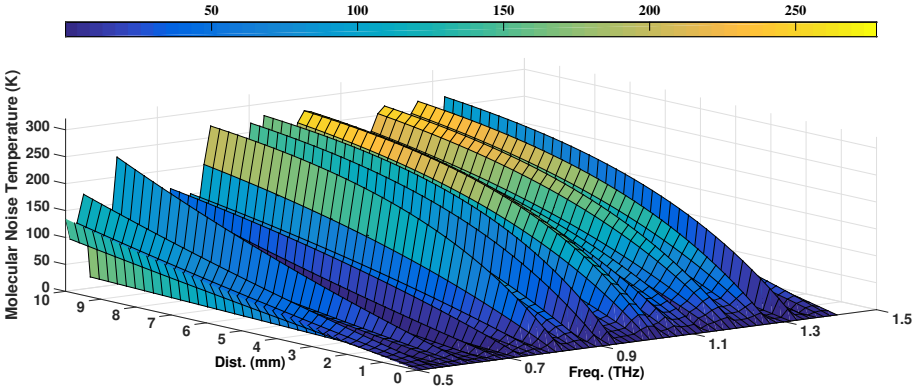

(b) Coll1 – 300k cells

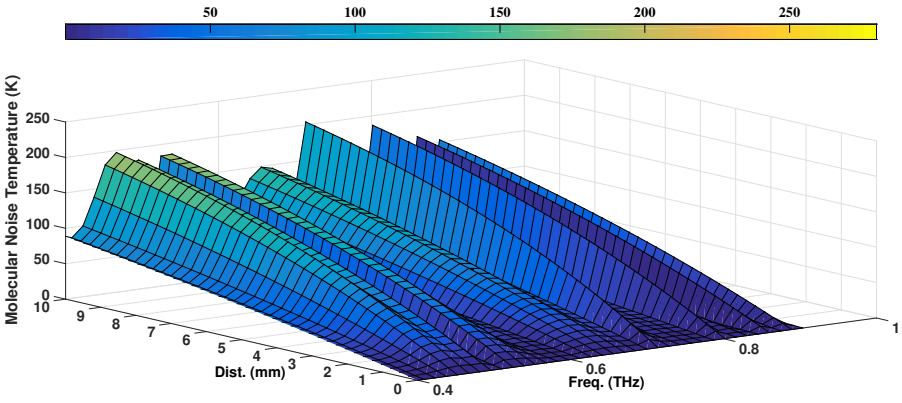

(c) Coll1 – 500k cells

Fig. 5.5 Molecular Noise Temperature as a function of frequency and distance of varying cell number density

sample (Table 5.1, coll1) with less number of fibroblast cells demonstrates refractive index values closer to that of water [2].

Similarly, absorption coefficient values (Fig.5.3(b)) are affected and decreased sharply for collagen with 500k cells. Other factors that could affect both material properties are atmospheric water vapours, gradual dehydration of samples (while performing the measurements) and etalon (also called Fabry-Perot) reflections. The first two scenarios can only be achieved in an ideal surrounding and later need further analysis. The presented value of absorption coefficient for figure 5.3(b) are higher due to high water content in the tissue and less contraction of cells. Maximum absorption coefficient can be measured in transmission mode by the dynamic range (DR) of the system. In this work, DR is expected to vary with the sample and is between 15-20 dB.

Table 5.1 Variation in cell numbers and collagen contraction

Sample	Cell No. (k=1000)	1 week old Diameter (cm)	2 weeks old Diameter (cm)	Contraction (approx.)
Coll1	100k	2.5	2	0.5
Coll3	300k	1.8	1.6	0.2
Coll5	500k	1.6	1.5	0.1

As DR approaches its maximum value, the noise increases rapidly and any absorption coefficient features after this are invalid. The working frequency for figure 5.3(a) is from 0.4 to 1.3 THz whereas for figure 5.3(b) it is 0.9-1.25 THz. For better understanding, the noise level and irrelevant absorption coefficient peaks are truncated from the results. The absorption coefficient values for coll1 and coll2 at 1 THz are 72 cm^{-1} and 95 cm^{-1} whereas for coll3, the value sharply decreases to 40 cm^{-1} at 0.8 THz. For coll3, the noise is high since absorption coefficient rolls-off after 0.9 THz and then sharply increases.

Measured refractive index and absorption coefficient values are used to calculate pathloss and molecular noise temperature underlying skin as the channel medium. Both the channel parameters as function of frequency and distance are illustrated in figure 5.4 and 5.5. Pathloss is shown in figure 5.4 for different cell number density. In reference [16] it was highlighted the total absorption depends on the number of molecules that propagating wave encounters. Although, in a real human skin one expects to observe multiple varying features such as hydration level, saline concentration, collagen fibre alignment and cells number density. The applied variation in fibroblast cell number demonstrates one of the important features of human skin conformation. It can be seen from figure 5.4 (c) that the pathloss at 0.9 THz is much lower than figure 5.4 (a) and (b) due to increased cell number density and reduced water

mass of collagen. As illustrated in figure 5.5 (a-c), variation in cell number density affects the molecular noise temperature keeping skin as the channel medium. For transmission distance up to 1mm, the noise is high for samples: Coll1 (Fig.5.5a) and Coll3 (Fig.5.5b), whereas for Coll5 (Fig.5.5c) the value steeply decreases. This is due to the fact that with increasing cell number density, the total water mass (hydration level) of collagen samples decreases. The results for both pathloss and molecular noise temperature demonstrate high dependence on molecular features and hydration level of the skin.

5.1.4 Collagen Fibre Alignment

A different set of collagen samples were prepared to investigate the fibre orientation and overall morphology. These fibroblast cell number density was slightly different (2×10^5, 4×10^5, 6×10^5 and 8×10^5) however the difference of 200% is still the same. The samples were first prepared using a critical point drier technique at the School of Engineering and Material Science (SEMS, QMUL). They were then fixed with glutaraldehyde 2.5% for 1 hour before dehydrating with a successive series of dilution in ethanol and then passed to the critical point drier.The samples were then brought to Nanovision Centre at Queen Mary University of London for scanning electron microscopy (SEM) imaging.

Fig. 5.6 Dried collagen samples glued to the metallic stage for SEM imaging

The imaging stage (Fig5.6) was prepared by sputtering it with thin (5-10 nm) layer of gold. The samples were fixed on a metal mount with a glue and left for drying for about 1-2 minutes. The stage chamber was then vacumed to a pressure of 2.58×10^{-4}mbar to

remove atmospheric water vapours. From figure 5.7 and 5.8, it can be seen the arrangement of collagen fibres in long parallel cylindrical shapes. As the number of cells increases, the sample's morphology seems to be more dense. Although, the fibres have the tendency to spread in random orientation, but they always grow on top of each other (Fig.5.7) to form a dense extra cellular matrix. In case of figure 5.9, the sample is imaged from one side, to measure the thickness (35.31 μm) of the sample. In addition to this, it can be inferred that the samples form layer of fibres always growing parallel to the plane suggesting a 2D geometry.

5.2 3D skin model - Organotypics Characterization

Cell culture refers to the removal of cells, such as fibroblasts and keratinocytes, from a tissue before their growth to a favourable artificial environment. In section 5.1, tissue culture of 2D skin monolayer-collagen, was discussed extensively. Recalling briefly, the cells were seeded in a plastic flask in an artificial environment aided by growth medium that supplies the essential nutrients such carbohydrates, vitamins, glucose, minerals etc., and are then left to proliferate in an incubator. Depending on the number of cells, they were then mixed with collagen type 1 reagent. However, there are certain missing links which prevents mimicking natural biological mechanisms. In such a method, communication between the cells is only restricted to the flat surface of the flask. The environment is non-physiologically uniform and the cells are not allowed to pile on top of one another, but are forced into monolayer morphology [17].

Skin is a multilayer heterogeneous organ and a monolayer model is primitive resulting in a homogeneous cell population. Some of the parameters that are overlooked includes: mechanical properties, communication between the cell (different cell types) and its matrix, and communication between adjacent cells. Organotypic cultures (also known as co-culture and 3D cell culture) provide the necessary complexity to the skin model by amalgamating both, epithelial layer and a mixture of extracellular matrix protein [section 5.1]- collagen and fibroblasts [18]. Skin performs various functions such as UV absorption, immune surveillance and act as sensory units for touch, temperature, pain and hydration [19]. These functions are nothing but generating body information through efficient communication between epidermis (epithelium tissue) and dermis (extra-cellular matrix/connective tissue). Epithelium and connective tissue are functionally interdependent units within organs and are integrated with nerves and muscle to varying degrees depending on their organ specific function [20].

The efficient 3D cell aggregation involves the formation of a base layer called scaffolding, essentially the dermis layer same as collagen (section 5.1.2). The third dimension is

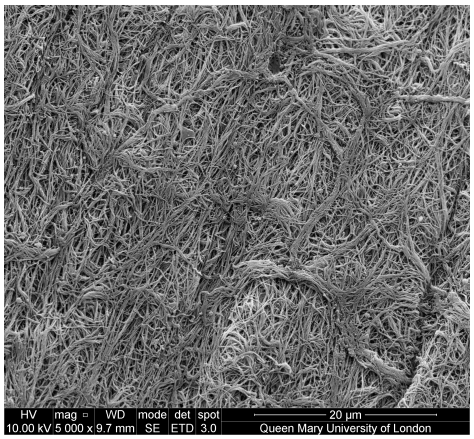

Fig. 5.7 Collagen fibres in cylindrical form aligned parallel to each other giving a final dense extracellular matrix

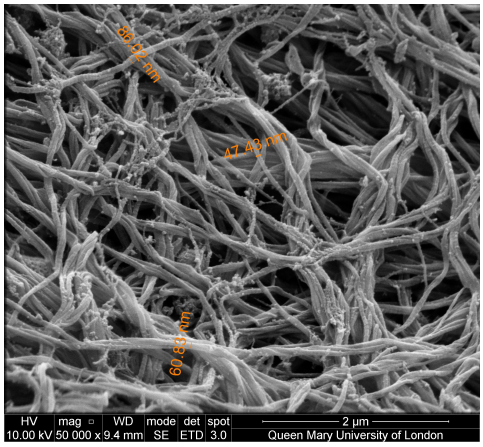

Fig. 5.8 Varying thickness of individual collagen fibres

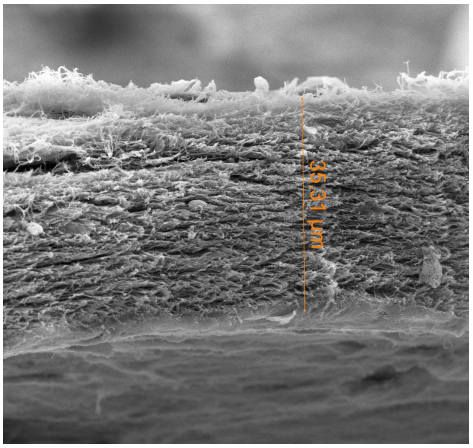

Fig. 5.9 Collagen sample are seen from one side of the sample. The sample is completely dry, hence the thickness reduces to 35.31 µm

introduced by culturing different cell types in a tissue specific formation. This is achieved by reconstructing human epidermis with the aid of proliferating and differentiating human keratinocytes [21, 22]. The final structure is prepared in an air-liquid interface environment with 2-3 weeks, wherein the epidermis equivalent covers collagen base layer. As reported in references [23], epidermis consists of carbohydrate polymers and stratum corneum lipids that organize as a liquid crystal to form a barrier to permeability of fluids.

In the field of biology and tissue engineering, the re-constructed artificial skin model are investigated for applications such as pathogen interactions,skin ageing, tissue repair (scars and burns),and drug trials. Similarly, in an era of inter-disciplinary research, 3D skin modelling has transpired to many engineering and physics domains. Some of the examples are, mechanical characterization [24], imaging [25], organ-on-chips [26] and 3D bio-printing [27]. In this section, the aim is to pioneer the electromagnetic characterization of organotypics in the THz region focusing on calculation of channel parameters for in-body nanonetworks.

5.2.1 Material and Methods of Organotypic Culture

All cell culture was performed in a laminar flow hood under aseptic conditions in accordance with standard tissue culture technique. Dermal fibroblasts (DF) isolation: Skin was incubated in 2.5 mg/ml dispase II (Sigma-Aldrich, Poole, UK) in PBS overnight at 4°C, then the epidermis was peeled off and discarded. The remaining dermis was excised into small pieces and incubated overnight in 0.5mg/ml collagenase D (Roche, Indianapolis, USA) at 37°C, 5% CO_2, 90-100% RH. The sample was briefly shaken well to release dermal fibroblasts from the dermis, then passed through a 100 µm filter to separate cells from dermal matrix. The cell suspension was centrifuged at 1000 rpm (rotation per minutes), 5 minutes. The supernatant was aspirated and the cell pellet was re-suspended in DMEM (Sigma-Aldrich, Poole, UK) and seeded in flasks for culture.

However, usage of primary keratinocytes has several disadvantages, for example, limited availability of fresh skin, limited in-vitro lifespan, and, in particular, the large donor to donor variation. By using an established immortalized keratinocyte cell line that can be kept in culture for prolonged time, such limitations can be circumvented [28]. NTERT is an immortalized keratinocyte cell line use for creating 3D-orgnanotypic skin equivalent models. NTERT keratinocytes were cultured in Keratinocyte serum free medium (K-SFM, Gibco, Paisley, UK) prior to use in the organotypic system. NTERT and DF were passaged using standard trypsinisation methods, except NTERT keratinocytes were neutralized using defined trypsin inhibitor (Gibco, Paisley, UK) since they were cultured in a serum-free media.

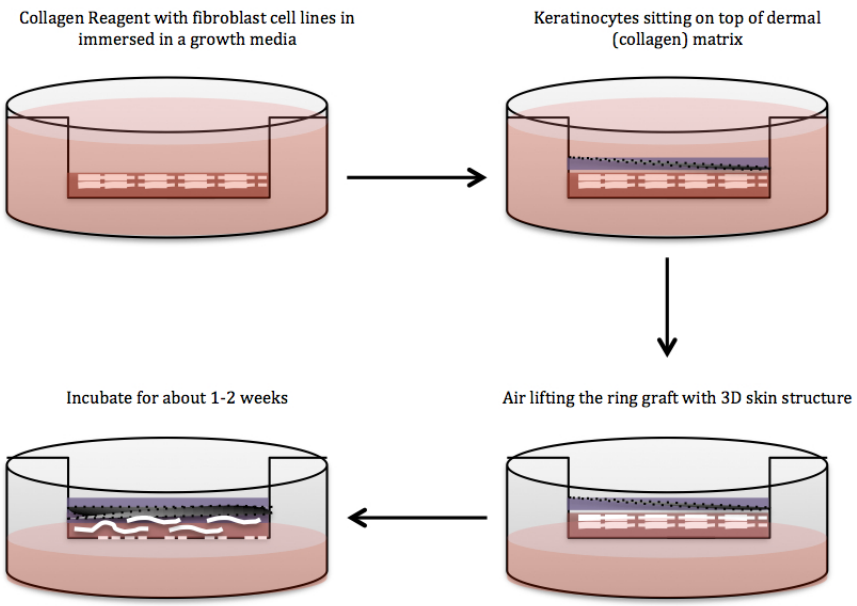

Fig. 5.10 Illustrated steps for organotypic 3D cell culture. The base layer is made of fibroblast cell line forming the dermis and epidermal layer is as a result of keratinocyte cell lines. The sample takes about 2 weeks to grow

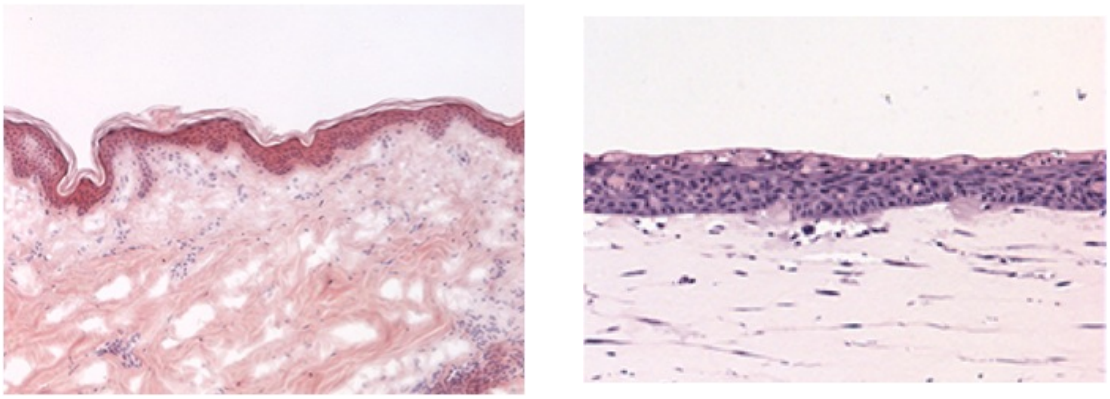

Fig. 5.11 Histology of normal skin (right) compared with NTERT organotypic (left). Organotypic Sections (left) of 0.5 μmimaged with standard light microscope, illustrating the presence of keratinocytes for epidermal layer. The light pink base is the dermis with fibroblasts and the keratinocyte starts to differentiate spreading as tiny dot-like features

Primary dermal fibroblast (1×10^5) per organotypic) were incorporated into ice-cold 4mg/ml rat-tail collagen 1 solution (Corning, MA, USA) with DMEM and neutralized with 0.5N NaOH. The collagen-cell suspension (350 µl) was pipetted into a 12 well plate hanging well insert (Millipore, Darmstadt, Germany) and allowed to polymerize for 30 min at 37°C to form a gel. Once polymerized, the culture was submerged in 2.5 ml DMEM and incubated at 37°C, 5% CO_2, 90-100% RH overnight. All culture media was aspirated and then 0.5 ml cell suspension of 1×10^5 NTERT immortalized keratinocytes were added atop the gel within a ring raft (also called cloning ring) in DMEM:F12 culture medium. An additional 2 ml DMEM:F12 was added in the well plate underneath the hanging well inserts and organotypics (Fig.5.10) were incubated at 37°C, 5% CO_2, 90-100% RH overnight. Organotypics were then airlifted by aspirating all culture media (both underneath and on top of the gel) and then replaced with 1 ml DMEM:F12 culture media in the wells underneath the hanging inserts. The organotypic cultures were incubated at 37°C, 5% CO_2, 90-100% RH for 14 days, with culture media was refreshed on a daily basis.

5.2.2 Optical Parameters and THz propagation channel characteristics of Organotypics

The organotypic samples of thickness 115 µm were measured at room temperature (23-24°C) via THz-TDS. The sample was measured in free space and fixed directly to the sample holder mount as shown in figure 5.12.

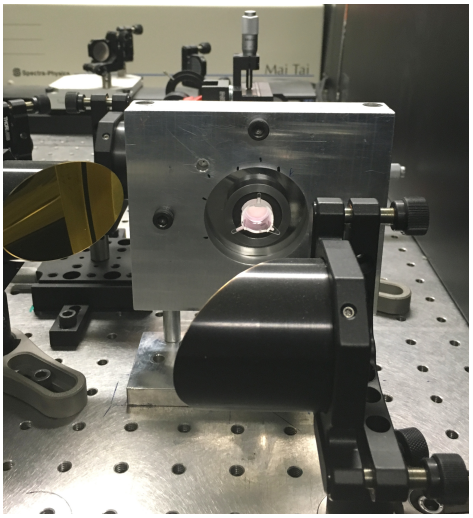

Fig. 5.12 THz-TDS set up for organotypic measurement. The plastic ring raft is fixed inside the metallic sample holder mount, making the sample suspended in free space

The samples were first taken out of the growth media and stored in an empty 12-well plate for about 10 minutes to let it naturally remove excess of media and later the residue was removed very carefully with a tissue paper. Epidermal cells consist predominantly of keratinocytes (95–97%),while collagen makes 70% of the skin [23, 29]. In this section, the 3D skin tissue as a combination of keratinocytes and collagen from fresh human skin is investigated for its optical properties (Fig.5.13) in the terahertz range. Keeping into consideration the absorption due to atmospheric water vapours, the refractive index and absorption coefficient are empirically calculated in the frequency domain.

From figure 5.13(a), the measured refractive index value at 1 THz is 3 and the value is quite consistent till 1.3 THz (Table 5.2). A steep fall and loss of data is observed after 1.4 THz. A stable working range is achieved from 0.85 THz to 1.4 THz. The non-linear curve fitting of the data again gives a stable value of 3 at 1 THz and very close value of 2.96 at around 1.3 THz with RMSE of 0.04, R-square value of 0.975 and adjusted R-square value of 0.969. Similarly, measured absorption coefficient values (Fig.5.13(b)) around 1 THz is 50 cm^{-1} and monotonically increases to 73 cm^{-1} at around 1.3THz. The theoretical fitting is done with RMSE as 0.06, R-square value as 0.989 and adjusted R-square value as 0.984.

Table 5.2 Measured Refractive Index and Absorption Coefficient of NTERT Organotypics

Frequency(THz)	Measured Refractive Index(n)	Absorption Coefficient (α,cm^{-1})
0.8	2.8	62.01
1	3	62.74
1.2	3	58.19

Table 5.3 Optical Parameters and THz Channel Characterization Metric for Organotypics at frequency of 1THz and distance of 100 μm

Refractive Index (n)	Absorption Coefficient, cm^{-1}	Pathloss(dB)	Molecular Noise Temperature (Kelvin)
3	50	25	30.81

The absorption coefficient is comparatively lower than excised skin tissue(section 4.4) and collagen(section 5.1.3) since the sample is thin and has less residual media. Keeping into consideration that the system's dynamic range affects the working range of frequency, refractive index of different tissue samples and collagen is compared with organotypics in table 5.4. Only consistent refractive index values are taken to provide a precise comparison.

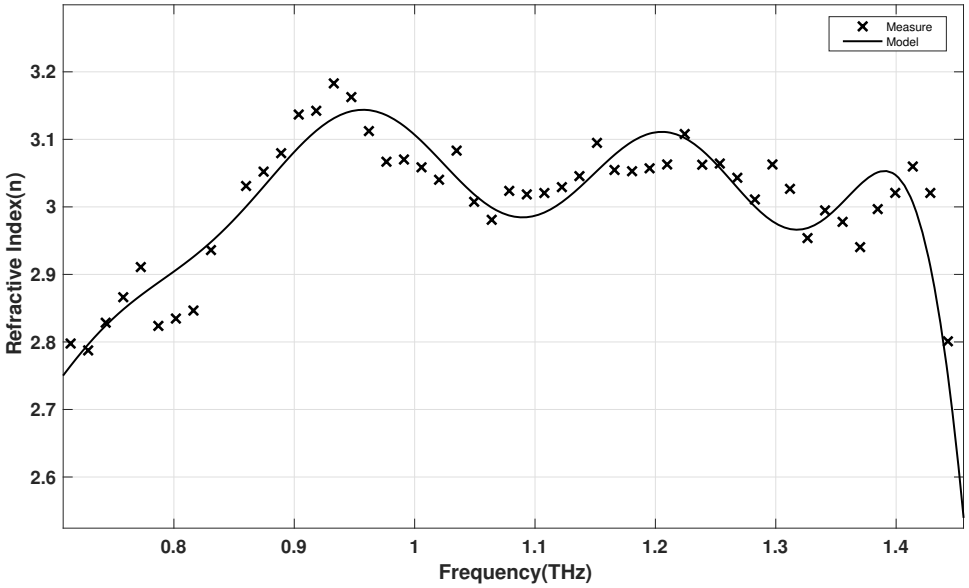

(a) Refractive Index for Organotypic

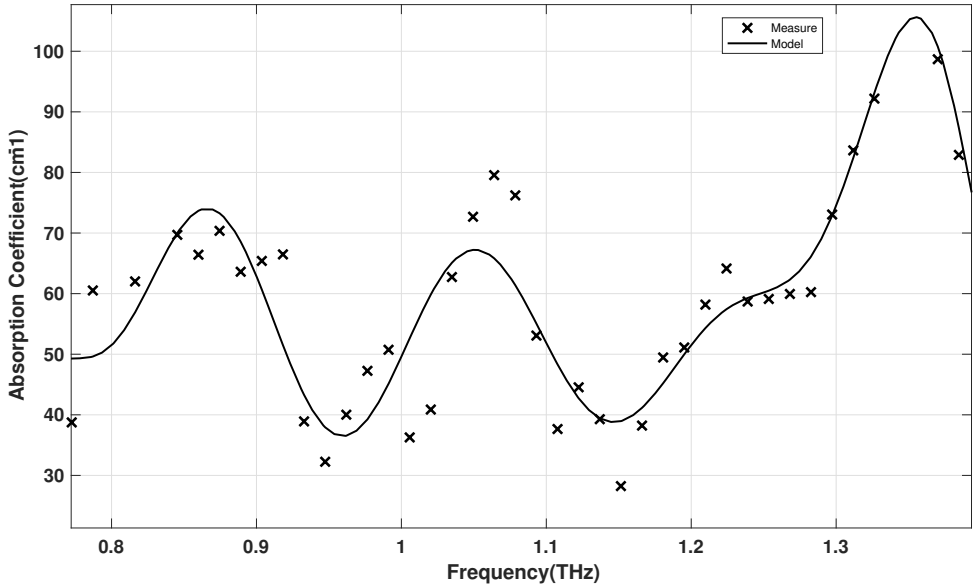

(b) Absorption Coefficient for Organotypic

Fig. 5.13 The optical parameters (a) refractive index and (b) absorption coefficient. The refractive index value is consistent from 0.9 to 1.3THz, where absorption coefficient vary with high spectral peaks at around 0.85THz and 1.1THz

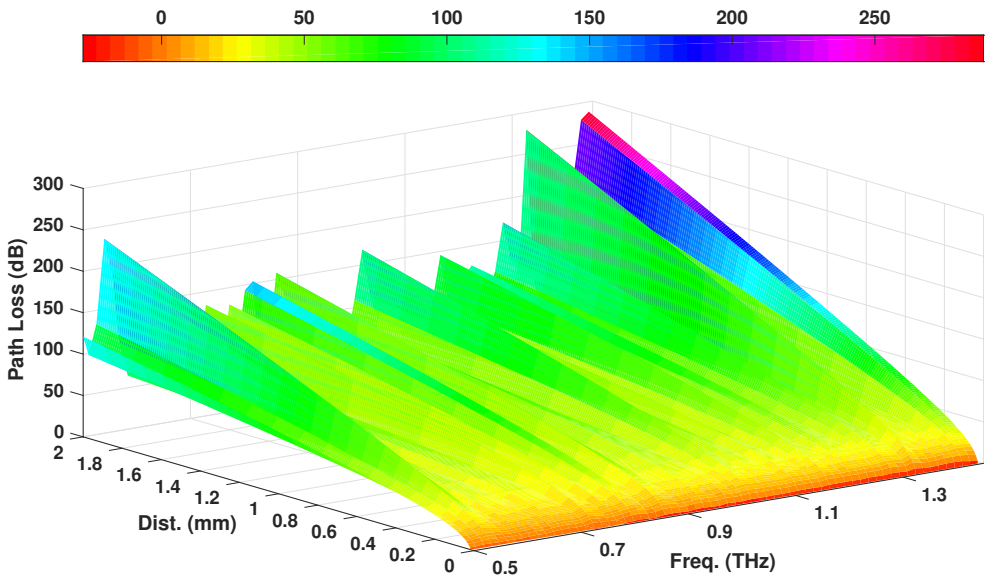

(a) Pathloss for organotypic

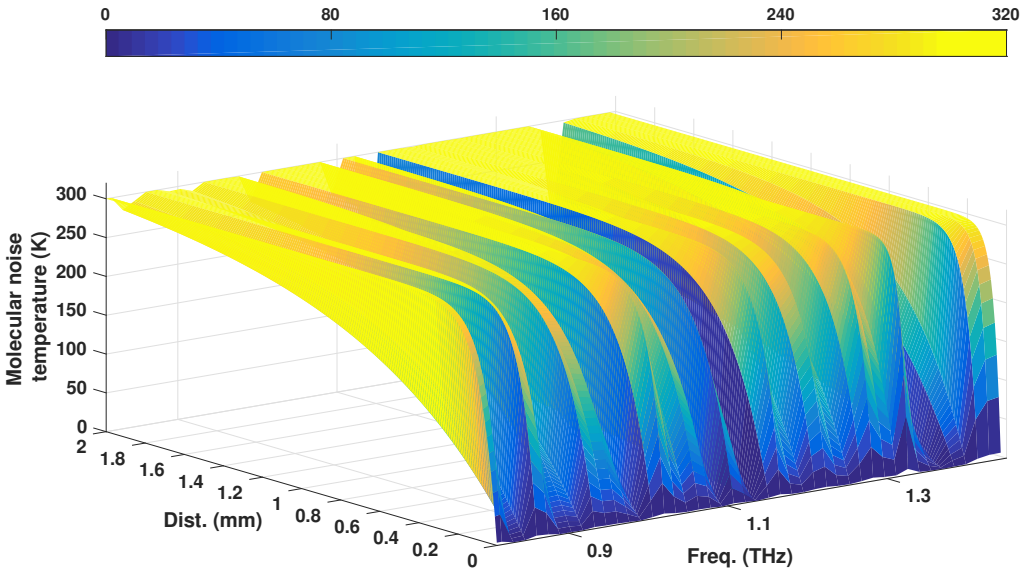

(b) Molecular noise temperature for organotypic

Fig. 5.14 The pathloss and molecular noise temperature for NTERT organotypics as function of distance and frequency

From the table, it might seem that refractive index of collagen with 100k cells, is the closest to freshly excised real skin, but morphologically it is significantly different. As explained in section 5.1.2, collagen represents the main protein of dermis layer of the skin, hence a more complex 3D organotypic structure is presented. Referring to [22], organotypics have been shown to have fairly similar morphology, expression of differentiation markers, and lipid properties compared with native human skin. As mentioned before (section 5.2.1), organotypics were added with 100k keratinocytes forming the epidermis sitting on top of 100k dermal fibroblast forming the dermis. Hence, when comparing refractive index value of collagen (with 100k fibroblasts) alone, addition of keratinocytes to organotypics could further vary the refractive index value. It is important to note that both 2D and 3D structures are engineered tissue substitutes, more variables such as other complex proteins, number of cells added, source of cells and tissue type could affect the overall morphology and subsequently the refractive index values. However, the advantage of skin substitute samples is the freedom to investigate individual components involved in the making of skin. For instance, THz-TDS of organotypics could help optimize the parameters involved in engineering such skin substitutes.

Table 5.4 List of samples measured with its refractive index value

S.no	Tissue Type	Refractive Index	Morphology
1	Breast	2.3	Epidermis and dermis with traces of blood
2	Abdomen	3.3	Dense tissue with both epidermis and dermis with traces of fat
3	Coll1	2.2	2D structure with artificially grown dermis layer abundant in collagen protien
4	Organotypic	3	3D structure with both epidermis and dermis layer

The above parameters: refractive index and absorption coefficient are applied to numerically evaluate the pathloss and molecular noise temperature for in-body networks (Fig.5.14 (a and b)). Both these parameters are function of distance and frequency. As explained from previous results, they increase with increasing frequency and distance. For molecular noise temperature, there are additional fluctuations due to atmospheric water vapour absorption. Again, analysing from the pathloss and molecular noise temperature values, to have successful operation of in-body networks, it is advisable to establish short-distance THz communication. The pathloss and molecular noise temperature for varying distances and frequencies is provided in table 5.3.

5.3 Chapter Summary

The complexity of skin as a channel medium is addressed in by varying the fibroblast cell number density. The results presented underlay the effects of heterogeneity of skin tissue on channel parameters specific to epidermal and dermal layer. The channel parameters depend on intricate molecular features of the human skin, which needs to be considered for in-body nanonetworks. Refractive and absorption coefficient value were obtained for varying cell number density keeping the thickness of the sample constant. Increase in fibroblast cell number density leads to collagen gel contraction and hence alters its molecular composition. This indicates to be one of the important variable factors in actual human skin. The refractive index and absorption coefficient value decreases with increased cell number density due to reduced water mass of the samples. The overall change in conformation of the collagen samples was included while calculating total pathloss and molecular noise temperature of THz wave channel. The complexity of real skin is further addressed by culturing 3D organotypic samples. The sample is densely populated with keratinocytes and fibroblast, together they make one of most important biological entities to investigate the THz wave propagation characteristics in the human skin. Morphologically, organotypics closely resemble human skin and could be optimized to investigate individual components such as stratum corneum, sweat ducts, blood vessels and many more. The effect of adding an additional layer and using dermal fibroblasts, resulted in change in optical properties and subsequently pathloss and molecular noise temperature. This suggests that, THz frequencies are sensitive to the complexity of skin and forms an excellent basis of in-body diagnostic nanodevices. The results demonstrated in this chapter, will be a stepping-stone for optimizing channel parameters of in-body nanonetworks along with a detailed analysis of skin composition.

References

[1] HH Mitchell, TS Hamilton, FR Steggerda, and HW Bean. The chemical composition of the adult human body and its bearing on the biochemistry of growth. *Journal of Biological Chemistry*, 168:625–637, 1945.

[2] Priyamvada Tewari, Martin O Culjat, Zachary D Taylor, Jonathan Y Suen, Benjamin O Burt, Hua Lee, Elliott R Brown, Warren S Grundfest, and Rahul S Singh. Role of collagen in terahertz absorption in skin. pages 71691A–71691A. International Society for Optics and Photonics, 2009.

[3] Steven L Jacques. Optical properties of biological tissues: a review. *Physics in medicine and biology*, 58(11):R37, 2013.

[4] Chi H Lee, Anuj Singla, and Yugyung Lee. Biomedical applications of collagen. *International journal of pharmaceutics*, 221(1):1–22, 2001.

[5] KR Foster and HP Schwan. Dielectric properties of tissues and biological materials: a critical review. *Critical reviews in biomedical engineering*, 17(1):25–104, 1988.

[6] S Gabriel, RW Lau, and Camelia Gabriel. The dielectric properties of biological tissues: II. Measurements in the frequency range 10 Hz to 20 GHz. *Physics in medicine and biology*, 41(11):2251, 1996.

[7] Peter H Siegel. Terahertz technology. *IEEE Transactions on microwave theory and techniques*, 50(3):910–928, 2002.

[8] Yun-Shik Lee. *Principles of terahertz science and technology*, volume 170. Springer Science & Business Media, 2009.

[9] Peter M Corridon, Ricardo Ascázubi, Courtney Krest, and Ingrid Wilke. Time-domain terahertz spectroscopy of artificial skin. pages 608007–608007. International Society for Optics and Photonics, 2006.

[10] AG Markelz, A Roitberg, and Edwin J Heilweil. Pulsed terahertz spectroscopy of DNA, bovine serum albumin and collagen between 0.1 and 2.0 THz. *Chemical Physics Letters*, 320(1):42–48, 2000.

[11] P Rompre, FA Auger, L Germain, V Bouvard, CA Lopez Valle, J Thibault, and A Le Duy. Influence of initial collagen and cellular concentrations on the final surface area of dermal and skin equivalents: a Box-Behnken analysis. *In vitro cellular & developmental biology*, 26(10):983–990, 1990.

[12] Luisiana X Cundin and William P Roach. Kramers-Kronig analysis of biological skin. *arXiv preprint arXiv:1010.3752*, 2010.

[13] Luigi Vitagliano, Rita Berisio, and Alfonso De Simone. Role of hydration in collagen recognition by bacterial adhesins. *Biophysical journal*, 100(9):2253–2261, 2011.

[14] V Ottani, M Raspanti, and A Ruggeri. Collagen structure and functional implications. *Micron*, 32(3):251–260, 2001.

[15] H Paul Ehrlich and Kurtis E Moyer. Cell-Populated Collagen Lattice Contraction Model for the Investigation of Fibroblast Collagen Interactions. *Wound Regeneration and Repair: Methods and Protocols*, pages 45–58, 2013.

[16] Josep Miquel Jornet and Ian F Akyildiz. Channel modeling and capacity analysis for electromagnetic wireless nanonetworks in the terahertz band. *IEEE Transactions on Wireless Communications*, 10(10):3211–3221, 2011.

[17] Jennifer Barrila, Andrea L. Radtke, Aurélie Crabbé, Shameema F. Sarker, Melissa M. Herbst-Kralovetz, C. Mark Ott, and Cheryl A. Nickerson. Organotypic 3d cell culture models: using the rotating wall vessel to study host–pathogen interactions. *Nat Rev Micro*, 8(11):791–801, November 2010.

[18] John W Haycock. 3d cell culture: a review of current approaches and techniques. *3D Cell Culture: Methods and Protocols*, pages 1–15, 2011.

[19] Johan PE Junker, Justin Philip, Elizabeth Kiwanuka, Florian Hackl, Edward J Caterson, and Elof Eriksson. Assessing quality of healing in skin: review of available methods and devices. *Wound Repair and Regeneration*, 22(S1):2–10, 2014.

[20] Eliah R. Shamir and Andrew J. Ewald. Three-dimensional organotypic culture: experimental models of mammalian biology and disease. *Nat Rev Mol Cell Biol*, 15(10):647–664, October 2014.

[21] Delphine Antoni, Hélène Burckel, Elodie Josset, and Georges Noel. Three-dimensional cell culture: a breakthrough in vivo. *International journal of molecular sciences*, 16(3):5517–5527, 2015.

[22] Gopu Sriram, Paul Lorenz Bigliardi, and Mei Bigliardi-Qi. Fibroblast heterogeneity and its implications for engineering organotypic skin models in vitro. *European journal of cell biology*, 94(11):483–512, 2015.

[23] Steven T Boyce and Glenn D Warden. Principles and practices for treatment of cutaneous wounds with cultured skin substitutes. *The American journal of surgery*, 183(4):445–456, 2002.

[24] A Oikarinen. Aging of the skin connective tissue: how to measure the biochemical and mechanical properties of aging dermis. *Photodermatology, photoimmunology & photomedicine*, 10(2):47–52, 1994.

[25] F Spöler, M Först, Y Marquardt, D Hoeller, H Kurz, H Merk, and F Abuzahra. High-resolution optical coherence tomography as a non-destructive monitoring tool for the engineering of skin equivalents. *Skin research and technology*, 12(4):261–267, 2006.

[26] Jungwoo Lee, Meghan J Cuddihy, and Nicholas A Kotov. Three-dimensional cell culture matrices: state of the art. *Tissue Engineering Part B: Reviews*, 14(1):61–86, 2008.

[27] Sean V Murphy and Anthony Atala. 3d bioprinting of tissues and organs. *Nature biotechnology*, 32(8):773–785, 2014.

[28] Vincent van Drongelen, Mogbekeloluwa O Danso, Aat Mulder, Arnout Mieremet, Jeroen van Smeden, Joke A Bouwstra, and Abdoelwaheb El Ghalbzouri. Barrier properties of an N/TERT-based human skin equivalent. *Tissue Engineering Part A*, 20(21-22):3041–3049, 2014.

[29] Hans-Jürgen Stark, Axel Szabowski, Norbert E Fusenig, and Nicole Maas-Szabowski. Organotypic cocultures as skin equivalents: A complex and sophisticated in vitro system. *Biol Proced Online*, 6(1):55–60, 2004.

Chapter 6

Conclusion and Future Research

Conventional communication paradigms are advancing with the passage of time, demanding high speed, multi-user functionality, efficient data transfer all in a small portable device. Nanotechnology is becoming a known reality for future communication devices. An assembly of nano-devices for a nanonetwork, is envisioned to sense, store and share the intricate details of the human body helping the medical sector. In this thesis, cornerstones of in-body communication for healthcare diagnostic applications were presented. Introduction to terahertz (THz) communication for in-body nanodevices with variation in skin morphology was the crux of this research investigation. The THz band for nanoscale (or short-range THz) communication ranging from 0.1-10THz has been explored for initially for in-door, short-range free space communication. However, by increasing the capabilities of devices around us at a macro-scale motivated to explore the capability of nano-devices. This concept led to several application in the medical field especially incorporating the THz frequencies which have already marked their niche in biomedical applications.

6.1 Contributions and Conclusions

Chapter 3, the imperative aspect of nanoscale in-body communication is the channel medium properties. In this chapter, kernels of THz characterization of skin tissue was presented. Key contributions are,

- Experimental investigation of channel medium was performed and human skin was the main focus of THz time domain spectroscopy. Skin being an inhomogeneous medium and early indicator to a person's health was proposed as a starting point to establish in-body communication.

- With the medical applications of Nanodevices, inhomogeneity of human body is still a big mystery. In this chapter, the basic variation of any tissue type - hydration was experimentally investigated. An iterative material parameter extraction algorithm was applied to extract the optical parameters.

- The standard optical imaging of the skin was done, to indicate the intricate features such as sweat duct and hair follicle contributing to the measurement data. The layered structure of skin including epidermis and dermis was measured with traces of top-most layer- stratum corneum. The samples were prepared for THz time domain spectroscopy in the transmission mode.

- The measurement optical parameters of THz time domain spectroscopy - refractive index and absorption coefficient were applied to numerically evaluate channel parameters - pathloss and molecular noise temperature.The time domain data in picosecond was converted to frequency domain by fast Fourier Transform. This gave both phase and magnitude value which were then used to get the ratio of transfer function of the sample under study and the reference. The channel parameters are based on radiative transfer theory depending on frequency and path length.

- Original Contribution - The results demonstrate the effects of skin dehydration on absorption coefficient and subsequently on channel parameters. It was highlighted that THz wave is sensitive to tissue hydration, hence water dynamics instead of being a hindrance to THz communication, became an excellent medium to sense various health conditions. The results of tissue dehydration shows that absorption coefficient is well below the <100 cm^-1 and this effects the pathloss and molecular noise temperature. Future in-body nanodevices can utilize these results to create a database of dehydrated tissue and further extend to related medical conditions. The channel parameters were evaluated and deemed suitable for short-range THz communication (less than 1mm) with minimal spectral featured in the THz domain.

Chapter 4, the channel medium optimization becomes complex as one dwells into understanding the skin morphology. The human body is a highly sophisticated machines wherein some part is linked to the other. In this chapter,

- Different tissue types were experimentally. Fresh skin tissue from different parts of the body were analyses and experimental results were presented. Throughout the measurement, the thickness was fixed at 200um by gently pressing the tissue and removing residual media. The ex-vivo measurement of fresh tissue is understandably the closest to actual live human skin.

- Tissue from different parts of body such as breast and abdomen was measured and optical parameters were extracted. The samples were obtained within a few hours of surgery and stored overnight in growth media to keep the morphology close to that of actual human skin. The samples were studied under standard light microscopy after performing the measurements.

- The optical properties of breast tissue was studied at different rotation angled analogous to real-time scenario. It was highlighted that human tissue, especially the dermis layer is a fibrous structure. Hence angled-dependent studies become important in case of any mechanical (pressure, temperature, or tissue-rupture) variations in the tissue.

- Both the tissues breast and abdomen have same layered structure, however with standard light microscopy results, the abdomen tissue is denser. Hence a slight variation in refractive index and absorption coefficient is seem. Other factors such as atmospheric water vapours and electronic noise from the optical bench do affect the working frequency range, signal to noise ratio and dynamic range.

- Original Contribution - Mapping the human skin by measuring different tissue types was the main focus of this chapter. A complete database involving variation in real-skin biological features such as hydration and tissue fibre density affect the optical properties and channel parameters. With the results presented, nanodevice location will highly depend on the tissue type and its optical properties. Fresh tissue refractive index varies between 2.3 -3.3 depending on water dynamics and fibre density. The angle-dependent measurement again highlight the complex morphology of the tissue and changes in fibre orientation that affects the pathloss and molecular noise temperature. A comparison of channel parameters of freshly excised breast and abdomen tissue highlights that with the same human body it is challenging to establish a universal in-body nanonetwork. However, focusing on details like presented in this thesis is a stepping stone for creating an in-body communication database applied for skin tissue.

Chapter5, the dehydrated and hydrated real skin tissue provides a spectrum of possible biological features that affects the channel medium for short-range THz communication. Skin is a heterogeneous layered structure and can be decided into three basics - stratum corneum, dermis and fat. In this chapter, dermis layer is investigated in detail,

- The dermis layer is artificially modelled using a standard tissue culture protocol. The focus is experimental investigation of collagen which is the main protein forming the extra-cellular matrix. Collagen was cultured using a reagent and fibroblast cells that

bind and proliferate to form the 2D matrix. This is a basic model of dermis layer mimicking the human skin layer where nutrients are provided with growth media.

- The samples were prepared by varying the fibroblast cell numbers. The key is to understand the dynamics of water and subsequent changes in optical parameters of the dermis layer.The cell number density was increased starting from 100k to 500k with a difference of 200%. The cells were first estimated by observing them in a standard light microscope using a haemocytometer. Rat-tail type I collagen was used as a base reagent for gel preparation, which was commercially bought. The gels were then incubated (5% CO2) for gelation at 37 degree for approximately 45 minutes. The contraction of the gels was observed and reported for over the period of two weeks. Increase in Fibroblast cell number density leads to collagen gel contraction and hence alters its molecular composition.

- The measurement of gels were carried out within half and hour of their exposure to room temperature. The signal level attenuation of collagen samples were compared with be compared with reference, where the peak intensity for is reduced to 5 mV for 500k cells and similarly for 300k and 100k. This presents the lossy behaviour due to absorption of transmitted THz wave through the samples. The same extraction algorithm was applied to record the refractive index and absorption coefficient values. It was shown as the cell number density increases the refractive index and absorption value decreases.

- The optical parameters for different cells numbers were used to evaluate the pathloss and molecular noise temperature. It was shown that not only channel parameters depends on frequency and distance but also intricate molecular features like collagen fibres. The results for both pathloss and molecular noise temperature demonstrate high dependence on molecular features and hydration level of the skin.

- The fibre density of collagen samples were separately studied under scanning electron microscope where sample number of fibroblast cells were estimated and a similar trend in contraction was observed. These fibroblast cell number density was slightly different (200k, 400k, 600k and 800k) however the difference of 200% is still the same. They were first dried to a point of no moisture and imaged under near to vacuum conditions. The fibres were observed to spread randomly but they always grow on top of each other. Spatially, the fibres are always in parallel to each other forming a dense extra cellular matrix.

- To further investigate the effects of layered structure , an epidermal layer with keratinocytes as its main constituent was added on top of a base dermal collagen layer. The form of tissue culture focuses on 3D structure called organotypics, addressing the dynamics between keratinocytes and fibroblasts forming a more advance dermal layer. NTERT keratinocyte cell line was used for creating 3D-orgnanotypic skin equivalent model. The cells were seeded in a plastic flask supplied with essential nutrients and and are then left to proliferate in an incubator. As before, collagen type 1 was used as the reagent to form the dermal layer and extended to forming an epidermis.

- The sample tend to contract and form a thin layer, and hence standard tissue sample holder was unsuitable. Instead, it was measured by mechanically fixing in the sample holder mount with a ring graft (used for growing the epidermal layer). The optical parameters were again extracted and applied to evaluate the pathloss and molecular noise temperature. In particular, absorption coefficient value was lower than the freshly excised tissue since the sample was very thin. The refractive index value was recorded to be very close to that of a real skin.The sample was also studied under standard light microscope highlighting the growth of epidermal on top of dermal layer.

- Original Contribution - Investigation of skin tissue molecular feature layer by layer was the highlight of this chapter. The skin substitute models offer potential insight to actual human skin morphology. A comparative study of 2D and 3D skin models were made and the results were together aligned with excised human skin. Organotypics are definitely a step closer to real human skin, but THz characterization of these samples helps to validate their biological nature. Not only the optical parameters are useful for channel parameters, in-body communication but optimizing the optical properties skin substitutes.

6.2 Future Research

The thesis presented an inter-disciplinary research with channel medium measurement and numerical evaluation of channel parameters as its main focus. The results and analysis can be further extended to enhance the capabilities of human body optical parameters, nanoscale THz communication, channel modelling and skin substitute applications. The work presented could open doors to:

- THz-TDS in reflection mode and nitrogen purging of the THz emitter path - The biological samples are lossy and vary in morphology and thickness. Reflection geometry

is convenient in regards to convenient placement of the tissue without the need for any sample holder. Different biological elements such as blood, sweat ducts, diseased tissue etc., needs to be characterized to extend the existing database for channel parameters. It would be interesting to integrate THz reflection mode with imaging making it a complete medical diagnostic tool. Current measurements are made in normal humid air, such fluctuations could lead to changes in phase information. Hence, future studies should include a comparative analysis of measurement with and without nitrogen purging (or dry air). This will further help the system to achieve an optimized repeatable state. Control parameters like time of nitrogen (or dry air) flow, pressure, humidity level will be helpful.

- An an extension to channel modelling for in-body nanonetworks, interference and noise due to cluster of nanodevices need to incorporated. Channel modelling needs some added functionality such as to explore the performance of multiuser; noise model such as body radiation and absorption noise due to variation in molecular features of the channel medium. Added extension could be effect on channel parameter due to changes in physical parameters like temperature, pressure, stress, rupture of tissue etc.

- Diabetes - THz technology has been utilized to study collagen which is essential for for forming the extracellular matrix in the dermis layer. Protein glycation contributes to skin ageing as it deteriorates the existing collagen by cross-linking. The elevated levels of glucose starts forming covalent adduct (chemical compound) with plasma proteins through a non-enzymatic process known as glycation. Accelerated skin ageing is especially noticeable in diabetic patients, where glycation is increased because of the high serum glucose level. Protein glycation and formation of advanced glycation end products (AGEs) play an important role in the development of diabetic complications.THz technology comes to aid with its ability to capture unique spectral features of biomolecules and associated activities with water inside the tissue. Such a technique could be of potential benefit to diagnose diabetes and related skin specific complications. Results presented in this thesis that characterization of collagen in the terahertz frequency range and further sugar variation with collagen protein can provide in-depth knowledge of diabetic conditions. The spectral signature obtained could be stepping in constructing a solid database for medical diagnostic devices such as THz diabetic device.

- These models are already popular in areas of skin grafting, toxicology, drug delivery etc., hence they are a potential candidates for testing the bio-compatibility of nano-devices and further establishing a non-network. Thus, THz TDS sensitivity to

biomolecular activity could be helpful in optimizing more artificial skin models to mimic real skin. Tissue culture is developing to add more real-like layers such as stratum corneum, blood vessels etc., hence it will be an exciting venture to utilize the attributes of THz radiation to study them.